JENERİK SAVAŞ UÇAĞI İÇİN AERODİNAMİK VERİ TABANI ELDE ETMEK AMACIYLA ÇOKLU DOĞRULUKLU VERİ BİRLEŞTİRME TEKNİKLERİNİN İNCELENMESİ

Burhan Necati KIZILOĞLU

YÜKSEK LİSANS TEZİ
SAVUNMA TEKNOLOJİLERİ ANA BİLİM DALI

SİVAS BİLİM VE TEKNOLOJİ ÜNİVERSİTESİ
LİSANSÜSTÜ EĞİTİM ENSTİTÜSÜ

OCAK 2024

ETİK BEYAN

Sivas Bilim ve Teknoloji Üniversitesi Lisansüstü Eğitim Enstitüsü Tez Yazım Kurallarına uygun olarak hazırladığım bu tez çalışmasında;

- Tez içinde sunduğum verileri, bilgileri ve dokümanları akademik ve etik kurallar çerçevesinde elde ettiğimi,
- Tüm bilgi, belge, değerlendirme ve sonuçları bilimsel etik ve ahlak kurallarına uygun olarak sunduğumu,
- Tez çalışmasında yararlandığım eserlerin tümüne uygun atıfta bulunarak kaynak gösterdiğimi,
- Kullanılan verilerde herhangi bir değişiklik yapmadığımı,
- Bu tezde sunduğum çalışmanın özgün olduğunu,

bildirir, aksi bir durumda aleyhime doğabilecek tüm hak kayıplarını kabullendiğimi beyan ederim.

……..
Burhan Necati KIZILOĞLU
31/01/2024

JENERİK SAVAŞ UÇAĞI İÇİN AERODİNAMİK VERİ TABANI ELDE ETMEK AMACIYLA ÇOKLU DOĞRULUKLU VERİ BİRLEŞTİRME TEKNİKLERİNİN İNCELENMESİ

(YÜKSEK LİSANS TEZİ)

Burhan Necati KIZILOĞLU

SİVAS BİLİM ve TEKNOLOJİ ÜNİVERSİTESİ

LİSANSÜSTÜ EĞİTİM ENSTİTÜSÜ

Ocak 2024

ÖZET

Aerodinamik veri setleri bir hava aracının uçuş performansı, uçuş dinamiğinin belirlenmesinde kulanılan önemli bir kaynaktır. Aerodinamik veri setleri farklı uçuş koşullarına karşılık gelen aerodinamik katsayıları içerir ve bu katsayılar farklı kaynaklardan farklı doğruluk değerlerinde elde edilebilmektedir. En doğru değerler uçuş testlerinden alınmakta olup, sonrasında büyük ve küçük ölçekli rüzgar testleri, hesaplamalı akışkanlar dinamiği simülasyonları ve nümerik çözücüler farklı doğrulukta aerodinamik veri elde edilmesinde kullanılır. Yüksek doğruluklu veri, hava aracına ait parametrelerin yorumunda doğru sonuçlar vermektedir ancak yüksek doğruluklu verilerin elde edilmesi iş gücü olarak maliyetli ve zaman alıcıdır. Çoklu doğruluklu veri birleştirme yöntemlerinin varlığı ile yüksek ve düşük doğruluklu verilerin kullanılması mümkün olmuştur. Böylece yüksek doğruluklu veriye ihtiyaç azalmış ve daha verimli, iş gücü ve zamandan tasarruf edilmiştir. Bu çalışmada kullanılan jenerik savaş uçağından elde edilen düşük ve yüksek doğruluklu veriler co-Kriging, çoklu-doğruluklu Gauss Süreç Regresyonu ve çoklu doğruluklu sinir ağları yöntemleri ile kullanılmıştır. Verilerin elde edilmesinde iki farklı veri kaynağı kullanılmıştır. Düşük doğruluklu veriler OpenVSP programında Vortex-Lattice metodu ve yüksek doğruluklu veriler ANSYS Fluent programında k-ω SST çözücü kullanılarak elde edilmiştir.Her iki kaynaktan -15 ile +15 derece hücum açısı aralığında kaldırma, sürükleme ve pitch moment katsayıları alınmıştır. Her iki veri kaynağından alınan veriler farklı miktarlarda kullanılarak test-caseler oluşturulmuş ve her üç yöntemin performansları incelenmiştir. Her üç yönteminde yüksek doğruluklu veri sayısının artmasıyla yönteme ait tahminlerinin yüksek doğruluklu veriler ile örtüştüğü belirtilmiştir. Co-Kriging yönteminde veri noktalarının yerinin değiştirilmesiyle tahmin performansının değiştiği bu yüzden co-Kriging yönteminin diğer yöntemlere göre daha hassas olduğu gözlemlenmiştir. MF-GPR yönteminin diğer yöntemler arasında en iyi tahmin sonuçlarını verdiği ve MF-NN modelinin eğitilmesinde düze yakın eğimlerde iyi tahmin yeteneğine sahipken, eğimi fazla durumda daha fazla yüksek doğruluklu noktaya ihtiyacı olduğu belirlenmiştir.

Bilim Kodu	:	93107
Anahtar Kelimeler	:	Çoklu-Doğruluklu Veri, Yüksek Doğruluklu Veri, Düşük Doğruluklu Veri, Veri Birleştirme Yöntemleri, Aerodinamik Veri Seti
Sayfa Adedi	:	116
Danışman	:	Dr. Öğr. Üyesi Yaşar OSTOVAN

INVESTIGATION OF MULTI-FIDELITY DATA FUSION TECHNIQUES TO OBTAIN AN AERODYNAMIC DATABASE FOR A GENERIC FIGHTER AIRCRAFT

(M.Sc. THESIS)

Burhan Necati KIZILOĞLU

SİVAS UNIVERSITY OF SCIENCE AND TECHNOLOGY

INSTITUTE OF GRADUATE STUDIES

January 2024

ABSTRACT

Aerodynamic data sets are an important source for determining the flight performance, stability and control, and flight dynamics of an aircraft. Aerodynamic data sets contain aerodynamic coefficients corresponding to different flight conditions. These aerodynamic coefficients can be obtained from different sources with different fidelity values. The most accurate values are obtained from flight tests, followed by large and small scale wind tests, computational fluid dynamics simulations and numerical solvers to obtain aerodynamic data of different fidelity. High-fidelity data provides accurate results for the interpretation of aircraft parameters, but obtaining high-fidelity data is labor costly and time consuming. With the availability of multi-fidelity data fusion methods, it is possible to use high and low fidelity data. This reduces the need for only high fidelity data and is more efficient, labor and time saving. The data obtained with the data fusion method is ensured to be high fidelity data. In this study, different data fusion methods were used using low and high fidelity data obtained from the generic fighter jet. These methods are co-Kriging, multi-fidelity Gaussian Process Regression and multi-fidelity neural networks. Two different data sources were used to obtain the data. Two different data sources were used to obtain the data. Low fidelity data were obtained using Vortex-Lattice method in OpenVSP program and high fidelity data were obtained using k-ω SST solver in ANSYS Fluent program. Lift, drag and pitch moment coefficients were obtained from both sources in the range of -15 to +15 degrees angle of attack. Test-cases were created using different amounts of data from both data sources and the performances of all three methods were analyzed. It is stated that the predictions of all three methods match with the high fidelity data as the number of high fidelity data increases In the co-Kriging method, it was observed that the prediction performance changed when the locations of the data points were changed, so the co-Kriging method was more sensitive than the other methods. It was determined that the MF-GPR method gives the best prediction results among the other methods, and while the MF-NN model has good prediction ability on flat and near flat slopes, but it needs more high fidelity data points in the data line with high curvature slope.

Science Code	:	93107
Key Words	:	Multi-Fidelity Data, High-Fidelity Data, Low-Fidelity Data, Data Fusion Methods, Aerodynamic Database
Page Number	:	116
Supervisor	:	Asst. Prof. Dr. Yaşar OSTOVAN

TEŞEKKÜR

Yaptığım bu yüksek lisans tezinin ciddi bir emek ve istikrarla hazırlanıp bitirilmesinin heyecanını ve gururunu yaşıyorum. Öncelikle yüksek lisans danışmanlığımı üstlenmiş, yüksek lisans tezi çalışması sırasında yardımlarını esirgememiş ve yüksek lisans tezimi sürdürürken konunun proje olmasında yardımcı olmuş, TAI LIFT UP+ projesi sayesinde Türk Havacılık ve Uzay Sanayi'de kısmi zamanlı çalışmamda emeği olan Doktor Öğretim Üyesi Yaşar OSTOVAN hocama danışmanlığı için çok teşekkür ediyorum. Bunun yanında her türlü desteği veren, yanımda olan ve tez yazmak istemediğimde beni isteklendiren aileme, her haftanın her günü birbirimize destek ve yardımcı olduğumuz ofis arkadaşlarıma ve adı geçmeyen diğer kahramanlarıma teşekkür ederim.

TABLE OF CONTENTS

Page

Page

LIST OF TABLES

Table **Page**

Table **Page**

LIST OF FIGURE

Figure **Page**

Figure **Page**

Figure **Page**

Figure **Page**

Figure **Page**

Figure **Page**

Figure **Page**

SYMBOLS AND ABBREVIATIONS

The symbols and abbreviations used in this study are presented below with their explanations.

Symbols	**Explanations**
Re	Reynolds Number
ω	omega

Abbreviations	**Explanations**
CFD	Computational Fluid Dynamics
DATCOM	The United States Air Force Stability and Control Digital DATCOM
DoE	Design of Experiment
k-ω SST	k-omega Shear Stress Transport
LF	Low-fidelity
LHS	Latin Hypercube Sampling
MF	Multi-fidelity
MF-cK	Multi-fidelity co-Kriging
MF-GPR	Multi-fidelity Gaussian Process Regression
MF-NN	Multi-fidelity Neural Network
MSE	Means Square Error
HF	High-fidelity
NS	Navier-Stokes
RANS	Reynolds Averaged Navier-Stokes
RBF	Radial Basis Function
RMSE	Root Mean Square Error
VLM	Vortex-Lattice Method

1. INTRODUCTION

Aerodynamic data sets are needed to understand whether an aircraft can meet the performance criteria and to predict the conditions under which it can perform. These data sets are obtained from various sources with different fidelity levels, and the places where each source with different fidelity levels is used differ. Depending on the level of the studies to be carried out, the data to be used must be reliable and produced in a short time. By producing data sets from these sources, engineers have information about the control, stability and performance analysis of the aircraft. In terms of reliability, the fidelity values of the data sources can be said to be flight tests, large- and small-scale wind tunnel tests, CFD analyses and various simple mathematical models, but if we compare them in terms of cost and time parameters, this order will be in the opposite direction. Creating aerodynamically high-fidelity datasets such as wind tunnels or flight tests can be costly and time consuming, while quasi-experimental mathematical methods such as DATCOM, ESDU or linear flow solvers such as Panel Method, Vortex Lattice Method are faster than other sources in creating datasets but behind in terms of reliability.

Since the data sets from the wind tunnels are generated under specified conditions and the cost of the data from the model is high and time consuming, a system that produces data close to the reliability of the wind tunnels, but in a fast and relatively less costly way, was searched for. With this system, it was concluded that the data would be obtained reliably without spending much time and that the need for other costly and time-consuming sources would be reduced. In this case, data of different reliability levels were obtained in a faster and easier way with the help of certain data fusion methods. As mentioned before, high reliability data sources are preferred for large studies and these data are generally obtained with the help of large- and small-scale wind tunnels. In order to obtain high-fidelity data sets such as wind tunnels more quickly, data from several sources should be fused with the help of certain methods and the accuracy of the obtained data set should be checked.

This master's thesis aims to produce and develop an aerodynamic database using multi-fidelity data fusion techniques. In the creation of aerodynamic data sets of aircraft, data sources of different accuracy are utilized and these sources can be of high and low fidelity. While low fidelity data sets can be obtained quickly, the creation of high-fidelity data sets is costly and time consuming. The problem here is that the data sets used to predict the

performance criteria of the aircraft should be of high fidelity, but as mentioned before, high fidelity data sources such as wind tunnels and flight tests are costly and time consuming. At this point, it is planned to create aerodynamic data sets of the aircraft using certain methods with less cost and time saving. Among these methods, the most widely used Kriging based estimation methods and artificial neural networks are considered. With two different methods, it is planned to obtain a new data set with multiple fidelity by using low and high-fidelity data at a certain data density and to train this data set. In this way, new data sets can be obtained by using a smaller amount of high-fidelity data. With this study, it will be useful in the formation of the aerodynamic database of the air vehicles that will be produced within the company and are currently in progress by creating data sets in a relatively less costly, practical and fast time.

2. LITERATURE REVIEW

The generation of aerodynamic data base for aircraft is mostly based on various classical methods such as wind tunnel tests, computational fluid dynamics simulations and flight tests. The data generated by these methods are used as high-fidelity data and these data are generated at different flight parameters (various angles of attack, Mach numbers, etc.). As the number of parameters increases, the size of the data set increases and more labor and time is required to create the data set. Different methods have been developed to reduce the labor and time required and to obtain high fidelity and accuracy data in an easier and faster way. In previous academic studies, faster and more reliable data were obtained by using aerodynamic data obtained by classical methods with the help of data fusion methods. This master's thesis aims to obtain and combine aerodynamic data of the generic fighter aircraft and to create a simple data set. For this purpose, firstly, data fusion methods in the literature are examined and explained in detail. Then, the wind test studies of the generic fighter jet model to be used are examined. Finally, the computational fluid dynamics tests of the same model are investigated and explained in detail.

2.1. Multi-Fidelity Data Fusion Methods

Aerodynamic databases are a collection of aerodynamic data for different aircraft and aerodynamic structures. These databases usually include data from experimental means such as large- and small-scale wind tunnel tests, numerical means such as computational fluid dynamics simulations, or combinations thereof, but in some cases flight tests are also used to create databases. In general, this data may include data on aerodynamic forces and moments, data describing the interactions between different parts and components of the aircraft, airflow data, aerodynamic constraints, shapes and sizes of aerodynamic surfaces, and performance data such as rate of climb, speed and range. These data are used to optimize the design of the aircraft, predict flight performance and simulate the aircraft. The creation of aerodynamic databases requires a great deal of time and cost, and the fact that these databases are always created using highly accurate data sources will prevent aircraft design and optimization from being performed quickly and efficiently. To avoid this situation, the use of multi-fidelity models will be faster and more efficient in designing and optimizing the aircraft, simulating flight dynamics and developing flight control algorithms.

Multi-fidelity models have been used especially in health and biology when data from different measurement devices need to be combined, and these models can also be used in aerodynamics. Multi-fidelity models are especially useful in cases such as aerodynamic databases where complex data sources with different fidelity levels need to be combined. Aerodynamic databases may contain data obtained under different flight conditions. These data are obtained using sources with different fidelity levels, and multi-fidelity models can help to obtain more accurate results by combining these data with different fidelity levels.

Aerodynamic data fusion is the process of combining data from aerodynamic data sources with different fidelity to create a larger data set. Aerodynamic data fusion aims to bring together data containing different variables such as different flight conditions, speeds, altitude values and deflection angles of aerodynamic surface geometries. These data can be test flights, wind tunnel tests, computational fluid dynamics calculations and other theoretical methods.

Aerodynamic data fusion is very important for the aerospace industry. This method is used to obtain more accurate results by combining data from different aerodynamic data sources. By considering the fidelity levels of the data with the data fusion method to be used, the differences between different data sources are eliminated and help to obtain more accurate results. Aerodynamic data fusion methods allow data of different fidelity to be processed simultaneously. This process saves time and labor. Aerodynamic data fusion methods improve data quality. Bringing together data from different data sources increases the reliability of the data and helps to eliminate false data. In addition, data fusion methods allow new information to be obtained by combining data from sources with different fidelity. This helps researchers to obtain more comprehensive results by using a larger data set. Finally, data fusion methods help to correct errors in the data. These advantages are why aerodynamic data fusion methods are widely used in the aerospace industry. Aerodynamic data fusion is important for obtaining more accurate results, increasing efficiency, improving data quality and correcting errors.

Models such as Kriging-based models, Response Surface models (RSM), Radial Basis Function (RBF) model, Variable Complexity Modeling (VCM) and machine learning model (ML) have been frequently used in aerodynamic data fusion studies in the literature. The most widely used of these data fusion models is the Kriging method. Before being used in

aviation, the Kriging method was used in areas such as mining, geology, agriculture and geography. The Kriging method is used to estimate data whose distribution is random. This method considers the measurement errors of the data from each source and calculates the weight of each data point. The Kriging method has an important parameter, the Kriging variance of the data. This variance is a measure of how accurate the estimated value is. When the number of data to be used in the Kriging method increases, the prediction reliability of the model increases, but one issue that the Kriging method lacks is the extrapolation process. The biggest disadvantage of the Kriging method is that the accuracy of the predictions made by extrapolation decreases. Co-Kriging, three-level Kriging (3LK), hierarchical Kriging (HK), Gradient enhanced Kriging (GEK), Gradient enhanced co-Kriging (GECK) are new methods developed based on Kriging method. Co-Kriging method differs from the Kriging method in that it is a method used to estimate the relationship between two or more variables and their relationship with each other. It estimates the variance of more than one variable using the covariance and correlation matrices of the variables. It can make a more precise estimate by using variances from different sources.

Lei et al. [1, 2], Amin et al. [3], Tang et al. [4], Kurt et al. [5], Ghoreishi and Allaire [7, 8], Pham, Kim, Tyan and Lee [9], Kuya et al. [10], Han et al. [11-13], Rosenbaum and Schulz [14], Parussini et al. [15], Rohit and Ganguli [16], Anhichem [24], Yixiang Deng et al. [17], Lin [18], Zhou et al. [23], Zhang [20], Rumpfkeil [21], Feldstein [25], Perdikaris [27], Mukhopadhaya [26], Xiao [19], Dong [22] have conducted studies using Kriging method in addition to other methods or to compare performance. In these studies, Kriging method is sometimes referred to as Gaussian Process Regression (GPR). In addition, some authors have contributed to the literature by developing new and advanced methods based on Kriging and changing the name of the model they proposed. Variable Fidelity Modeling is a modeling approach where models with different levels of fidelity are used together. This approach aims to obtain more accurate results by using data of different fidelity. By using different functions, the relationship between data with different fidelity can be found and data fusion is performed using the VFM method. These functions are scaling function, increment function and hybrid function. There are studies in the literature where all three functions are used separately. The scaling function uses the ratio between high fidelity data and low fidelity data. There are several potential problems with using this function. The first one is that the assumption will not work if the number of low fidelity data takes the value zero. In addition, as the number of low-fidelity data approaches zero, the value of the

function grows excessively and the prediction errors are the main reasons for these problems. The Increment function operates using the difference between high and low fidelity data. It can be used safely except in the absence of data in one of the data sources. Hybrid function aims to use both increment and scaling functions together. Vinh Pham [9], Ghoreyshi [29], Han [11, 12], Nguyen [30], Zastawny [32], Rumpfkeil [21], Tyan [33], Belyaev [34] have conducted studies using VFM method. The Radial Basis Function method is a mathematical method used especially for machine learning problems such as classification and regression analysis. This method mostly uses the Euclidean distance function to estimate the location of the data. It mostly uses the Gaussian function to estimate the location of the data. Apart from this, different basis functions such as linear, cubic and multi-quadratic are also used. In RBF regression, the model is trained using a set of input and output pairs. The aim of the algorithm is to produce output values corresponding to the input values. The RBF regression model consists of three layers. These are the input layer, the hidden layer and the output layer. The input layer contains the input values in vector form. In the hidden layer, the data is processed using the basic functions described above. In the output layer, the predicted data is obtained. During training, the algorithm also determines the most appropriate center point in the dataset and the weight values associated with the functions. The RBF method can be used for problems with non-linear relationships between input and output variables. The RBF method is advantageous because it has the ability to fit complex data without overfitting and does not have many parameters to be optimized in terms of computational efficiency. Lei et al. [1], Tyan et al. [33] have conducted studies using the RBF model.

Response Surface Modeling is a statistical technique used to represent the data obtained with a mathematical model. The RSM method is used to understand and optimize the relationships between input and output values entering the system. RSM is based on multiple regression analysis and is used with design of experiments. The RSM method examines the individual variables of the model and determines their effects. Taking these effects into account, it is used to predict the response of the system to the input value. This method can be used to obtain optimum results more efficiently by reducing the time and cost required to generate data. Keajne [6], Kuya et al. [10], Tang et al. [28] have conducted studies using Response Surface Modeling method. Variable complexity modeling (VCM) is a method that can be used to combine data with different levels of fidelity. It works by adjusting the complexity of the model to capture differences between different datasets. For

example, it can be used to build a predictive model by combining both low-fidelity and high-fidelity data. VCM balances the differences between datasets by reducing the influence of low-fidelity data and increasing the influence of high-fidelity data. He et al. [2], Tang et al. [4], Kurt et al. [5], Tang et al. [28], Nguyen et al. [30, 31], Tyan et al. [33], Kou [40] combined data with different fidelity using Variable Complexity Modeling. Aerodynamic data fusion using machine learning is an increasingly popular method for combining and analyzing aerodynamic data from different sources. This method provides faster and more accurate results than traditional data fusion methods in parallel with the developing technology and increasing processing capacity of computers. Machine learning algorithms commonly have an input layer, a hidden layer and an output layer. Mathematical operations called activation functions are performed between each layer. The values given in the input layer go through a series of operations and are displayed as a prediction value in the output layer. Gomec [35], Kurt [36], Wang [37], Tao [38], Chen et al. [41].

Lei et al. [1] aimed to obtain high-fidelity aerodynamic data in an efficient way by using a multi-fidelity surrogate model to obtain high-fidelity data. RBF (Radial Basis Function) and Kriging were chosen as multi-fidelity model methods and these methods were discussed. While the RBF method is used to generate the low-fidelity model, the Kriging method is used to generate the high-fidelity data. After creating the model, the authors tested the model on two cases and noted that they obtained satisfactory results from both study cases. These two studies are engineering examples of aerodynamic force coefficients and aerodynamic heat flow, respectively. In the first case, data were taken from the wind tunnel using two different test conditions and were selected as primary and secondary data sources. Six different aerodynamic forces are planned to be estimated with angle of attack and sideslip angle as test variables. In the second example, the aerodynamic heat flow data fusion of the aircraft was performed and the data were obtained from computational fluid dynamics (CFD) and wind tunnel data. In conclusion, multi-fidelity surrogate modeling such as Kriging and RBF are efficient methods for obtaining high fidelity aerodynamic data. In another study by Lei [2], he aimed to obtain a new high-fidelity dataset from low and high-fidelity data using deep neural networks as a data fusion method. In his study, in order to interpret the performance of deep neural networks, he also used VCM and co-Kriging method to obtain a data set and compared the methods. In the engineering test problem, Euler and Navier-Stokes simulations were performed using the NACA0012 airfoil model. Aerodynamic coefficients were obtained for various Mach number and angle of attack values. In the study,

the aerodynamic coefficient data obtained from simulations using the Euler solver are considered as low-fidelity, while the aerodynamic coefficient data obtained from simulations using Navier-Stokes are considered as high-fidelity. This study predicts that wind tunnel or flight test data can be used in addition to the Euler and Navier-Stokes data obtained from the CFD method to get better results, more complex aerodynamic problems can be solved by giving more input-input variables using deep neural networks, the model will improve and the error values will decrease as the number of data increases.

Amin et al. [3] aimed to create an efficient and effective working environment for the provision and management of aerodynamic data for reentry vehicles in this study. It stated that due to the wide range of flight regimes and the large amount of aerodynamic force data required for each regime, it is necessary to build an aerodynamic data table for reentry vehicles. In the study, interpolation and data fusion techniques were applied in order to advance the accuracy of the data. It is aimed to reduce the need for high-fidelity data as well. The author interpolated the low-fidelity data with the Kriging method and determined the trend of the data set. The few high-fidelity data were combined with the reorganized low-fidelity data using the co-Kriging method. All these methods continued by adding new data to the dataset until the root mean square error (RMSE) value of the dataset matched the predetermined RMSE value. In this study, the low-fidelity data set was obtained using Euler-CFD solvers and the high-fidelity data set was obtained using Navier-Stokes-CFD solver. Tang et al. [4] studied a new method for aerodynamic data generation using CFD tools using design of experiments (DoE) and data fusion. The study aims to improve the efficiency of the data generation process by converting data sets of various fidelity into a single data set and using adaptive design of experiments With the variable-complexity modeling (VCM) method, which is one of the data fusion methods, it is desired to obtain a data set with better accuracy than other data sets by combining low-fidelity data with high-fidelity data. In the study, the VCM method was considered to be used together with the increment function. In the study, Euler simulations were used for low-fidelity data and Navier-Stokes (NS) simulations were used for high-fidelity data and the data were generated by calculating at different Mach numbers and angles of attack. As a result, a comparison was made between this approach and conventional general design methods, showing that this approach significantly reduces the time required for data generation. Kurt et al. [5] wanted to create an aerodynamic dataset of the F-16 fighter jet and stated that the aerodynamic dataset is obtained from high-fidelity data, it takes a very long time to produce and the cost of these

works is high. In his study, he aimed to obtain a high-fidelity dataset by using the data fusion method he proposed for a dataset containing a small number of high-fidelity and a large number of low-fidelity data. In this way, he obtained a high-fidelity data set in a shorter time without using a completely high-fidelity data set. He used methods such as VCM and Kriging in the creation of the resulting high-fidelity data set and created low-fidelity data with semi-empirical methods such as DATCOM and high-fidelity data with wind tunnel test data. While obtaining the data in the study, C_d, C_l and C_m coefficients parameters were created to correspond to different horizontal tail deflection angles with an angle of attack between 0 and 30 degrees at Mach 0,2 at sea level. VCM and co-Kriging estimates were made with these data. The data in the CL and alpha graph, CD-alpha graph and CM-alpha graph between -20 and 20 degrees at Mach 0,2 were applied for both data fusion methods and both methods produced satisfactory and highly accurate data. The results of the study show that co-Kriging provides more accurate results, while the VCM method tends to oscillate in the absence of highly accurate data. In Keajne's study [6], it is aimed to use experimental design, response surface method and data fusion methods together to provide wing optimization with computational fluid dynamics through drag estimation. In this study, it is desired to create a multi- fidelity response surface model (RSM) over the transonic wing. Using experimental data and CFD data, the most accurate model will be created by examining the variations on drag by changing the parameter properties of the wing at constant lift coefficient. Instead of using the least squares method, Kriging method was used which is the most commonly used regression method. Then compared data obtained using Tadpole with data obtained using Kriging, data obtained using MGAERO with data obtained using Kriging, and finally data obtained by combining Tadpole and Kriging data with data obtained using MGAERO. It is seen that the correlation is good when comparing the data obtained with the Tadpole solver and the Kriging method, but the correlation deteriorates when comparing the MGAERO and Kriging method. When the data obtained by combining the data of Tadpole and Kriging methods are correlated with MGAERO, it is stated that the correlation is better than the MGAERO-Kriging correlation alone and worse than the Tadpole-Kriging result.

Ghoreishi and Allaire [7] reported that different data sources are used in estimation and design decisions for complex systems and these data sources have different fidelity and number of data. A multi-fidelity co-Kriging model was applied, which aims to create an accurate prediction of the data of interest by utilizing data from all models. In the first case,

three analytical single-parameter input and output equations with different fidelity values are defined as low, high and highest fidelity, respectively. In the two-dimensional CFD modeling example, the design space of NACA0012 was created using XFOIL and SU2 from computational fluid mechanics programs. For this example, Mach number and angle of attack are the input parameters and the lift coefficient are the desired output parameter. Another data source with the highest fidelity is needed and this data source is specified as a real-time wind tunnel. The results show that the new high-fidelity dataset is very close to the wind tunnel data used for validation and that the model becomes more efficient and the error values gradually decreases as the number of data used in the fusion increases. In another study.

Ghoreyshi et al. [8] conducted a study for sampling and data fusion operations based on obtaining an aerodynamic database for flight simulation. There are objectives in the study which is to obtain high-fidelity aerodynamic databases and is to perform geometry optimization with reference to the initial geometry and to perform data fusion using the initially created aerodynamic data table. The passenger airplane model was used for this process. The data source used for low-fidelity data is DATCOM. The high-fidelity data was obtained from the CFD method. Kriging method was preferred for combining high and low-fidelity data. In order to create the aerodynamic database efficiently and cost-effectively, the design of the experiment was performed using the Latin Hypercube Sampling model, which is an improved version of the Monte Carlo model. the Kriging method is performed for data fusion. They plotted the variations of drag, lift and moment coefficients with respect to the angle of attack. In the result, it was stated that the Kriging method gave effective results. According to Pham et al. [9], developing an aerodynamic dataset is a critical structure used in many engineering applications such as high-fidelity flight simulations and design optimizations, and this dataset must be very large and highly accurate in order to be used in a wide range of operational concepts in real systems. Here, it is planned to create a high-fidelity aerodynamic dataset by using 3 different degrees of fidelity through various fidelity and hierarchical kriging approach. The VFM metamodel was chosen in this study to solve the problem through multi-fidelity models. However, the VFM method was modified and an alternative VFM model was created and this algorithm is referred to as three-level Kriging (3LK). With the 3LK method, three different data sets (low, medium, high) are created instead of two, and a new low-fidelity data set is developed using low- and medium-fidelity data, and these data are combined again with high-fidelity data to create a new data set that

gives more accurate and precise results. To test the targeted algorithm, the study created two examples, one analytical and one aerodynamic, and compared them using other data fusion methods. In the example of creating an aerodynamic database for the Clark Y airfoil, Mach number and angle of attack values were assigned as variables. Mach number values ranged from 0.1 to 0.8 and angle of attack values ranged from -20 to 20 degrees and data were obtained using three different method. Other data fusion methods such as co-Kriging, Hierarchical Kriging (HK) and Improved Hierarchical Kriging (IHK) were compared with the 3LK method and Mean Absolute Error (MAE), Maximum Absolute Error (MaxAE) and Coefficient of Multiple Determination (R^2) were used for error measurement. Four data fusion methods were tried in the database where lift and drag coefficients will be generated and it was observed that the 3LK method gave the best result. In addition, when high fidelity data are added to increase the efficiency of the models, it is stated that co-Kriging and Kriging methods significantly reduce the error values and create data with high precision and accuracy. Kuya et al. [10] tried to explain a methodology to minimize the effects of systematic errors and to generate more accurate data by using co-Kriging and Response Surface Model (RSM) methods. The study investigates the performance of an inverted wing of a racing car in generating vortex under the ground effect. The low and high-fidelity data sources used for data fusion are CFD code and wind tunnel tests, respectively. According to the results of the test, Polynomial Response Surface model (PRSM) and co-Kriging method give close results but the error values is lower in co-Kriging method.

Han et al. [11] developed a new and practical co-Kriging method to be used in surrogate model-based aerodynamic analysis and optimization by making a new approach to the construction of the co-Kriging covariance matrix. They aimed to improve the prediction accuracy of the method by adding gradient information from data obtained from different data sources. They tried to create a general model using the aerodynamic force and moment coefficients of the RAE2822 airfoil and validate this model with their proposed method. In this test, a model was created using co-Kriging and VFM models. The data were accepted as low or high fidelity according to different element numbers in the Euler-DLR-TAU solver. In another test, different solvers were used for different data sources for the same airfoil. Euler solver was chosen for low fidelity data while RANS solver was used for high fidelity data. For the analysis results, the co-Kriging method gives more accurate results than the VFM method. A different study by Han et al. [12] proposes an alternative method for variable fidelity modeling. In this study, a co-Kriging method is used to combine high and

low fidelity surrogate models for aerodynamic data prediction. This study presents a new method to improve the use of surrogate models in aerodynamic design. A predictive model is created and drag polar and aerodynamic force and moment coefficients of the RAE2822 airfoil are obtained. In addition, The VFM method was used in a test case and the bridge function was used. In the single-parameter analytical example, high and low fidelity models were represented by different analytical equations. According to the results of the test case, the dataset generated with the VFM model showed more consistent results with less error values than the data obtained with the Kriging method only. In the second example, the aerodynamic data of the RAE2822 wing were modeled based on Euler and Navier-Stokes (NS). The data to be merged with the Co-Kriging method consists of two parameters, Mach number and angle of attack. It is planned to obtain drag, lift and moment coefficients as output values. In the analysis made as a result of data fusion, it was observed that the error values of the data produced by co-Kriging is very low. Another study by Han [13] proposes a new approach to improve the accuracy of variable-fidelity surrogate models. The proposed approach involves using a combination of gradient-enhanced Kriging (GEK) and a generalized hybrid bridge function (GHBF) to improve the fidelity of variable-fidelity models. The GEK method transfers the gradient information of high-fidelity data to the surrogate model, while the GHBF method combines high- and low-fidelity data using a weight function In the test, the derivation and combination of aerodynamic force and moment coefficients with respect to angle of attack variation is tested using the RAE2822 airfoil. Low-fidelity data were obtained from the Euler solver using the TLR TAU code and high-fidelity data were obtained from the RANS solver. The results show that using GEK and GHBF improves the accuracy of variable fidelity surrogate models significantly more than the traditional Kriging method. The precision value of the GEK method increases in proportion to the amount of data used. The GHBF method, which is used in multi-fidelity model building, produces efficient models with a low error values and a high precision value when the increment or scale function is used.

Rosenbaum and Schulz [14] presents a comparative analysis of various sampling strategies for building Kriging metamodels in aerodynamics. The authors suggest that accurate and efficient surrogate models can be developed using Kriging, a statistical technique used for interpolation and prediction of output data. The paper compares different sampling strategy for building Kriging metamodels. These are Kriging and Gradient-enhanced Kriging (GEK) methods. The authors evaluate the effectiveness of these methods using a dataset of

aerodynamic coefficients generated from computational fluid dynamics simulations. The model they use for their method is the RAE2822 airfoil. Using this airfoil, drag, lift and moment coefficients are obtained using with for two different input parameters which are Mach number and angle of attack. The data sources used are RANS-CFD for high-fidelity data and Euler-CFD for low-fidelity data. For each data source, an experimental design space consisting of 20, 30, 40 and 100 datasets were created using the Latin Hypercube sampling model (LHS) to obtain aerodynamic coefficient data at different angle of attack and Mach value ranges. Parussini et al. [15] propose a method called Gaussian Process Regression (GPR) to improve the prediction and efficiency of random fields by combining data from multiple sources with different degrees of fidelity. The author's proposed method is based on recursive Bayesian techniques and recursive co-Kriging. The proposed method can be used in model-based simulations for multi-fidelity data fusion. The multi-fidelity Gaussian process (MF-GP) approach uses a set of basis functions to capture correlations between low- and high-fidelity data and builds a joint model describing the correlation between the two data sources. The authors verify the performance of the MF-GP method through numerical experiments on the stochastic Burger equation and Rayleigh-Bénard convection test problems. The results show that the MF-GP method is more accurate and computationally efficient than the traditional GP regression approach when low-quality data are used and its number increases. In a study by Rohit and Ganguli [16], presented a method to perform uncertainty quantification (UQ) of beam vibration using both coarse and fine quality element meshes. The method is based on co-Kriging, a statistical interpolation technique used to estimate values at unobserved locations based on observations at other locations. A joint Kriging model is created that combines information from both sources to predict the response at new locations. The data sources used are the Spalart-Allmaras model and the k-ω Shear Stress Transport (k-ω SST) model with low and high-fidelity, respectively. The results show that the co-Kriging based multi-fidelity approach is able to accurately predict the data in addition to lower computational cost compared to using only fine mesh. Deng et al. [17] present a novel approach to multi-fidelity data fusion using gradient-enhanced Gaussian process regression. The authors describe a method for fusing data from multiple sources with different levels of fidelity and cost to create a more accurate model. The method is called Gradient-enhanced co-Kriging (GECK) and is referred to as a method that combines data from different sources and gradient information. The effectiveness of the proposed method is tested in several numerical experiments and an engineering case study. The engineering case study involves an analysis to predict the displacement of a structure under

external loads. In addition, the proposed method is found to have better accuracy when compared to GE-Kriging. In another comparison, GE co-Kriging method was found to be more accurate than the standard co-Kriging method. This study by Lin [18] proposes a model for combining data from different sources to improve prediction accuracy. The authors use Portion of Gradient Enhanced Multi-Fidelity Gaussian Process Regression (PGEMFGPR), a probabilistic model widely used in machine learning for regression tasks. In the engineering test case, the authors performed data fusion on the NACA 0012 airfoil using Gradient Enhanced Kriging (GEK), Gradient Enhanced Generalized Hybrid Bridge Function (GEGHBF), Gradient Enhanced Multi-Fidelity Gaussian Process (GEMFGP) and the proposed method and the result shows that although all four methods give very close results, the proposed method is the most efficient method by giving the best performance in three different error types. The results show that the proposed model outperforms the other models in terms of accuracy, especially when the input data is high dimensional and noisy.

Xiao [19] proposes an extended Co-Kriging interpolation method that allows the use of data with varying levels of fidelity. The proposed method is applied to a complex engineering problem involving the estimation of the output of the pressure field around an airfoil. When the airfoil problem is analyzed, data from three different fidelity data are used to obtain lift and drag coefficients. For comparison, when the lift and drag coefficients generated after combining data with two and three different fidelity data with the co-Kriging method are compared with the actual values, it is observed that the error value of the model using data with three different fidelity is lower. As a result, the proposed method was tested for all three test case and it was stated that the model using data with three different fidelities has a smaller error value compared to other models in the data obtained after data fusion. Zhang et al. [20] discussed the use of data fusion for multi-fidelity aerodynamic applications. The study uses data of four different fidelities. These are empirical methods, Vortex-Lattice method (VLM), Euler solver, RANS solver. To test their proposed method, the authors used the DC-1 airplane as a reference and found the aerodynamic force coefficients of the airplane. The test was performed between Mach number between 0,2 and 0,9 and angle of attack between -5 and 15 degrees. 20 low- fidelity and 6 high- fidelity test data and co-Kriging method were used for data fusion. The process was continued until the error value was below 10 percent. With each addition of high-fidelity data to the dataset, the error value decreased and the data fusion process became more efficient. In this work, Rumpfkeil [21] discusses techniques for building multi-fidelity surrogate models for aerodynamic

performance predictions. The method used in the study is Variable Fidelity Modeling (VFM). In this method, the increment function is used. The low and high-fidelity data sources used in the study are Euler-CFD and RANS-CFD solver, respectively. The authors used two analytical and one engineering example to test the proposed method. In the engineering example, the steady turbulent flow through the NACA 0012 airfoil is analyzed. As a result, the proposed method results in faster computations, reduced computational costs and increased accuracy. Moreover, multi-fidelity surrogate models are computationally more efficient while achieving the same accuracy as high-fidelity models. In this study by

Dong [22], he discusses a Kriging-based multi-fidelity data fusion approach. With this method, the author aims to model the relationships between dissimilar data and then use these models to predict missing data. The method proposed in the study involves combining models with multiple levels of fidelity using Kriging method. This method is intended to use lower fidelity models to improve the accuracy of higher fidelity models and to cover a larger design space. The effectiveness of the method is tested on an autonomous underwater vehicle hull stability analysis example and an analytical problem. The results show that the proposed multi-fidelity level data fusion method performs better than single-fidelity level models. Zhou et al. [23] proposed a new approach to combine data from multiple sources with different levels of fidelity. The authors propose the use of a generalized hierarchical co-Kriging model to combine data from high and low-fidelity sources. The authors prepared analytical and engineering test cases to evaluate the effectiveness of the proposed approach. As an engineering example, the lift coefficient of the NACA 0012 airfoil was estimated. In the engineering example, HF Kriging (only high-fidelity sampling Kriging), hybrid Kriging-scaling (HKS), hierarchical Kriging (HK), Kennedy and Hogan (KOH) and generalized hierarchical co-Kriging (GCK) methods were used and compared. CFD data of two different fidelity levels were used in this test. The Euler model was chosen for low-fidelity data and the RANS model was chosen for high-fidelity data. The results show that using the generalized hierarchical co-Kriging (GCK) model provides more accurate predictions than traditional Kriging and other data fusion methods. Anhichem et al. [24] discuss the application of multi-directional data fusion to airplane wing pressure distributions. The authors used a Gaussian Process Regression approach with a weight function to model the pressure distribution at different points on the wing surface. The data sources used in the study which were Pressure Tap Point, dynamic pressure-sensitive paint (DPSP), RANS, XFLR5. The model used in the study is the RBC12 semi-wing-fuselage model and the model

used in the study was tested as a 1/17,5 scale scaled downsized model. The authors conclude that multi-directional data fusion has the potential to considerably increase aircraft design and analysis efficiency and accuracy.

Feldstein [25] presents a method for multidisciplinary analysis of blended-wing-body (BWB) structures using data fusion with multiple sources with different levels of fidelity. Gaussian Process Regression (GPR) method is used for this purpose. The method also considers the data uncertainty between data sources and ensures that the combined data is statistically appropriate. In this study, data improvement analysis is performed on the stability and control analysis of the BWB model under different flight conditions. The data sources used for this study are wind tunnel tests, CFD analyses and Vortex-Lattice method in order of high to low-fidelity. It is aimed to obtain lift, drag and moment coefficients from these control surfaces. The uncertainty values of the data obtained using the data fusion method with GPR are less than the data obtained from the wind tunnel alone, RANS, Euler, and other low fidelity methods, according to the study conducted with output values from three different data sources. Mukhopadhaya [26] discusses the development of a methodology for creating aerodynamic databases for use in aerospace engineering applications. The methodology involves the use of multi-fidelity modeling techniques that combine data from multiple sources to create a more accurate and reliable model. The methodology proposed by the authors is referred to as Gaussian Process Regression (GPR). With this method, a new system has been created for the development of multi-fidelity modeling techniques and the elimination of uncertainties in CFD calculations. The study states that the databases will be created using three differently fidelity data sources: computational fluid dynamics simulations (CFD), Vortex-Lattice models and wind tunnel experimental data. The three different databases were used to create all configurations for the NASA CRM model. First, a single data source was used, then the number of data sources was increased to estimate the aerodynamic force coefficients varying with the angle of attack. In order to test the effect of varying the number of high-fidelity data on the model, the authors tested the error relationship of the number of high-fidelity data and concluded that increasing the number of high-fidelity data makes the model more efficient and reliable for all aerodynamic coefficients. Furthermore, the authors mentioned that the databases acquired through the suggested approach have applications in the aerospace industry, including shorter design cycle times, higher dependability, and lower costs. Perdikaris [27] presented a work that proposes new algorithms for combining information from multiple

sources to build accurate models that are efficient in terms of data requirements. The focus of the work is on multi-fidelity modeling, which refers to the use of data from multiple sources and multiple levels of fidelity to build a more accurate modelThree different methods were used in the study. These are Gaussian Process Regression (GPR), Multi-fidelity modeling with recursive Gaussian processes (NARGP) and Nonlinear information fusion algorithms (AR1). The methods proposed by the authors were tested with three analytical and engineering test cases. This engineering example is based on numerical simulations to generate a response surface modeling of the Nusselt number value of the flow through a cylinder. Since the Nusselt number is a function of Reynolds (Re), Richardson (Ri) and convection angle φ, tests were performed at different Re, Ri and φ angles. Low-fidelity data were obtained from empirical models and high-fidelity data were obtained from the Navier-Stokes equation. When the data fusion process was tested using three methods, it was discovered that the NARGP method overlapped with the real data to a large extent, the GP method overlapped with the real data but had a lower correlation value than NARGP, and the AR1 method had a high correlation value but a higher error value. Tang et al. [28] present an approach for investigating the design space of high-speed civil transportation using aerodynamic response surface approximations (RSM) in this paper. The authors suggest a method for predicting the aerodynamic response of an aircraft to changes in design variables such as wing form, engine placement, and fuselage geometry using Response Surface Modeling (RSM). The resulting data is used to create aerodynamic response surface models as a function of the design variables. The response surface models are then used to perform optimization studies to find the optimal design that meets the performance requirements. In this study, Variable Complexity Modeling method is used with scale function to combine data from high and low-fidelity data sources. In order to compare the VCM method in the study, it was compared with response surface models designed to be optimum according to drag force and range. The results showed that RS models are effective and fast in creating design space. The model using RSM is successful in reducing the noise effect and saves up to 5 processor hours compared to the VCM method.

In this study, Ghoreyshi et al. [29] evaluate the combination of data from low-fidelity aircraft aerodynamic models with high-fidelity computational fluid dynamics results to create aerodynamic models for flight dynamics analysis. The methods used to obtain low-fidelity data were two different Vortex-Lattice codes and DATCOM data. The codes used in the Vortex-Lattice method, which is selected as low-fidelity, is Tornado code. The aircraft

model to be used in the study is a general-purpose UAV and Euler and RANS simulations are used as high-fidelity data sources. The fusion of low-fidelity data with high-fidelity CFD data resulted in improved and efficient predictions of aerodynamic forces and moments at a reasonable computational cost. The data fusion method used in the study is Variable Fidelity Modeling, where the increment function is used to fuse the data. In the example problem, one (angle of attack) and three (angle of attack, Mach number, side slip angle) aerodynamic parameter variables were used separately to test the efficiency and accuracy of the data fusion process. In the data fusion process with a single parameter variable, using DATCOM and RANS-CFD data, and it was noted that the accuracy and reliability of the data set increased with the increase in the number of high-fidelity data. The results were also found to be effective when data fusion was performed with VLM code and RANS-CFD. In this work, Nguyen [30] presents a new approach to design unmanned combat aerial vehicles (UCAV) using models of different fidelity. The authors propose the use of a Variable Complexity Modelling (VCM) to combine different data sources and optimize the design of the UCAV system. In this way, they suggest that task and weight analyses can be performed using more accurate data. The authors conducted several tests to evaluate the effectiveness of the proposed approach. The high-fidelity data source required for model testing was selected as CFD-RANS and the Euler-CFD solver was selected as the low-fidelity data source. A new data set was obtained by using these data with the VCM method. The obtained data were tested as a function of the weight factor as a function of the take-off weight of the airplane and the results showed that the data generated by the VCM method were close to the reality, highly accurate and reliable. The results show that the use of multi-fidelity models can lead to more accurate and efficient UCAV designs compared to traditional single-fidelity models. This study presents an efficient approach for designing UCAV systems using multi-fidelity models. In a different study, Nguyen et al. [31] propose a new approach to multidisciplinary aircraft conceptual design. Traditional techniques entail employing a fixed complexity model, which is inflexible enough to account for changes in design parameters and requirements. The authors propose a modified Variable Complexity Modeling (mVCM) - which is more efficient and accurate. Aircraft Design Synthesis program was used for low-fidelity data and AADL3D-CFD code was used for high-fidelity data. In the test results, it was observed that the three functions in the data fusion process made with the VCM method did not approach with high-fidelity data. When the three functions were compared with the mVCM method, it was observed that the scaling and hybrid functions agreed with the high-fidelity data. In the comparison of aerodynamic force

coefficients on the wing, the CFD method was first compared with low fidelity data and then with mVCM. The result showed that the MVCM method has less error value than the low-fidelity data. They compared their proposed approach to the traditional constant complexity approach and found that their approach is more efficient and accurate. Zastawny [32] introduced the use of variable-fidelity modeling in modern aircraft design. The paper describes the concept of Variable-Fidelity Modeling (VFM) and its applications in aircraft design. In the study, the low-fidelity data source (Bhatnagar-Gross-Krook) is obtained in the inviscid solution using the BGK code and the high-fidelity data source is obtained in the inviscid with coupled boundary layer solution. The model used in the test is the NACA 632-215 airfoil in two dimensions. The performance of the VFM model was measured by increasing the number of high-fidelity data. The Viscous Full-Potential method was determined as low-fidelity and TAU simulations were determined as high-fidelity, and it was concluded that if only high-fidelity data was used. As a result, it was observed that the VFM method is an effective and efficient method for creating databases and its accuracy gradually increases as the number of high-fidelity data used increases.

Tyan et al. [33] propose an approach to optimize airfoil design by using models of varying fidelity levels. For this purpose, models with different fidelity levels are used to explore the design space. Then, with the help of Radial Basis Function Networks-Radial Basis Function network (RBFn), these models are combined using Global Variable Fidelity Modeling GVFM. This approach is beneficial in that models at lower fidelity levels provide data for models at higher fidelity levels and also allow for a wider range of design space to be covered. The method to be used for data fusion is Global Variable Fidelity Modeling (GVFM), which, like the VCM method, uses low-fidelity data and aims to obtain high-fidelity data with the help of a scaling function. The proposed method is tested separately for one analytical and two engineering problems. The common analytical problem used in previous studies was also tested here and very similar results were obtained. The other test is about the transonic flow analysis of the RAE2822 airfoil. In the transonic pressure coefficients contouring process performed by optimizing the RAE2822 airfoil using the GFVFM method, it is observed that the pressure distribution on the airfoil is more regular and the shock formation is closer to the edge of attack. As a result, GVFM, as an improved version of the existing VCM method, was found to converge to high-fidelity data faster and using less data than VGFM. Belyaev et al. [34] investigate the method of surrogate model building using data fusion instead of using completely factorial design in spacecraft

aerodynamics problems. In the study, fused assumption, local fidelity solution method and fused solution assumption technique are used. The data sources to be used for data fusion in the study are wind tunnel tests for high-fidelity and CFD code (Euler, RANS) for low fidelity data respectively. The study aims to create a meta-model and automatically interpolate multidimensional data. In the results, it was observed that the data generated with the local-fidelity method had a large amount of uncertainty in the design space where high-fidelity data were missing and the data were inconsistent and unreliable. In the data fusion process with the merged solution method, efficient approaches with high-fidelity were made. In the solution with the fused assumption, the results are stated as the most reliable. Gomec et al. [35] conducted a research that proposed a new approach to improve the aerodynamic performance of aircraft. The authors propose the use of neural networks and genetic algorithms to optimize the aerodynamic database of the aircraft. The proposed approach involves training neural networks to estimate the aerodynamic coefficients of the aircraft based on input parameters such as angle of attack, flow rate and other relevant variables. The neural network models are then integrated with genetic algorithms to optimize the database by iteratively improving the prediction accuracy of the neural network. The authors conducted several tests to evaluate the effectiveness of the proposed approach. In these tests, a simple 1^{st} and 2^{nd} order polynomial curve fitting technique is compared with the proposed method. The results show that the use of neural networks and genetic algorithms significantly improves the accuracy of the aerodynamic database and the aircraft has better aerodynamic performance. In addition, it is stated that with the Neural Network Genetic Algorithm (NNGA), fifty percent less CFD analysis is needed. As a result, this study presents a promising approach to improve the aerodynamic performance of aircraft using advanced machine learning techniques. Kurt et al. [36] describe the implementation of an aerodynamic database simulation using neural networks and genetic algorithms. The goal of the simulation is to estimate the aerodynamic forces acting on an airplane based on design parameters. The authors used neural networks to model the complex relationships between the design parameters and the resulting aerodynamic forces. They also use a genetic algorithm to optimize the parameters of the neural network model. The authors demonstrate the effectiveness of their proposed approach by applying it to a simplified aerodynamic simulation problem. They compare the performance of their neural network model with that of a conventional computational fluid dynamics (CFD) model and show that the neural network model can achieve similar fidelity levels with significantly reduced computational cost. This study demonstrates the potential of using neural networks and genetic algorithms

to create accurate and computationally efficient aerodynamic simulations. The authors optimized the parameters of the neural network model using genetic algorithms to create a simulation that is both accurate and efficient.

Wang et al. [37] propose a multi-model fusion method for the optimization of high aspect ratio wings in air vehicles. The optimization process involves the use of a genetic algorithm to optimize the wing design parameters while simultaneously considering the structural integrity and aerodynamic performance of the wing. Structural integrity is evaluated using a finite element analysis (FEA) model, while aerodynamic performance is evaluated using a computational fluid dynamics (CFD) model. The low and high-fidelity data to be used in the analyses were determined using Sparat-Allmaras (SA) and Navier-Stokes (NS) models with different grid numbers. In the test, a three-dimensional wing model based on the $NACA64_a816$ airfoil is used to obtain the lift and drag coefficients and L/D ratio. The proposed method is applied to the optimization of a high aspect ratio wing for a small unmanned aerial vehicle (UAV). The results show that the multi-model fusion method can effectively improve the performance of the wing compared to using a single simulation model. In addition, the genetic algorithm is shown to be an effective method to optimize the wing design parameters. As a result, this study demonstrates the effectiveness of the proposed multi-model fusion method to optimize the design of high aspect ratio wings in air vehicles. Tao and Sun [38] propose a deep-belief network (DBN) based model to improve the efficiency and accuracy of aerodynamic design optimization. The authors propose to use a surrogate model based on deep learning that can predict the performance of a design at a low computational cost. The proposed approach is demonstrated on a complex aircraft design optimization problem where the objective is to maximize the lift and minimize the drag of the aircraft. In this design problem, reliable aerodynamic design optimization is performed for the wing and airfoil under Mach number uncertainty. The airfoil used is RAE2822 and the wing model is DLR-F6. The authors compare the performance of the deep learning-based surrogate model with the performance of conventional surrogate models and show that the deep learning-based model outperforms the standard model in terms of both accuracy and computational efficiency. Renganathan et al. [39] present a Bayesian inference for combining data from multiple sources with varying levels of fidelity. This method aims to improve the accuracy and reliability of predictions by integrating data from different sources. The weights of each source are estimated using a maximum likelihood approach or a Bayesian approach, depending on the availability of data. The authors demonstrate the

effectiveness of their method by performing two case studies. These are the RAE2822 airfoil in transonic flow and the Common Research Model (CRM) model. The data sources used in the test are wind tunnels with noisy and incomplete data for high-fidelity datas and deterministic but biased numerical simulations for low-fidelity datas. The output parameter to be obtained in the test is the pressure coefficient distributions over the wing section. The results show that the method can provide more accurate predictions than a single data source and that the proposed method can quantify the uncertainty in the predictions. The author has presented a useful method for combining data from multiple sources to improve the accuracy and reliability of predictions. Kou and Zhang [40] propose a computational approach that combines Variable Complexity Modeling (VCM) to obtain accurate and efficient predictions of aerodynamic forces on airfoils. The study involves combining low-fidelity and high-fidelity models to predict nonlinear and unsteady effects arising in aerodynamic flows. The authors demonstrate the effectiveness of their method on an unsteady moving two-dimensional airfoil. The results show that the multi-fidelity modeling can provide accurate and efficient predictions of aerodynamic forces. The study states that this method can be used to obtain more accurate and efficient estimates and the multi- fidelity modeling framework for nonlinear unsteady aerodynamics of airfoils provides a useful tool for predicting aerodynamic forces. Chen et al. [41] conducted a study to fuse data from multiple sources with different fidelity levels using convolutional neural networks (CNN). The authors present a multi-fidelity data fusion study using Convolutional Neural Networks (MFDA-CNN), which involves training multiple CNN's over different fidelity levels of the data and then using a fusion network to fusion the outputs of the CNN's. The results show that MFDA-CNN outperforms other methods, including those using only a single fidelity level or simpler fusion techniques. Through testing, MFDA-CNN is a usable approach for integrating data from multiple sources at different levels of fidelity and can be applied to a wide range of machine learning tasks.

2.2. Computational Fluid Dynamics Simulations

Berg et al. [42] investigated various flow conditions on an F-16-like model built by NLR. These flow conditions include various performance factors including engine power settings. The research was carried out by performing a calculation based on the Euler equation. The results show that the calculation method captures the main features of the flow, such as the vortices at the strake and wing tip and the complex shock structure on the wing, quite well.

Comparison of the calculated and measured pressure distributions shows that the accuracy of the results is satisfactory. However, small differences were observed due to the absence of viscous terms in the Euler method. It is suggested that a method based on the Navier-Stokes equations should be used to investigate these viscous effects. Rizzi and Luckring [43] wanted to obtain wing pressure values under two different flow conditions using CFD method to compare and validate the F-16XL fighter jet model. These two different flow conditions are high angle of attack at low speed and low angle of attack in transonic flow. Hybrid RANS, URANS models were used as turbulence modeling. The results show that in low speed high angle of attack flight, the leading-edge vortex effects on the wing pressures are inaccurate by about 15-25%. Also, in transonic low angle of attack flight, the pressure predictions were generally in good agreement with flight test results. However, there were significant differences in some pressure distributions on the undersurface of the fuselage and on the undersurface of the wings. In the study by Akgun et al. [44] the drag effects of the fuselage, wing and tail of the F-16 fighter aircraft model were investigated. Ansys Fluent CFD method was used to analyze the model used. For each sub-part of the model, analyses were performed in subsonic, transonic and supersonic regimes at different Mach numbers. Friction due to pressure and drag due to viscous effect are shown for the fuselage, wing and tail parts of the airplane. The results show that the fuselage is the part that produces the most drag in supersonic and subsonic flows, and that the drag due to viscous effects in subsonic flows and pressure drag in supersonic flows are more effective. Kodavanla et al. [45] tested the F-16 fighter jet model at different Mach numbers (Mach 0,6 and 1,2) and investigated the flow dynamics in the study. CFD method was used to explain the performance parameters of the model. For the turbulence model, k-ε model (Realizable) and k-w SST models were used. The solver was chosen as "density-based" since the simulation is fully compressible flow. Pressure, drag force and buoyancy were calculated in the CFD study. The relationship between velocity and pressure was investigated by adjusting the angle of attack to increase by 5 degrees between 0 and 15 degrees. As a result, it is stated that the mesh quality used in the F-16 fighter jet has a key role for the accuracy of the results, static, dynamic pressures and aerodynamic forces were obtained from the CFD study and the pressure temperature and velocity variations on the model surface were analyzed and compared with reference data.

In this study, Sharma et al. [46] investigated viscous, incompressible and steady flow on F-16 aircraft using computer modeling techniques and compared the modeled results with

experimental results using a wind tunnel. The study developed a computational model of the F-16 and then created a finite computational domain. Aerodynamic coefficients such as pressure coefficient, lift coefficient, drag coefficient were obtained by applying certain boundary conditions by flying the aircraft at Mach 2 and at 50 000 feet above sea level and the results were compared with experimental results. In the study by Matak et al. [47] the aerodynamic properties of NACA 64_a-204, the airfoil of the F-16 fighter jet, were evaluated by numerical analysis of compressible and turbulent flow at high Mach number using CFD. Ansys Fluent CFD method was used in the study and the results were generated with RANS, k-w SST turbulence models. The aerodynamic properties of geometries with varying geometries were analyzed. Separate wing configurations were created for subsonic and supersonic flows. Lift, drag coefficients and C_L/C_D coefficient were obtained by using varying turbulence models at angles of attack ranging from 0 to 12 degrees. As a result, it is seen that at certain angles of attack, the C_L/C_D value of configuration 0 (subsonic flow) is better than configuration 1 (supersonic flow), and as the angle of attack increases, the drag and lift coefficient values of the subsonic configuration are better than configuration 1.

Peiris et al. [48] evaluated the aerodynamic behavior of the F-16 aircraft by performing Computational Fluid Dynamics (CFD) analyses. CFD simulations were performed in both subsonic and supersonic flight regimes. To validate the results, CFD analyses were performed with two different turbulence models. A full scale CATIA solid model of the F-16 aircraft was used to create a computational mesh and then CFD simulations were performed mainly with Fluent ANSYS. The aerodynamic characteristics of the F-16 were estimated in terms of lift coefficient and drag coefficient for angles of attack between 0° and 40°. When comparing CFD predictions between turbulence models, the formation of two large leading-edge vortices at Mach number 0,6 was observed on the main wings. At supersonic speed, we analyzed the formation of shock waves and expansion fans around the aircraft by studying the static pressure change. To further investigate the flow over the main wings, the surface static pressure variation and pressure coefficient variation at different span positions were also studied. Kostić, Bengin, Rašuo [49] develop a unique numerical approach for obtaining the fundamental aerodynamic characteristics of an aircraft and to enable the method's extensive use in the analysis of some aerodynamic characteristics of an aircraft without the need of empirical methods in this study. The AGARD-B model was tested in the T-38 trisonic wind tunnel. The size of the model was chosen according to the test area of the tunnel, with a length of 0.98 m and a diameter of 0,115 m. The lift, drag and

moment coefficients were obtained to compare the CFD data of the same model in the wind tunnel. The wind tunnel which can reach Mach 0,6; 0,8 and 1,6. On the CFD side, tests were performed at the same Mach numbers at -4- and 12-degrees angles of attack with different mesh configurations. The k-ε SST turbulence model was used in the tests. In this comparison, it is observed that the aerodynamic coefficients generated by the numerically and experimentally tested model are in great agreement. Huband et al. [50] tested the F-16A fighter jet in a transonic flow field at average angles of incidence using the Navier-Stokes equations. In their numerical study, they tested the F-16A fighter jet at Mach 0,85- and 16-degrees angle of attack to obtain lift and drag coefficients from their tests. It is stated that the numerical test data obtained matches the experimental results and the drag coefficient exceeds the experimental data by 8 percent. At the same time, the lift coefficient from the calculated pressure distributions were similar to the wind tunnel data.

Ramli et al. [51] stated that owls fly silently and this ability significantly reduces noise pollution. In his study, authors investigated the noise reduction ability of the NACA0012 wing by serrating it from the front, back and both sides. In addition, the effect on the drag and lift coefficients of the wing was observed. The test was carried out in a wind tunnel using two different Reynolds values (20 000 and 40 000) at angles of attack of 2 and 30 degrees. In the results, it was observed that both models (normal and serrated) gave similar results at the first Reynold value. When the Reynold value was changed, it was stated that there was a large increase in the lift coefficient and the lowest drag coefficient was observed in the model with serrated trailing edge. The study by Pandya, Sreevanshu et al. [52] states that the design, development and production of radio-controlled air vehicles has recently gained importance. The authors discuss the design methodology, material selection, measurement techniques as well as aerodynamic characteristics obtained from wind tunnel tests and numerical simulations. In the study, a scaled-down radio-controlled model was placed in a low-speed wind tunnel and dynamic pressure measurements were made at speeds of 19 m/s and 25 m/s at angles of attack of -5 and 35 degrees. Aerodynamic measurements were made by measuring 6 components using a load-cell. Numerical simulations were performed using the Spalart-Allmaras turbulence model in ANSYS Fluent program. When the lift and drag coefficient data from the wind tunnel and CFD tests were analyzed, it was determined that the CFD data were compatible with the wind tunnel data. Kai et al. [53] conducted low-speed wind tunnel tests of a 3D printed morphing wing structure. It was stated that morphing wings were chosen because of their important contributions to fuel technology

and environmentalism. Two different wing models were chosen for wind tunnel tests. These are NACA0012 and NACA0024 respectively. It was decided to take data with a 6-axis force sensor in the wind tunnel with 600x600mm test area dimensions. The flow in the wind tunnel was set to 10m/s and data was taken between -30 to +30 degrees angle of attack. In the measurements, it was observed that the wing model with morphing structure produced higher lift coefficient at the same angles of attack compared to the rigid wing model. In addition, it was observed that the stall angle of the morphing wing structure increased and the lift coefficient of the morphing structure did not decrease suddenly after the reaching stall angle. In the study by Jun et al. [54] CFD calculations of NACA23012 airfoils in rime and glaze icing conditions were performed in three-dimension wing. These tests were carried out in the Icing Research Tunnel. Data on surface points were collected with a 3D laser scanner and these data points were converted into grids with Geomagic software. It was made suitable for numerical calculation using the Pointwise program. RANS, URANS turbulence models were used in the numerical study. In the test performed at Mach 0.10 and 0.18 at angles of attack of -9 and 18 degrees, the angle of attack was limited to between 0 and 10 degrees for the wind tunnel. The data obtained from the wind tunnel and CFD tests were converted into pressure coefficient and calculated along the chord. In the comparison, it was stated that there was a very close correlation between the experimental and numerical results in the Rime Ice geometry, but it was added that there were some differences in the results on the lower surface of the wing. As a result of this differences, the lift coefficient deviated from the experimental data. In the Glaze Ice geometry study, large differences were observed between the experimental and numerical results and it was stated that these differences may be due to the flow separation around the horn. Vadake et al. [55] analyzed the ClarkY-14 airfoil at different angles of attack in turbulent flow condition. Numerical analyses were performed in the STAR-CCM+ program and experimental tests were performed in the AEROLAB Educational Wind Tunnel. Numerical analyses were performed using the k-w SST turbulence model. The airfoil was tested at angles of attack of -4 to 12 degrees at speeds of 80, 100 and 120 mph respectively. Numerical analyses were performed with and without the balance sensor. According to the results, the CFD results match the wind tunnel test results closely. The presence of the balance sensor does not disturb the flow on the wing and does not affect the test results.

3. MATERIAL AND METHODS

In this thesis, different data fusion methods are applied using aerodynamic data. Data fusion makes it feasible to obtain a single data set using data from two or more different data sources. Here, the two different data sources represent high and low-fidelity data sources. Low-fidelity data is easy to access and produce and can be produced quickly, while high-fidelity data requires more time and processing power. The aim of data fusion methods is to obtain new high-fidelity data by using low-fidelity data together with low-fidelity data, which requires less time and cost, since using only high-fidelity data in data set production is costly in terms of time and labor. For this purpose, different data fusion methods such as co-Kriging, Gaussian Process Regression, Kriging, RBF have been used in previous academic studies. In this thesis, these methods will be used separately on aerodynamic data to perform data fusion and the efficiency of the methods will be discussed. In the study, aerodynamic data will be obtained through computational fluid dynamics simulations and experimental methods such as wind tunnel testing. In the data to be obtained, data fusion methods will be applied so that the data from the wind tunnel will be less than the data from the computational fluid dynamics simulations.

Numerical and experimental methods will be used to obtain the aerodynamic data to be used in the study. In order to obtain numerical and experimental data, an aircraft model is needed. It was decided that this model would be a fighter jet model. Since the model should have the same dimensions for aerodynamic analysis, the model was adjusted to have a blockage value of 1 percent with respect to the test chamber of the wind tunnel. [56] The fighter model was taken from VSPHangar, the digital library of the OpenVSP program.

3.1. OpenVSP Software and Data Acquisition Process for Low-Fidelity Model

The fighter jet model was opened in OpenVSP version 3.35.3 and the structural features of the model were examined and the necessary changes were made. In these changes, the main wing airfoil shape was replaced with the NACA 64A-204 wing profile used in the generic fighter jet. The horizontal wing airfoil shape was also replaced with the NACA 64A-204 airfoil like the main airfoil. Since the data to be obtained should be consistent, the dimensions of the model were adjusted so that the blockage value was 1 percent according to the wind tunnel. The newly created fighter model with the modified airfoil was analyzed aerodynamically using the VSPAero add-on in the OpenVSP program.

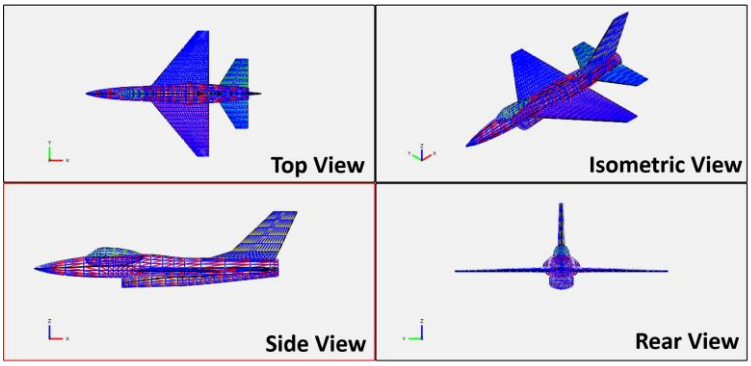

Figure 3.1. View of generic fighter jet model from different angles in OpenVSP program

The angle of attack limits of the motion mechanism used in the model wind tunnel are limited between -15 to +15 degrees. In order for the tests to be compatible with each other, the test range was set between -15 to +15 angle of attack. The maximum speed of the wind tunnel to be used is 30 m/s and the Reynolds value corresponding to 30 m/s in the analysis to be performed is calculated as in the equation shown in Eq. 3.1. In the calculation, the Reynolds value was calculated as approximately 310 000 for the fighter jet model and 1 485 000 for the wind tunnel test room.

$$Re = \frac{\rho * V * L}{\mu} = \upsilon * V * L \tag{3.1}$$

Table 3.1. Aerodynamic parameters calculation for Reynolds Number

Parameters	**Values**
Model Length	167,11 mm
Wind Tunnel Test Room Length	800 mm
Velocity	30 m/s
Density	1,082 kg/m^3 (@1285m)
Dynamic Viscosity	1,75E-5 Pa.s
Reynolds Number (for aircraft)	309 965
Reynolds Number (for wind tunnel wall)	1 485 257

The VSPAero plugin contains two different solvers. These are Vortex-Lattice Method and Panel Method. [57] Both solvers are based on the full potential equation and can be used for twisting and deflection of wing models. However, Vortex-Lattice Method gives more efficient results for thin airfoil theory modeling while Panel Method gives more accurate results for thick wings.

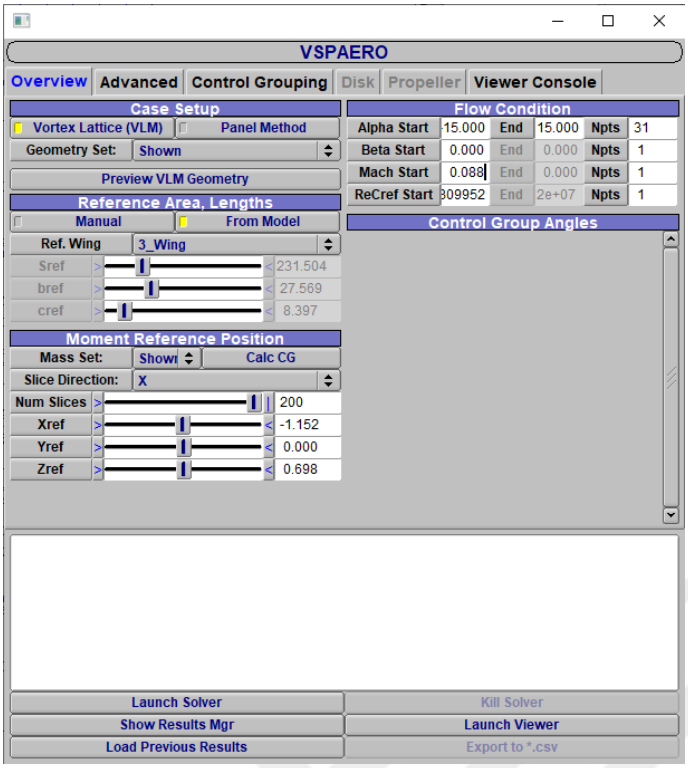

Figure 3.2. VSPAero add-on and interface for current test case

Since the wingspan of the model is not infinitely long and the wing thickness does not infinitely small, it was decided not to use the Vortex-Lattice method based on the thin airfoil theory. The Vortex Lattice Method will be used instead. In the aerodynamic analysis; lift, drag and moment coefficients of the model were obtained. These aerodynamic coefficients will be compared with data from other sources and will enter the data fusion process.

3.2. Computational Fluid Dynamics Software and Data Acquisition Process for High-Fidelity Model

The model of the .vsp plugin via OpenVSP was converted to solid modeling format such as STEP or IGS using the “Trimmed Surface” command in the program. The solid model was opened using the Solidworks software and checked for distortion on the model surface. After the check, the model was cut from the symmetry plane in order to finish the CFD results faster and to save processing power. The half model was converted to Parasolid (x_t) format for import into ANSYS Fluent. From the "Geometry" tab in ANSYS Fluent, the model was set to the desired angles of attack and ready for CFD tests.

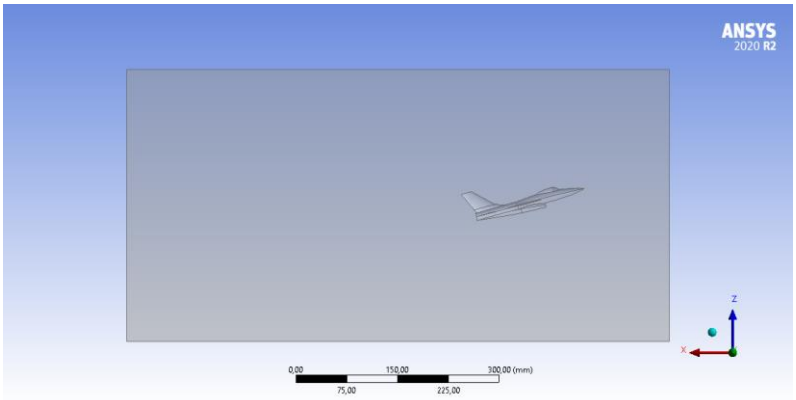

Figure 3.3. Preparation of generic fighter aircraft model for cfd simulation test at positive 15 degrees angle of attack

In order for the generic fighter jet model to give a good result in computational fluid dynamics simulations, the boundary conditions, the solver model to be used, the outputs to be obtained and the reference parameters were determined. Accordingly, in the computational fluid dynamics simulation to be used, data were taken at odd numbered angles of attack in positive and negative directions starting from 0 degrees in the range of -15 degrees to +15 degrees angle of attack. Since the maximum speed that the wind tunnel can reach is 30 m/s, the speed of the flow coming from the inlet section is set to 30 m/s. Some parameters of the wind tunnel were taken as reference for obtaining a high accuracy data set. Examples are the maximum speed of the wind tunnel of 30 m/s and the size of the test chamber chosen as the domain for the CFD simulation. The angle of attack between -15 and 15 degrees is the limit of the load cell. The k-ω SST turbulence model was used to better visualize the effects on the wings of the model and the boundary effects in the test chamber. The test case is matched with the wind tunnel in one-to-one scale and the model is positioned in the test chamber according to the location of the string of the wind tunnel. In the CFD study, tetrahedron mesh was selected and applied from tetrahedron and hexahedron mesh types. The main reason for choosing tetrahedron mesh in this study is that it is more adaptive and effective in complex geometries such as the generic jet aircraft geometry used in this study. [61] For the same geometry, tetrahedron mesh contains more elements than hexahedron mesh and the computational cost increases. However, tetrahedron mesh has better accuracy in complex geometries. Many calculations were made while meshing the model. First of all, it was decided that the dimensionless parameter y+ of the model home test chamber walls should be 1 or close to 1. The y+ parameter characterizes the thinness or thickness of the boundary layer. Low or extremely high values of y+ affect the accuracy of the results. Eq. 3.2 shows the equation for y+ and its parameters.

$$y^+ = \frac{\rho * V_x * y}{\mu} \tag{3.2}$$

Here ρ represents the density of the fluid, V_x the velocity of the fluid, y the distance in the boundary layer and μ the dynamic viscosity of the fluid. τ_w and C_f represent wall shear stress and skin friction coefficient respectively.

$$u_t = \sqrt{\frac{\tau_w}{\rho}} \tag{3.3}$$

$$\tau_{w=\frac{1}{2}} * C_f * \rho * U_\infty^2 \tag{3.4}$$

$$C_f = \frac{0{,}0026}{Re^{\frac{1}{7}}} \tag{3.5}$$

[58] In order to find the first layer thickness of the model, the Reynolds (Eq. 3.1), y+ formula (Eq. 3.2) friction velocity formula (Eq. 3.3), wall shear stress formula (Eq. 3.4) and skin friction coefficient (Eq. 3.5) values must be found. The first layer thickness equation is shown in (Eq. 3.6).

$$\Delta s = \frac{y^+ * \mu}{u_t * \rho} \tag{3.6}$$

Table 3.2. Parameters and values required for first layer thickness calculation for generic fighter aircraft in CFD calculations

Parameters	**Values**
Density	1,082 (@1285m)
Dynamic Viscosity	1,75E-5 Pa.s
Reynolds Number (for aircraft)	309 965
Velocity	30 m/s
Skin Friction Coefficient	0,000427
Wall Shear Stress	0,207941
Friction Velocity	0,438385
y^+ Value	1,0
First layer thickness (for aircraft zone)	0,00001167 m = 0,0116 mm

Table 3.3. Parameters and values required for first layer thickness calculation for wind tunnel test room in CFD calculations

Parameters	**Values**
Density	1,082 (@1285m)
Dynamic Viscosity	1,75E-5 Pa.s
Reynolds Number (for wind tunnel wall)	1 485 257
Skin Friction Coefficient	0,000341
Wall Shear Stress	0,166236
Friction Velocity	0.391967
y^+ Value	1,0
First layer thickness (for wind tunnel zone)	0,0000130 m = 0,013 mm

Knowing the Reynolds value helps us to know whether the flow is in a laminar or turbulent state. Knowing the type of flow makes it easy to know the thickness of the boundary layer formed by the flow passing over the model. [59] Flows up to 2320 Reynolds are considered laminar, flows between 2320-4000 Reynolds are considered transitional and flows above 4000 Reynolds are considered turbulent. In this case, the generic aircraft test case is a turbulent flow. The type of flow and the length of the model play a role in determining the thickness of the boundary layer. The following table shows the boundary layer thickness according to the Reynolds value.

Table 3.4. Calculation of boundary layer thickness values corresponding to different Reynolds Number values

Flow Type	Reynolds Number Range	Boundary Layer Thickness
Laminar	Re<2320	$\delta = \frac{4{,}91 * x}{\sqrt{Re}}$
Turbulent	$5*10^5<Re<5*10^7$	$\delta = \frac{0{,}368 * x}{Re^{\frac{1}{5}}}$
Turbulent	$1{,}8*10^5<Re<4{,}5*10^7$	$\delta = \frac{0{,}252 * x}{Re^{\frac{1}{6}}}$
Turbulent	$2{,}9*10^5<Re<5*10^8$	$\delta = \frac{0{,}201 * x}{Re^{\frac{1}{7}}}$

Since generic jet aircraft model and wind tunnel test chamber have turbulent Reynolds number, the boundary layer thickness of the generic jet aircraft model is calculated as 4,904 mm and the boundary layer thickness of the wind tunnel test chamber is calculated as 17,162 mm. When the default "Growth Rate" ratio is left as 1,2 in the "Inflation" command in the ANSYS Fluent program, 25 layers are required for the generic fighter jet model and 31 layers

for the wind tunnel test chamber. The closer the Aspect Ratio (AR) ratio is to 1, the better the accuracy of the results. However, aspect ratio values up to 100 are acceptable. [60] In terms of convergence, since high aspect ratio causes flux imbalance and divergence, it is stated that the results will be good up to a maximum value of 40. In the CFD study, the aspect ratio values were set to 20, 25, 30, 35 and 40 respectively, and the mesh was discarded and test cases with 22,6 million, 16,8 million, 13,3 million, 10,8 million and 9,2 million elements were created, respectively.

Table 3.5. Parameters to use for mesh dependency in computational fluid dynamics simulations

Aspect Ratio	Element Size (mm)		Number of Elements
	aircraft	wall	
40	0,48	0,532	9,2 million
35	0,42	0,4655	10,8 million
30	0,36	0,399	13,3 million
25	0,3	0,3325	16,8 million
20	0,24	0,266	22,6 million

Increasing or decreasing the number of elements in CFD simulations will change the accuracy of the solution result and the calculation time. A low mesh density in the CFD study will result in a fast calculation but poor accuracy of the results; a high mesh density will result in a long calculation time but high accuracy of the results. For this reason, the mesh dependency test was performed to examine and optimize the effect on the result according to different element numbers. In the mesh dependency process, five different meshes with 22,6 million, 16,8 million, 13,3 million, 10,8 million and 9,2 million elements were compared respectively.

Table 3.6. Mesh dependency comparison and error calculations

Number of Element	Lift Coefficient	Drag Coefficient	Moment Coefficient
9,2 million	0,12970426	0,076269816	-0,002690582
10,8 million	0,12913205	0,076341459	-0,002677028
13,3 million	0,12813372	0,075983031	-0,00265108
16,8 million	0,12823649	0,075892042	-0,002651999
22,6 million	0,1280069	0,075716188	-0,002667788

According to Table 3.6, mesh dependency study was performed according to different element numbers. The results of the study for each coefficient are shown as follows.

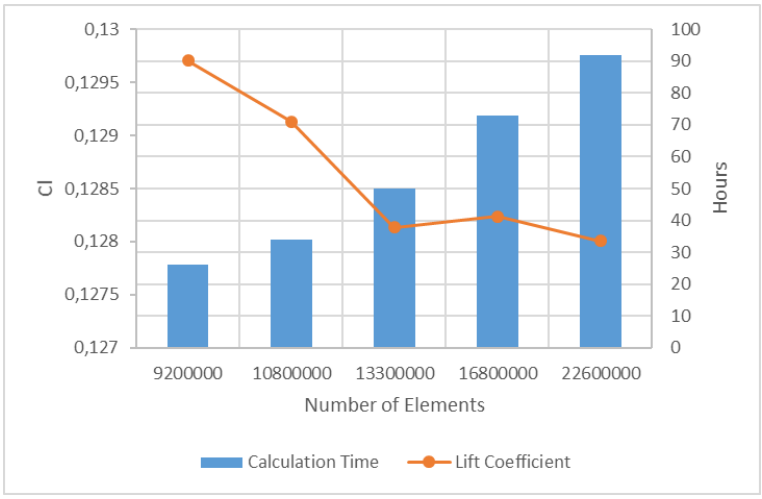

Figure 3.4. Mesh dependency test for lift coefficient

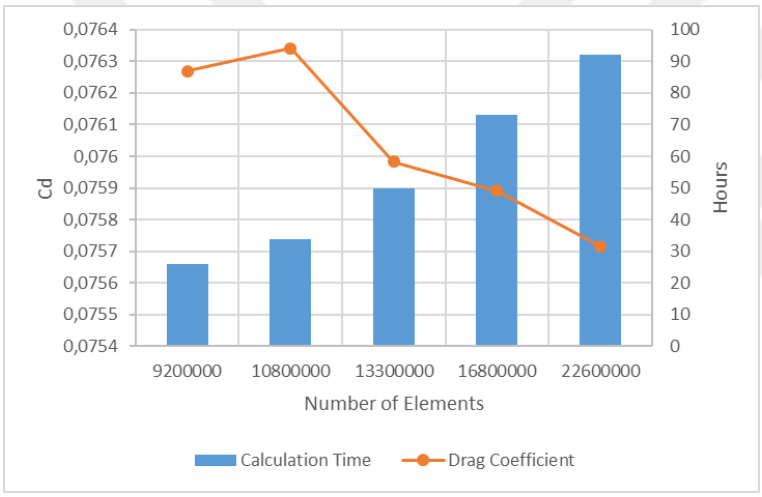

Figure 3.5. Mesh dependency test for drag coefficient

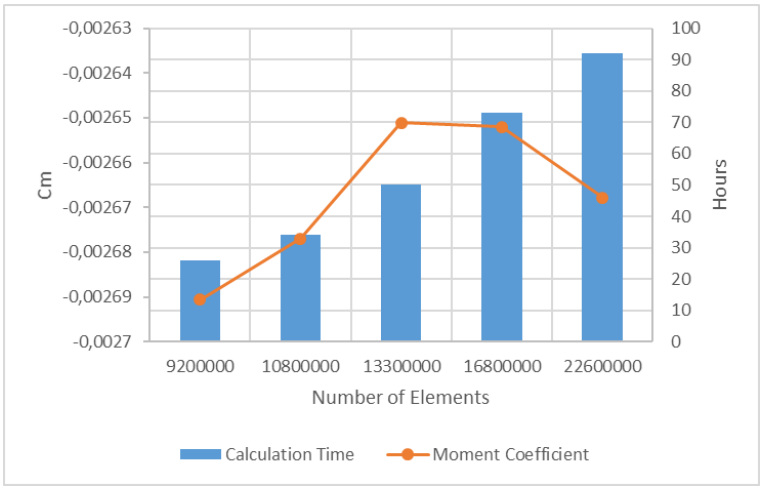

Figure 3.6. Mesh dependency for pitch moment coefficient

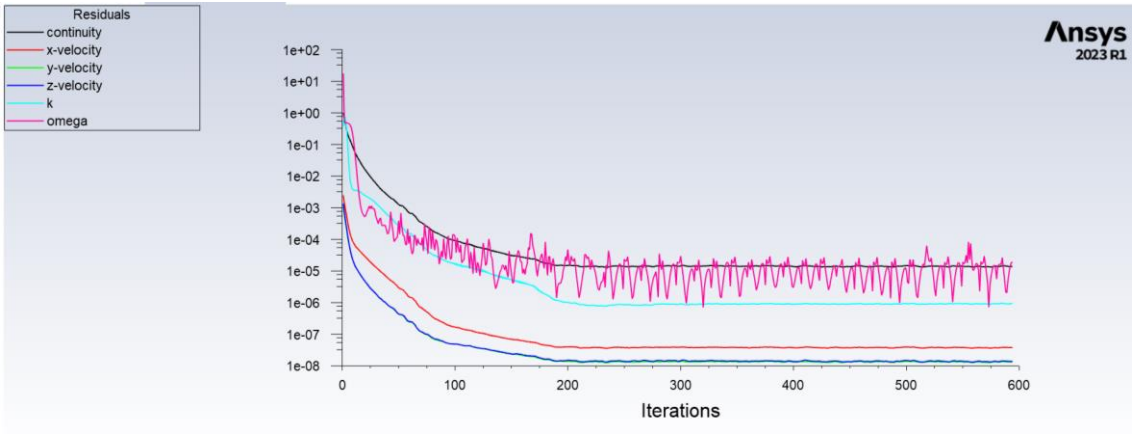

Figure 3.7. Convergence of Ansys k-ω SST solver parameters

As can be seen, the results varied with the increase in the number of meshes and the changes in the amounts of the values decreased after 13,3 million meshes. Here, the solution with 13,3 million meshes will give the optimum result for the solution. However, it is desirable that the performance of the computer used is limited and the time required to obtain data is not too long. Therefore, simulations with 10,8 million meshes were used. Tests using 10,8 million meshes take approximately 34 hours.

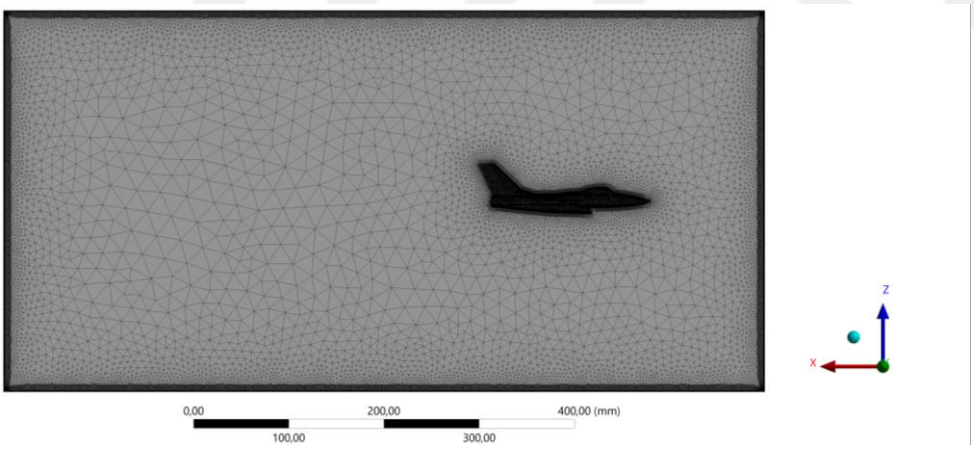

Figure 3.8. Created test case’s mesh ratio equal 35.

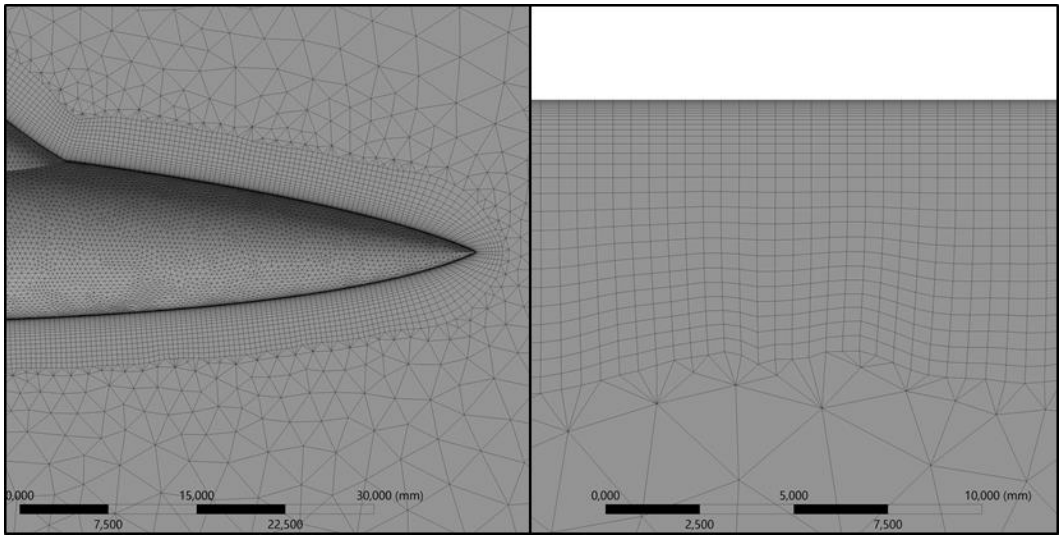

Figure 3.9. Created aircraft's (left) and test section wall's (right) inflation layers for aspect ratio equal 35.

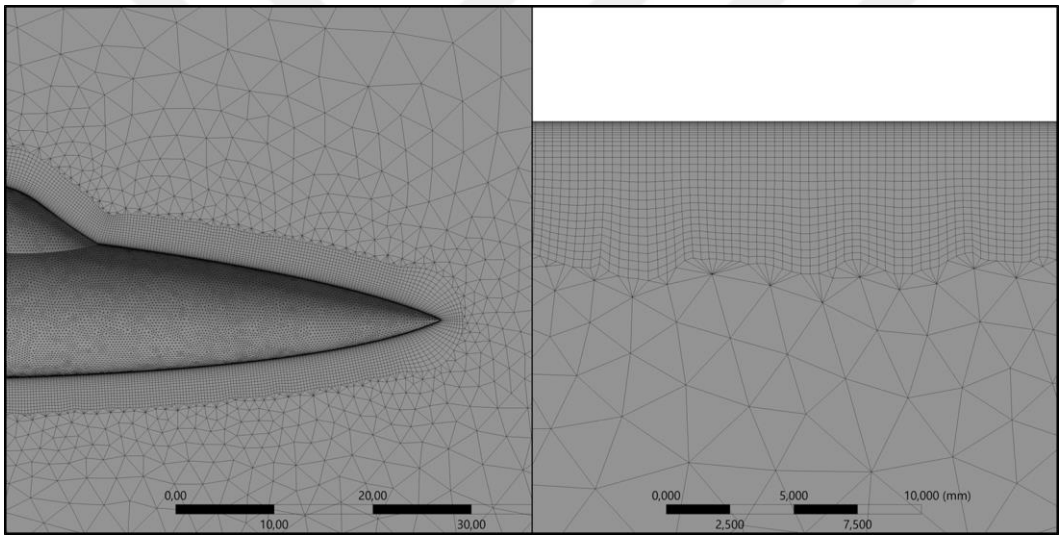

Figure 3.10. Created aircraft's (left) and test section wall's (right) inflation layers for aspect ratio equal 25.

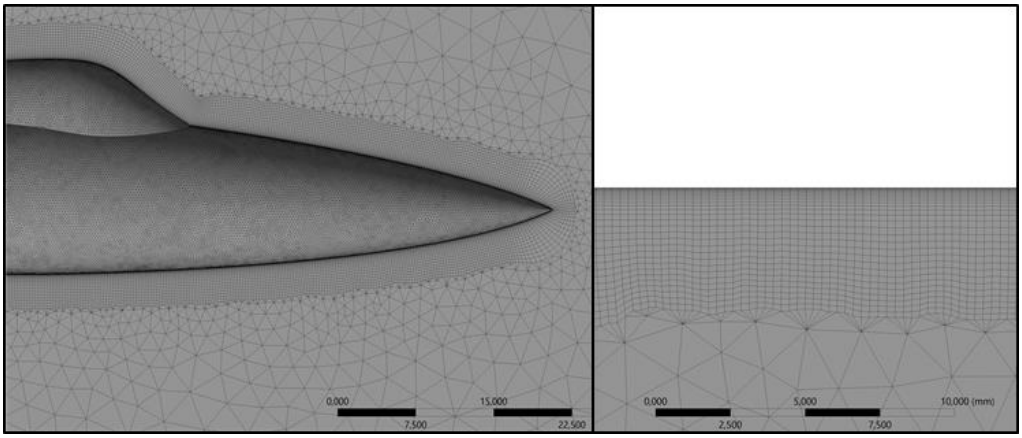

Figure 3.11. Created aircraft's (left) and test section wall's (right) inflation layers for aspect ratio equal 20.

Looking at the time per analysis graph, it was seen that the times of test cases with 9,2 million and 10,8 million element counts were close to each other. For ease of calculation and to save time, it was decided to use the test case with 10,8 million elements and to use the other data in this way. The test with 10,8 million meshes was chosen due to the performance limits of the computer used and the need to avoid long computation times.

3.3. Multi-Fidelity Gaussian Process Regression (MF-GPR)

Gaussian Process Regression (GPR) method is basically a regression model. With this method, the probability of each data point in the data set having a certain value is associated with the distribution in the data set. For each point in the data set, there is an estimate and an uncertainty value for that estimate. With this method, using these data points, the relationships between these points are calculated and new predictions are developed. In places where the data points of the data set are limited, the Gaussian Process Regression method can accurately relate the data to each other. Multi-fidelity Gaussian Process Regression method creates different GPR models for data coming from different sources. Each model has its own mean and covariance functions. Since low-fidelity data is more abundant in the dataset, it is used to capture the trend. Then, high-fidelity data is added to create a specific model to change and correct the trend. The information learned in the data set with a low-fidelity level is transferred to the data set with a high level of fidelity. In this way, the use of data points with a high level of fidelity becomes more effective and cost-effective.

In the Multi-fidelity Gaussian Process Regression data fusion process using data of different fidelity which low fidelity data was obtained from OpenVSP software, high fidelity data

from Computational Fluid Dynamics simulation results. The data obtained were compared with the Computational Fluid Dynamics simulation data in a benchmark comparison. Different numbers of data were used to optimize the performance of the data fusion process. Different combinations were made and their performance was compared.

The mean of this GP model is believed to be 0 value everywhere. In such circumstances, 9the covariance function, k(x,x'), is what connects one observation to another. The 'squared exponential' is a frequent choice for common case. All the Gaussian Process Regression formulas are taken from Reference [62].

$$k(x,x') = \sigma_f^2 exp\left[\frac{-(x-x')^2}{2l^2}\right] \tag{3.7}$$

The data is often noisy from measurement errors. Therefore, noise should be added to the outputs and expressed as such.

$$y = f(x) + \mathcal{N}(0,\sigma_n^2) \tag{3.8}$$

Here;

$$k(x,x') = \sigma_f^2 exp\left[\frac{-(x-x')^2}{2l^2}\right] + \sigma_n^2\delta(x,x') \tag{3.9}$$

$$K = \begin{bmatrix} k(x_1,x_1) & k(x_1,x_2) & \cdots & k(x_1,x_n) \\ k(x_2,x_1) & k(x_2,x_2) & \cdots & k(x_2,x_n) \\ \vdots & \vdots & \ddots & \vdots \\ k(x_n,x_1) & k(x_n,x_2) & \dots & k(x_n,x_n) \end{bmatrix} \tag{3.10}$$

$$K_* = [k(x_*,x_1) \quad k(x_*,x_2) \quad \dots \quad k(x_*,x_n)] \tag{3.11}$$

$$K_{**} = k(x_{**},x_*) \tag{3.12}$$

The data can be represented in a multivariate Gaussian distribution as follows.

$$\begin{bmatrix} y \\ y_* \end{bmatrix} \sim \mathcal{N}(0, \begin{bmatrix} K & K_*^T \\ K_* & K_{**} \end{bmatrix}) \tag{3.13}$$

Here T represents the matrix transpose and y_* denotes the situational probability value. The value of y_* in a Gaussian distribution can be calculated in the following formula.

$$(y_*|y) \sim \mathcal{N}(K_*K^{-1}y, K_{**} - K_*K^{-1}K_*^T) \tag{3.14}$$

Formulas are used to calculate the mean value and variance of y* in the distribution, respectively. In this way, a GPR model is created using the available data. This model is created separately for low fidelity and high fidelity data.

$$\bar{y_*} = K_* K^{-1} y \tag{3.15}$$

$$var(y_*) = K_{**} - K_* K^{-1} K_*^T) \tag{316}$$

The basic algorithm of the Multi-fidelity Gaussian Process Regression method is shown below.

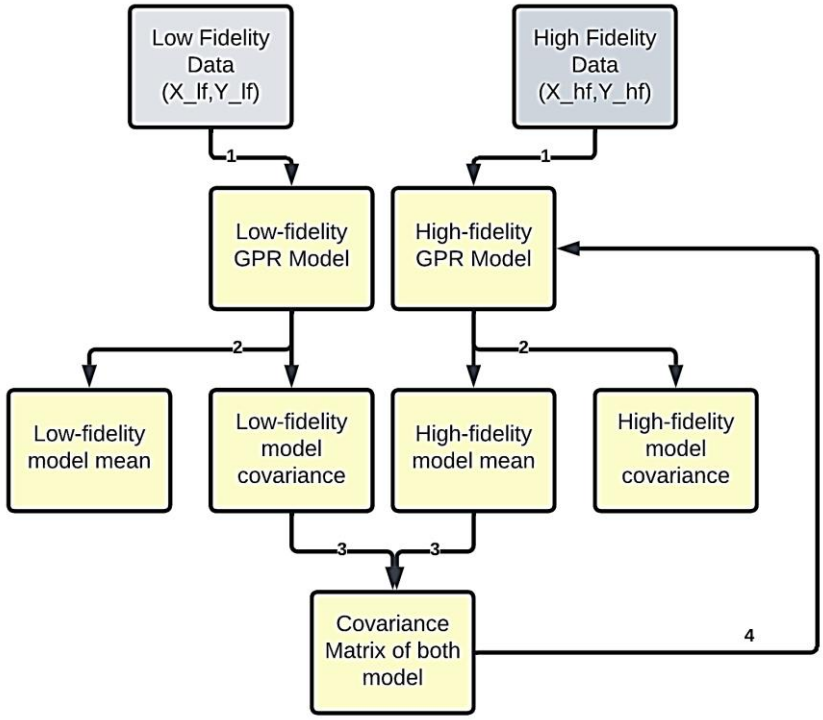

Figure 3.12. Flowchart of multi-fidelity gaussian process regression algorithm

3.4. Multi-Fidelity co-Kriging (MF-cK)

Co-Kriging method is a Kriging based regression model. This model aims to reduce the use of costly high-fidelity data by combining data sets of different fidelity levels. The method creates a Kriging method for each dataset with different levels of fidelity. These Kriging models include the predicted value and covariance matrix of each data point. The covariance matrix of the data set with a low level of fidelity is combined with the covariance matrix of the data set with a high level of fidelity. The low-fidelity model is used to determine the general trend. The data obtained from this model is transferred to the high-fidelity model.

The high-fidelity model is updated according to the information transferred by the low-fidelity model. The created multi-fidelity co-Kriging model is trained by adding new data points until it is ready to make predictions for new points.

In the Multi-fidelity co-Kriging data fusion process using data of different fidelity which low fidelity data was obtained from OpenVSP software, high fidelity data from Computational Fluid Dynamics simulation results like before in the Multi-fidelity GPR method. In a different way, firstly, low and high fidelity data points were combined to obtain a new high fidelity data points. Different numbers of data were used to optimize the performance of the data fusion process. Reference [63] was used for the construction of the Co-Kriging model.

To build the co-Kriging model, the dataset with high-fidelity data should be a subset ($X_e \subset X_c$) of the dataset with low-fidelity. First, the previously obtained data are put into a cluster together.

$$Y = \begin{pmatrix} Y_c(X_c) \\ Y_e(X_e) \end{pmatrix} = \left[Y_c(x_c^{(1)}) \quad \cdots \quad Y_c(x_c^{(n)}) \quad \cdots \quad Y_e(x_e^{(1)}) \quad \cdots \quad Y_e(x_e^{(n)}) \quad \ldots \right]^T \tag{3.17}$$

The co-Kriging data fusion method is an interpolation model based on Kriging. The relationship between high and low fidelity data is determined using a scaling parameter which is hyperparameter in the general model and used in optimization process.

$$Z_e(x) = \rho * Z_c(x) + Z_d(x) \tag{3.18}$$

$Z_c(x)$ and $Z_e(x)$ represent the Gaussian model for high-fidelity and low-fidelity data. The function $Z_d(x)$ defines the difference between high fidelity data and low fidelity data. The procedure for high fidelity data to be estimated is shown in Eq 3.19.

$$\hat{y}_e = \hat{\mu} + c^T C^{-1}(y - 1\hat{\mu}) \tag{3.19}$$

$$\left\{ c = \begin{bmatrix} \hat{\rho}\hat{\sigma}_c^2 \psi_c(X_c, x) \\ \hat{\rho}^2 \hat{\sigma}_c^2 \psi_c(X_c, x) + \hat{\sigma}_d^2 \psi_d(X_e, x) \end{bmatrix} \right\} \tag{3.20}$$
$$\hat{\mu} = 1^T C^{-1} Y / 1^T C^{-1} 1$$

The covariance matrix values required for the predictions to be made with the co-Kriging method are found by the formula in Eq. 3.21.

$$C = \begin{bmatrix} \sigma_c^2 \psi_c(X_c, X_c) & \rho\sigma_c^2 \psi_c(X_c, X_e) \\ \rho\sigma_c^2 \psi_c(X_c, X_e) & \rho^2\sigma_c^2 \psi_c(X_c, X_e) + \sigma_d^2 \psi_d(X_e, X_e) \end{bmatrix} \quad (3.21)$$

Here, $\psi_c(\cdot,\cdot)$ ve $\psi_e(\cdot,\cdot)$ define the correlation matrix between two different data points. The correlation function is calculated as in Eq. 3.22.

$$\psi\left(x^{(i)}, x^{(j)}\right) = \exp\left(\sum_{m=1}^{n} \theta_m{}^2 \left(x_m^{(i)} - x_m^{(j)}\right)^2\right) \quad (3.22)$$

Here, θ_m is a hyperparameter variable.

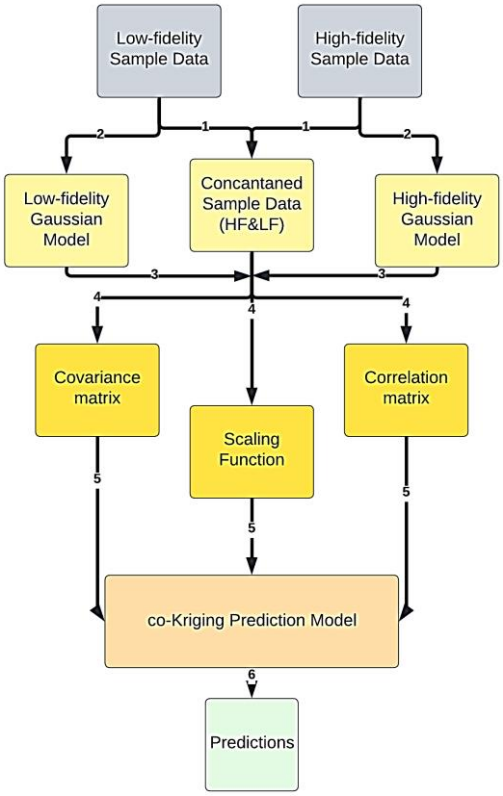

Figure 3.13. Flowchart of multi-fidelity co-Kriging data fusion algorithm

3.5. Multi-Fidelity Neural Network (MF-NN)

The artificial neural networks used in this method are a structure built in layers, based on the human brain and nervous system. It basically consists of input layer, hidden layer and output layer. Data is sent to the input layer, multiplied by the weight values of the neuron, evaluated with the activation function, and the result is produced. The number of layers and the number of neurons used in the layer contribute to improving the solution and determining the weights. Neural networks go through two types of processes to gain the ability to learn.

These are forward propagation and back-propagation algorithms. In the forward propagation algorithm, data moves from the input layer to the output layer and output is produced. In the back-propagation algorithm, like the forward propagation algorithm, data enters the input layer and moves to the output layer, the result is produced and then the error value is found. Each weight value is updated according to the error value. In this process, the weights are updated until the desired error value is achieved.

Low fidelity data is taken from OpenVSP software; high fidelity data is taken from computational fluid dynamics simulation. For machine learning models, it is known that the more data the better the model will be trained. Therefore, Kriging interpolation was applied for low and high fidelity data. In this way, other unknown data points were obtained by interpolation method and sent to the multi-fidelity neural network data fusion method. These two different fidelity data were combined and a new high fidelity data was obtained. The obtained data was compared with computational fluid dynamics simulation tests and the performance was analyzed.

In order to create a multi-fidelity neural network model, it is necessary to determine the number of layers of the model, the number of neurons in each layer and the activation functions to be used in each layer. Some activation functions and their formulas are shown in the table below.

Table 3.7. Activation Functions

Activation Function	Formula for the Function
Sigmoid Activation Function	$f(x) = \frac{1}{1 + e^{-x}}$
Tanh Activation Function	$f(x) = \frac{2}{1 + e^{-2x}} - 1$
Lineer Activation Function	$f(x) = x$
ReLU Activation Function	$f(x) = \max(x, 0)$
Softmax Activation Function	$f(x) = \frac{e^{x,i}}{\sum_k e^{x,k}}$

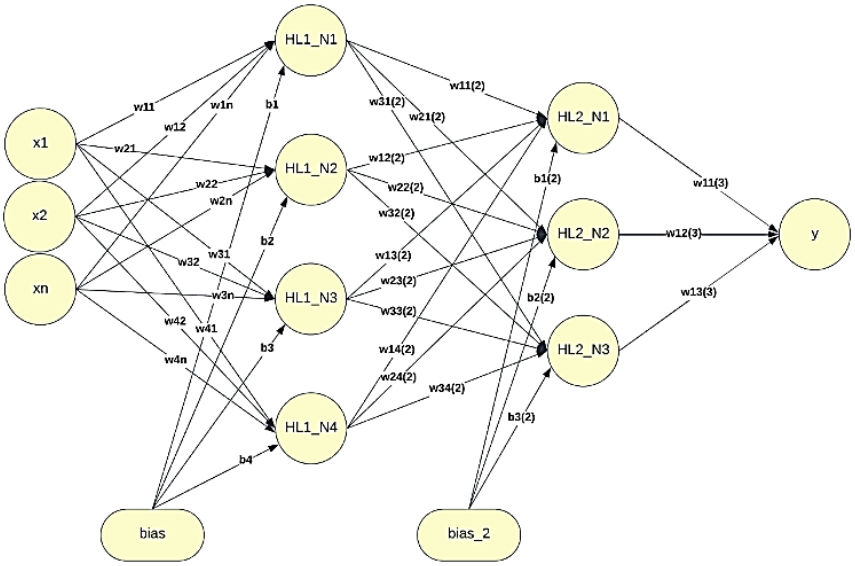

Figure 3.14. An example of neural network diagram

The feed-forward algorithm underlying the neural network model is calculated as follows.

$$X = [x_1 \quad x_2 \quad \cdots \quad x_n] \tag{3.23}$$

$$HL1_{N1} = x_1 * w_{11} + x_2 * w_{12} + \cdots + x_n * w_{1n} + b_1 \tag{3.24}$$

$$HL1_{N2} = x_1 * w_{21} + x_2 * w_{22} + \cdots + x_n * w_{2n} + b_2 \tag{3.25}$$

$$HL1_{N3} = x_1 * w_{31} + x_2 * w_{32} + \cdots + x_n * w_{3n} + b_3 \tag{3.26}$$

$$HL1_{N4} = x_1 * w_{41} + x_2 * w_{42} + \cdots + x_n * w_{4n} + b_4 \tag{3.27}$$

Converting the formulas Eq. 3.23-3.27 into matrix format will result in the following matrix operation. It is expressed as in Eq. 3.28.

$$\begin{bmatrix} HL1_{N1} \\ HL1_{N2} \\ HL1_{N3} \\ HL1_{N4} \end{bmatrix} = [x_1 \quad x_2 \quad \cdots \quad x_n] \begin{bmatrix} w_{11} & w_{21} & w_{31} & w_{41} \\ w_{12} & w_{22} & w_{32} & w_{42} \\ \vdots & \vdots & \vdots & \vdots \\ w_{1n} & w_{2n} & w_{3n} & w_{4n} \end{bmatrix} + \begin{bmatrix} b_1 \\ b_2 \\ b_3 \\ b_4 \end{bmatrix} \tag{3.28}$$

$$HL1^*_{N1} = \sigma(HL1_{N1}) \tag{3.29}$$

$$HL1^*_{N1} = \frac{1}{1+e^{-HL1_{N1}}} \tag{3.30}$$

For example, if the activation function to be used is chosen as "sigmoid function", the equation is written as follows. A different activation function can improve the model prediction by changing the calculating operations and output results. The expression HL1_N1* represents the value of the layer that has been processed with the activation

function. When all these operations are performed for the other layers and the neurons belonging to the layer, the output value in the final layer is obtained.

$$y^* = \left(HL2_{N1} * w_{11}^{(3)} + HL2_{N1} * w_{12}^{(3)} + HL2_{N1} * w_{13}^{(3)}\right) \quad (3.31)$$

$$y = \sigma\left(HL2_{N1} * w_{11}^{(3)} + HL2_{N1} * w_{12}^{(3)} + HL2_{N1} * w_{13}^{(3)}\right) \quad (3.32)$$

The algorithm in which all these operations are performed is the feed-forward algorithm. The data used in this algorithm helps to get output using weight vector and bias values.

Another algorithm used is the back-propagation algorithm. This algorithm is based on updating the weight matrix and bias value according to the error value between the output value and the actual value. By updating the weight matrix and layer bias values, the output value is obtained by using the feed-forward algorithm again. This process takes one iteration. This process continues until the desired error value is achieved. In this case, the model is ready for prediction using the final weight matrix and bias values obtained. The most commonly used error models in multi-fidelity neural network data fusion method are "mean squared error (mse)" and "root mean squared error (rmse)" models. Among these error models, the "mean squared error" error model was selected and used.

$$MSE = \frac{1}{N}\sum\left(y_{target} - y\right)^2 \quad (3.33)$$

$$RMSE = \sqrt{\frac{1}{N}\sum\left(y_{target} - y\right)^2} \quad (3.34)$$

Once the error value is found, the weight vectors are updated in each layer to backwards direction. Using each updated vector, the weight vectors in the previous layer are also changed. The formula for updating the weights is expressed as follows.

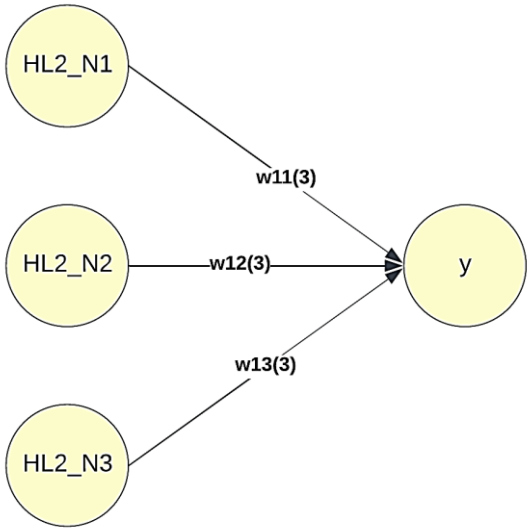

Figure 3.15. Schematic of the process of updating the weight vector $w_{11}^{(3)}$ for the backpropagation algorithm

$$\frac{dE}{dw_{11}} = \frac{dE}{dy} * \frac{dy}{dy^*} * \frac{dy^*}{dw_{11}^3} \tag{3.35}$$

The elements in the formula shown in Eq. (3.35) are obtained in the following equations.

$$\frac{dE}{dy} = \frac{d\left(\frac{1}{N}\sum\left(y_{target}-y\right)^2\right)}{dy} \tag{3.36}$$

$$\frac{dy}{dy^*} = \frac{d\left(\sigma\left(HL2_{N1}*w_{11}^{(3)}+HL2_{N1}*w_{12}^{(3)}+HL2_{N1}*w_{13}^{(3)}\right)\right)}{d\left(HL2_{N1}*w_{11}^{(3)}+HL2_{N1}*w_{12}^{(3)}+HL2_{N1}*w_{13}^{(3)}\right)} = y^* * (1-y^*) \tag{3.37}$$

$$\frac{dy^*}{dw_{11}} = \frac{d\left(HL2_{N1}*w_{11}^{(3)}+HL2_{N1}*w_{12}^{(3)}+HL2_{N1}*w_{13}^{(3)}\right)}{dw_{11}^3} \tag{3.38}$$

The formulas used here refer to updating the weight vector between the output layer and the last hidden layer.

The following equations were used to update the weight vector of the previous layer. Using the previous operations, the weight values w^3_{11}, w^3_{12}, w^3_{13} of the last layer were found. The updated weight expressions are indicated with a star sign.

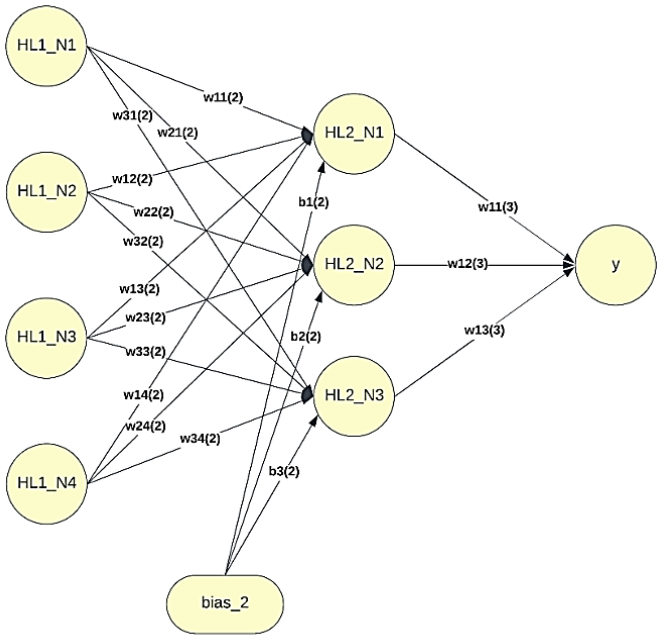

Figure 3.16. Schematic of the process of updating the weight vector $w_{11}^{(2)}$ for the backpropagation algorithm

$$\frac{dE}{dw_{11}^{(2)}} = \frac{dE}{dy} * \frac{dy}{dy^*} * \frac{dy^*}{dHL2_{N1}^*} * \frac{dHL2_{N1}^*}{dHL2_{N1}} * \frac{dHL2_{N1}}{dw_{11}^2} \tag{3.39}$$

$$\frac{dE}{dy} = \frac{d\left(\frac{1}{N}\Sigma\left(y_{target} - y\right)^2\right)}{dy} \tag{3.36}$$

$$\frac{dy}{dy^*} = \frac{d\left(\sigma\left(HL2_{N1} * w_{11}^{(3)} + HL2_{N1} * w_{12}^{(3)} + HL2_{N1} * w_{13}^{(3)}\right)\right)}{d\left(HL2_{N1} * w_{11}^{(3)} + HL2_{N1} * w_{12}^{(3)} + HL2_{N1} * w_{13}^{(3)}\right)} = y^* * (1 - y^*) \tag{3.37}$$

$$\frac{dy^*}{dHL2_{N1}^*} = w_{11}^{3*} \tag{3.40}$$

$$\frac{dHL2_{N1}^*}{dHL2_{N1}} = (HL2_{N1}) * (1 - HL2_{N1}) \tag{3.41}$$

$$\frac{dHL2_{N1}}{dw_{11}^2} = HL1_{N1} \tag{3.42}$$

Using the above equations, the weight vector between the hidden layers is updated. In this way, the weight vectors between other neurons are updated.

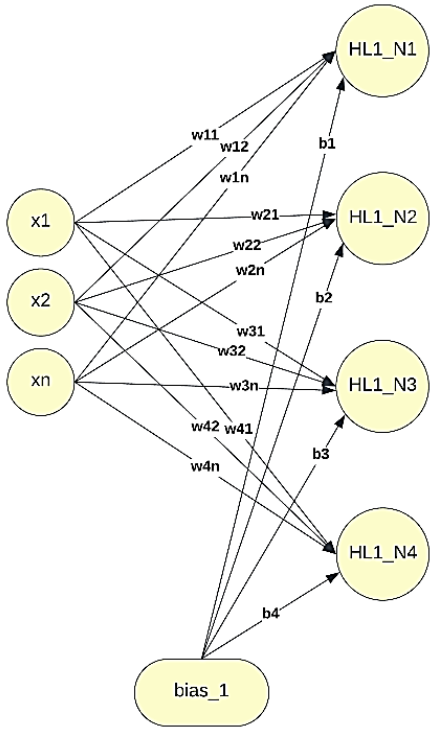

Figure 3.17. Schematic of the process of updating the weight vector $w_{11}^{(1)}$ for the backpropagation algorithm

In order to update the weight matrix between the input layer and the hidden layer, the updated weight vectors calculated from the previous layers are needed. The weight vectors between these two layers are calculated using the following equations.

$$\frac{dE}{dw_{11}^{(1)}} = \frac{dE}{dy} * \frac{dy}{dy^*} * \frac{dy^*}{dHL2_{N1}^*} * \frac{dHL2_{N1}^*}{dHL2_{N1}} * \frac{dHL2_{N1}}{dHL1_{N1}^*} * \frac{dHL1_{N1}^*}{dHL1_{N1}} * \frac{dHL1_{N1}}{dw_{11}^1} \tag{3.43}$$

$$\frac{dE}{dy} = \frac{d\left(\frac{1}{N}\Sigma\left(y_{target}-y\right)^2\right)}{dy} \tag{3.36}$$

$$\frac{dy}{dy^*} = \frac{d\left(\sigma\left(HL2_{N1}*w_{11}^{(3)}+HL2_{N1}*w_{12}^{(3)}+HL2_{N1}*w_{13}^{(3)}\right)\right)}{d\left(HL2_{N1}*w_{11}^{(3)}+HL2_{N1}*w_{12}^{(3)}+HL2_{N1}*w_{13}^{(3)}\right)} = y^* * (1-y^*) \tag{3.37}$$

$$\frac{dy^*}{dHL2_{N1}^*} = w_{11}^{3*} \tag{3.40}$$

$$\frac{dHL2_{N1}^*}{dHL2_{N1}} = (HL2_{N1}) * (1-HL2_{N1}) \tag{3.44}$$

$$\frac{dHL2_{N1}}{dHL1_{N1}^*} = w_{11}^{2*} \tag{3.45}$$

$$\frac{dHL1_{N1}^*}{dHL1_{N1}} = (HL1_{N1}) * (1-HL1_{N1}) \tag{3.46}$$

$$\frac{dHL1_{N1}}{dw_{11}^1} = x_1 \tag{3.47}$$

Using all these equations, with the error obtained after the feedforward process, the back-propagation algorithm is applied and the weight values are updated from the output layer to the input layer and the feed-forward process is started again. All these processes are shown in the picture below.

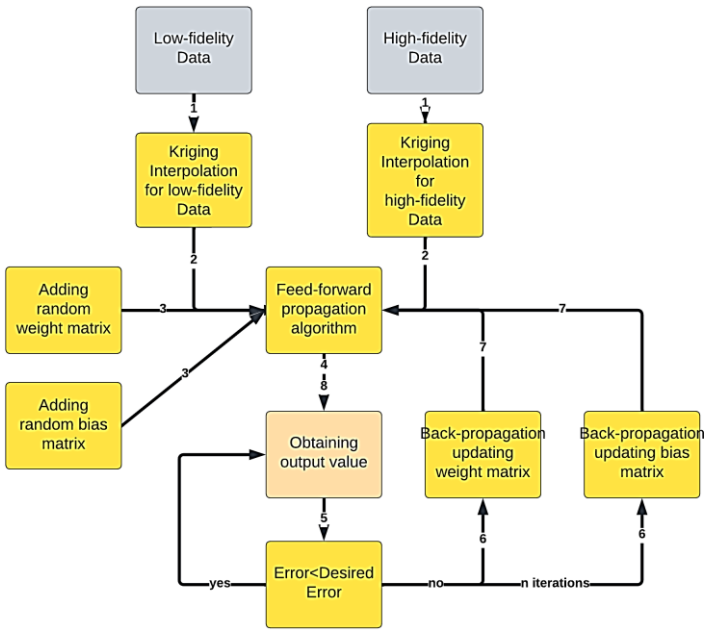

Figure 3.18. Flowchart of multi-fidelity neural network data fusion algorithm

4. RESULTS AND DISCUSSION

In this thesis, two different data sources were obtained with low and high fidelity and these data were analyzed using three different methods. Low fidelity data was obtained using OpenVSP with the Vortex-Lattice method solver. The high fidelity data were obtained using the k-w SST solver in ANSYS Fluent software. In this section, these data are used in different quantities to investigate the performance of the data fusion models used. The data were generated by randomly selecting points without design of experiments (DoE). In this section, three different data fusion methods are investigated and their performances are observed. At the same time, the performance of the model is investigated with increasing low fidelity data. The differences between the time required to obtain high fidelity data and the production performance of multi-fidelity data fusion models are investigated.

4.1. co-Kriging Data Fusion Method

Three different data sources were used in this data fusion method. First, low and high fidelity data were combined. Fewer high fidelity data and more low fidelity data were used. The data obtained as a result of the fusion will have higher fidelity than the low fidelity data. For this purpose, the performance of the data fusion process was examined by using different numbers and fidelity types of data. Accordingly, the test-case prepared to measure the performance of the co-Kriging method is shown in the table below.

Table 4.1. Test case of co-Kriging method to estimate data fusion performance

Case Number	Low-fidelity test samples	High-fidelity test samples
1	31	5
2	31	7
3	31	9
4	31	11
5	15	5
6	15	7
7	15	9
8	15	11

All these test cases were performed for the lift, drag and pitch moment coefficient obtained from the fighter jet model. For testing all the test cases, 31 low-fidelity and 17 high-fidelity data were obtained separately and random sample data sets were generated from them. Here, each high-fidelity data was obtained in 34 hours and the low-fidelity data in approximately 19 seconds. These data sets were used to estimate the lift coefficient of the model and the

results are listed below.

4.1.1. co-Kriging method prediction to obtain lift coefficient

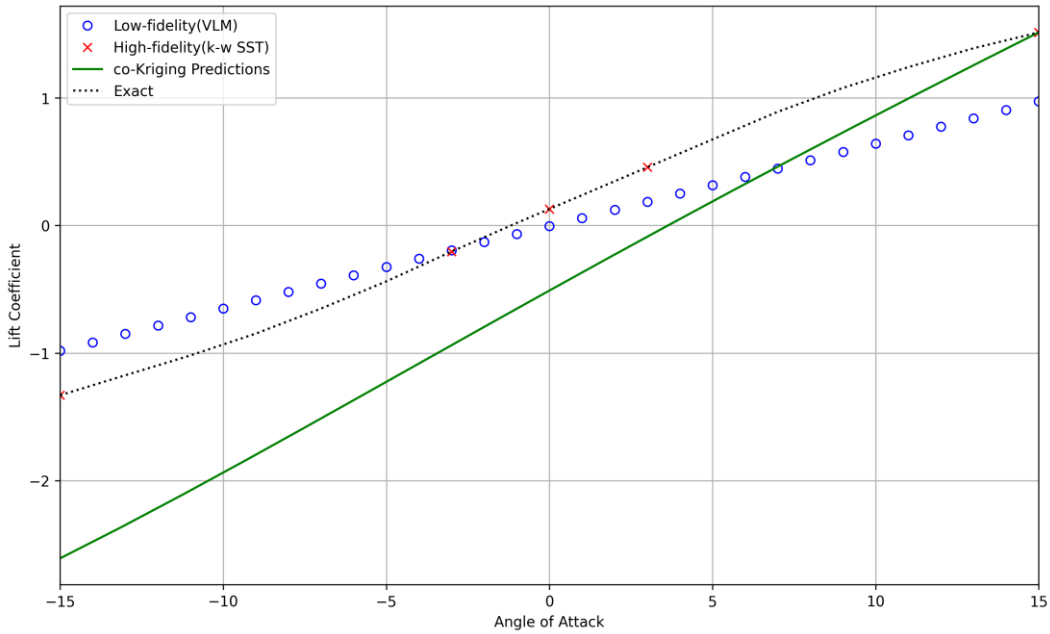

Figure 4.1. co-Kriging lift coefficient estimate using 31 low-fidelity and 5 high-fidelity data corresponding to test case 1

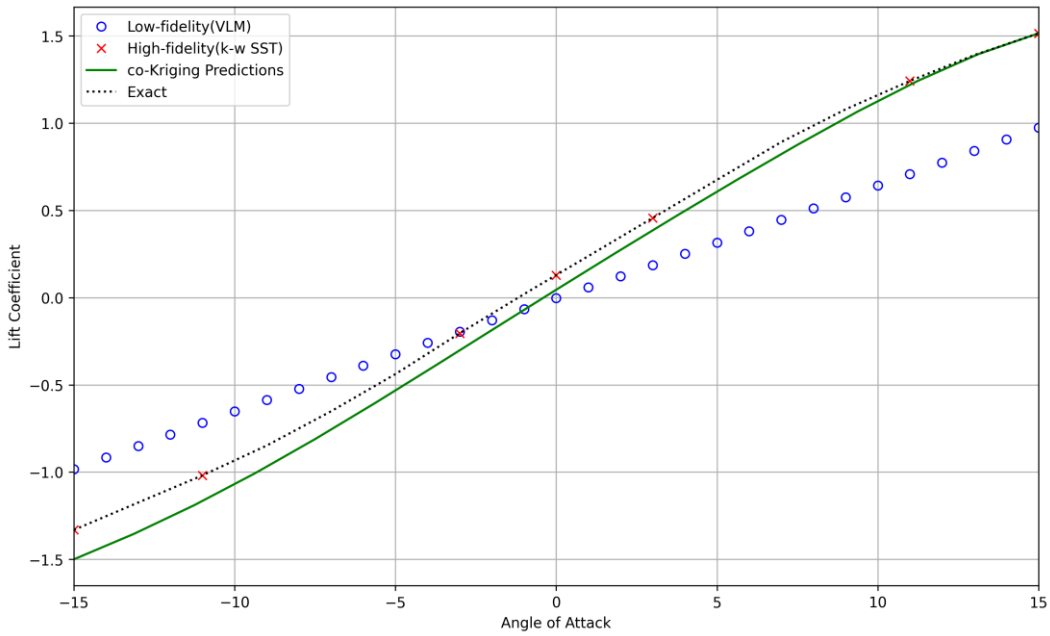

Figure 4.2. co-Kriging lift coefficient estimate using 31 low-fidelity and 7 high-fidelity data corresponding to test case 2

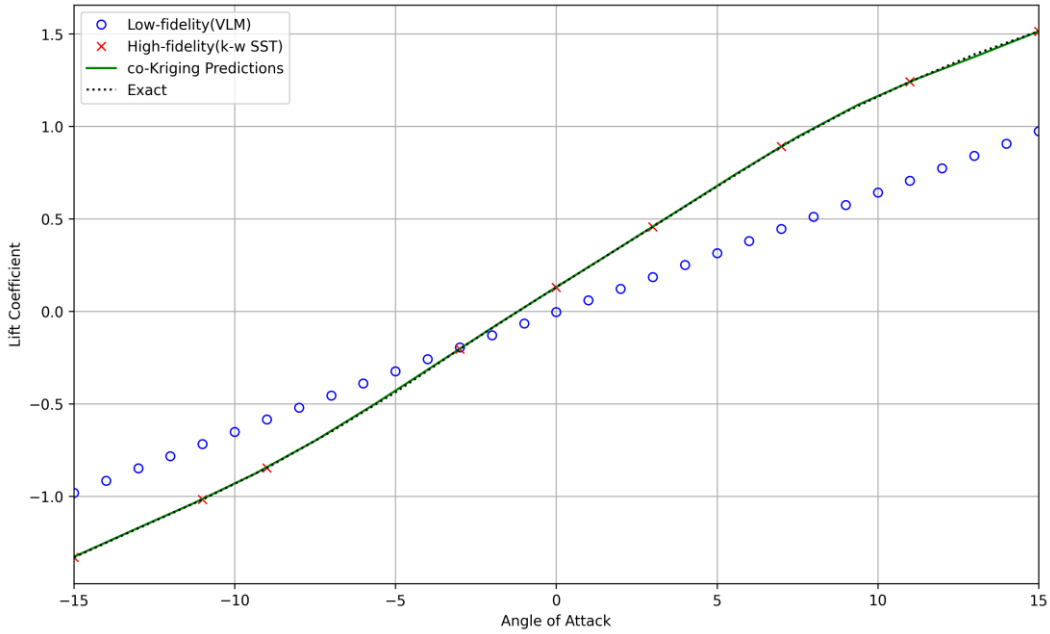

Figure 4.3. co-Kriging lift coefficient estimate using 31 low-fidelity and 9 high-fidelity data corresponding to test case 3

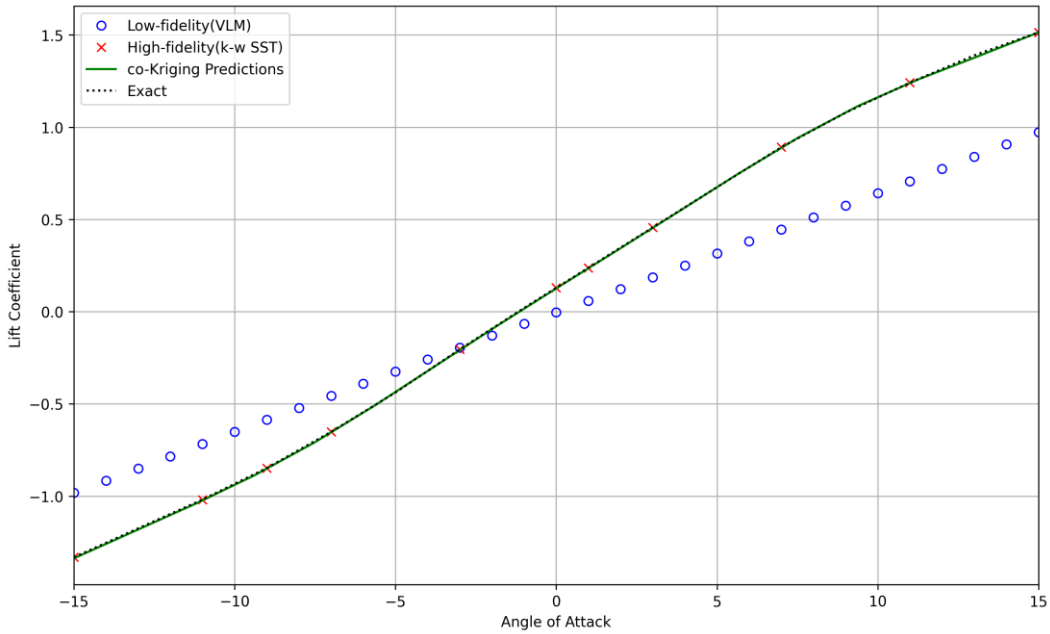

Figure 4.4. co-Kriging lift coefficient estimate using 31 low-fidelity and 11 high-fidelity data corresponding to test case 4

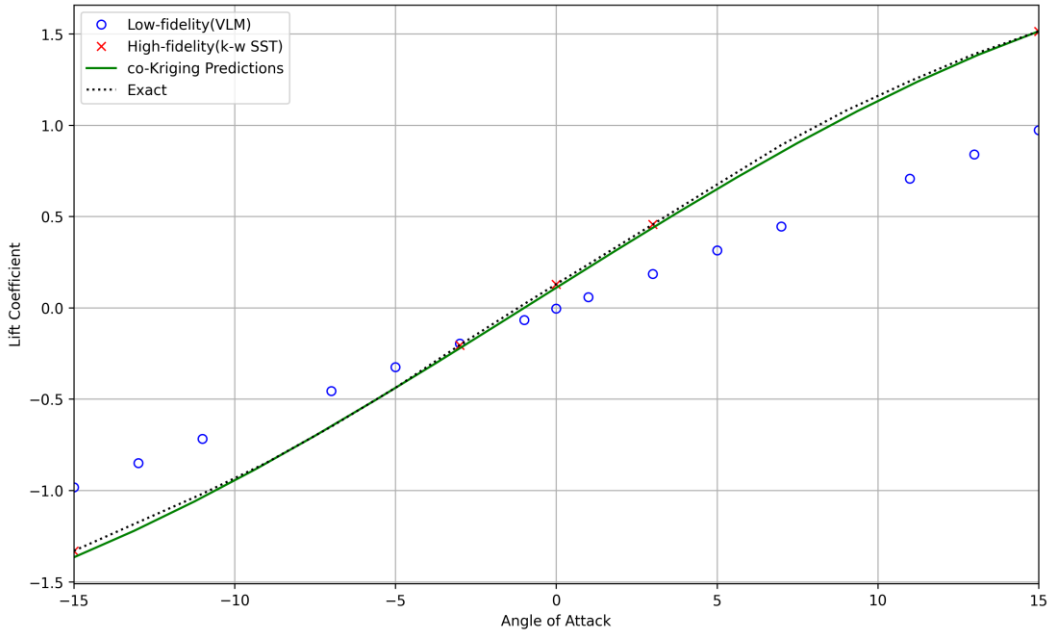

Figure 4.5. co-Kriging lift coefficient estimate using 15 low-fidelity and 5 high-fidelity data corresponding to test case 5

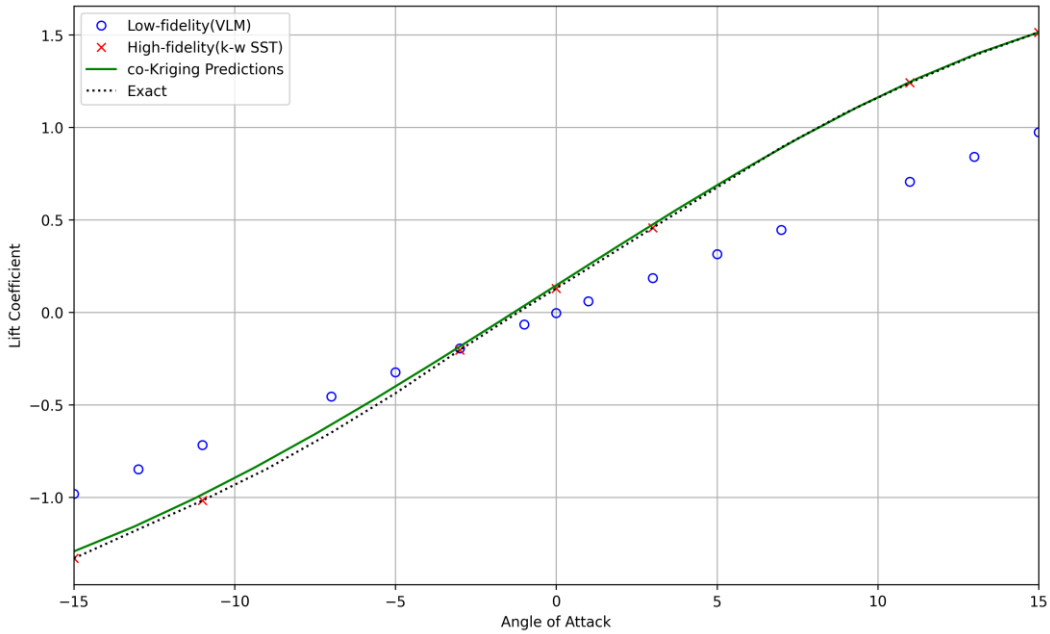

Figure 4.6. co-Kriging lift coefficient estimate using 15 low-fidelity and 7 high-fidelity data corresponding to test case 6

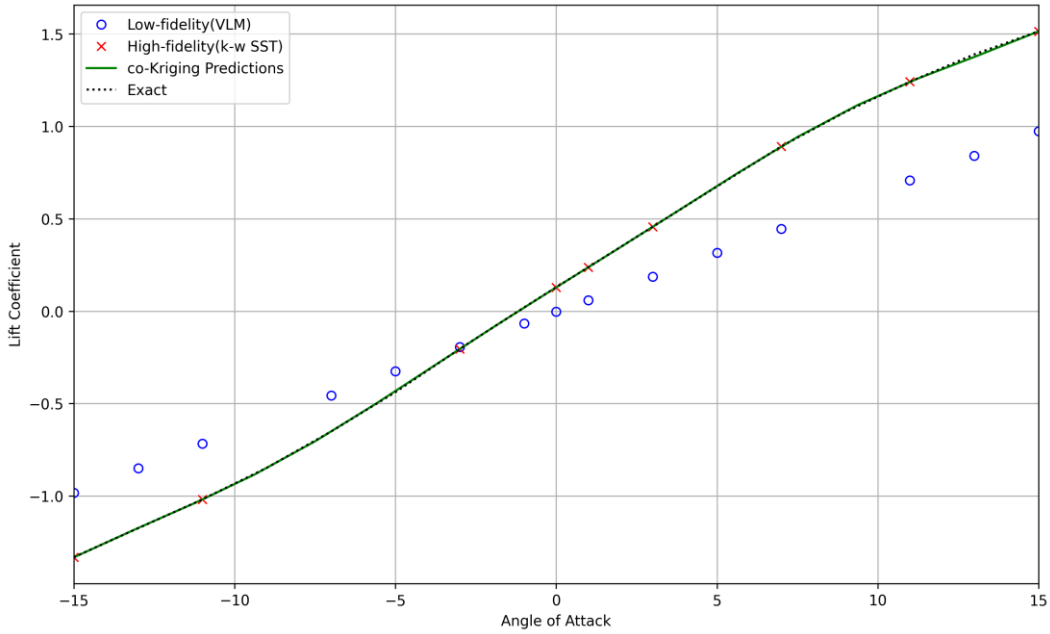

Figure 4.7. co-Kriging lift coefficient estimate using 15 low-fidelity and 9 high-fidelity data corresponding to test case 7

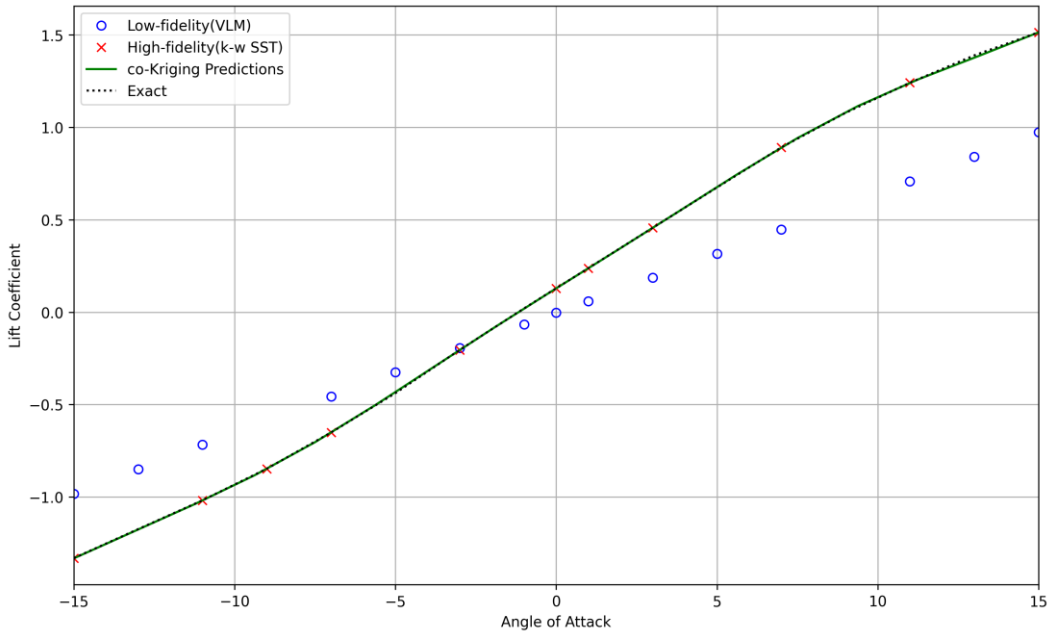

Figure 4.8. co-Kriging lift coefficient estimate using 15 low-fidelity and 11 high-fidelity data corresponding to test case 8

Table 4.2. Error values for co-Kriging method lift coefficient estimation

Test Case Number	Mean Square Error (MSE)	Data Configuration
1	0,5595651912549	31 Low and 5 High Fidelity Data
2	0,0145149851968	31 Low and 7 High Fidelity Data
3	0,0029226826647	31 Low and 9 High Fidelity Data
4	0,0026485282381	31 Low and 11 High Fidelity Data

Table 4.3. Error values for co-Kriging method lift coefficient estimation

Test Case Number	Mean Square Error (MSE)	Data Configuration
1	0,002924136	15 Low and 5 High Fidelity Data
2	0,00273631	15 Low and 7 High Fidelity Data
3	0,00285235	15 Low and 9 High Fidelity Data
4	0,00103612	15 Low and 11 High Fidelity Data

While obtaining the lift coefficient values with the co-Kriging method, the same amount of low-fidelity data was used and the number of high-fidelity data was increased. It was observed that when the number of high fidelity data increased, the predictions approximated the actual values and when 11 high fidelity data were used, the predictions overlapped with the actual values to a great extent. In testcase number of 5,6,7 and 8 with 15 low fidelity datasets, the high fidelity data points did not change and the predictions overlapped with the actual values. Here, with the increase in the number of low-fidelity data, the trend line lost its dominance and the predictions made by the co-Kriging data fusion method started to give more accurate results since the high-fidelity data showed the correct points. Similarly, with the increase in the number of high fidelity data, the predictions made started to overlap more and more with the actual values. Looking at the error values for each test case, the mean squared error values decrease as the number of high fidelity data increases.

4.1.2. co-Kriging method prediction to obtain drag coefficient

Sample test cases for estimating the drag coefficient of the model are listed below.

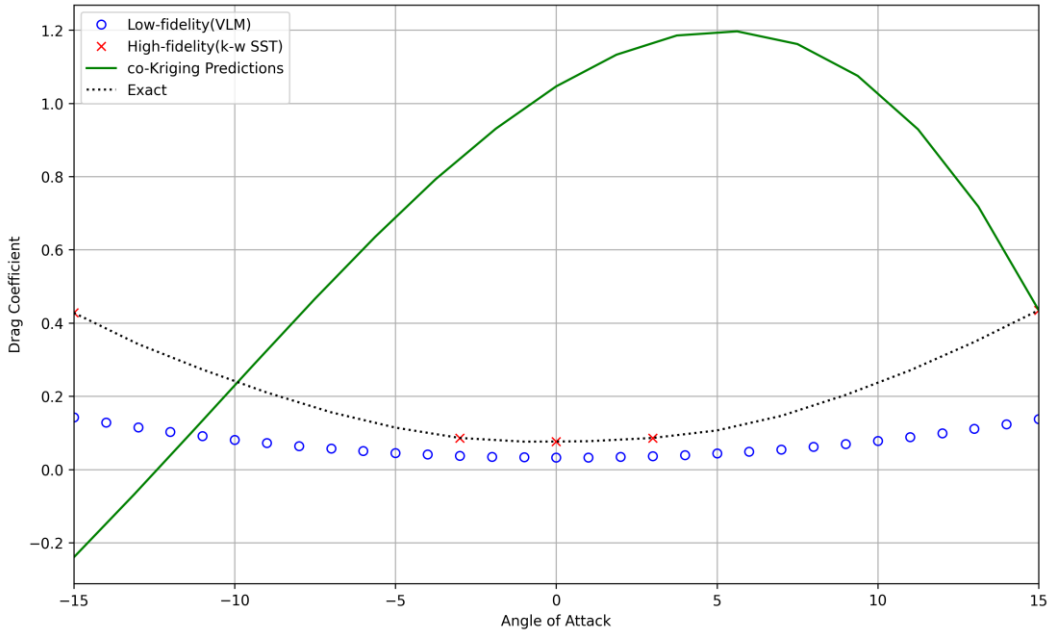

Figure 4.9. co-Kriging drag coefficient estimate using 31 low-fidelity and 5 high-fidelity data corresponding to test case 1

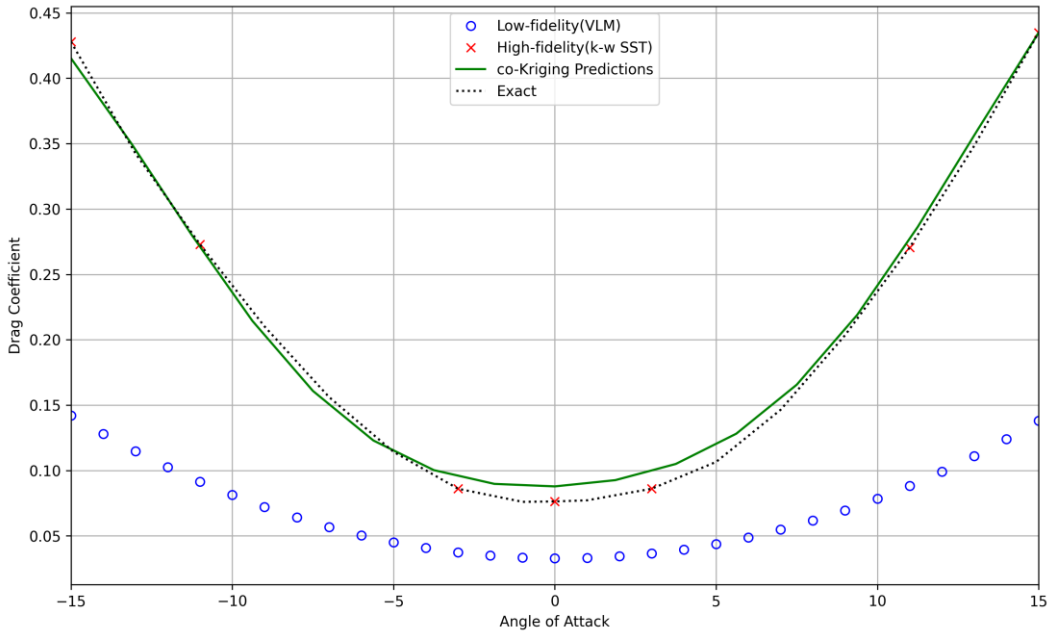

Figure 4.10. co-Kriging drag coefficient estimate using 31 low-fidelity and 7 high-fidelity data corresponding to test case 2

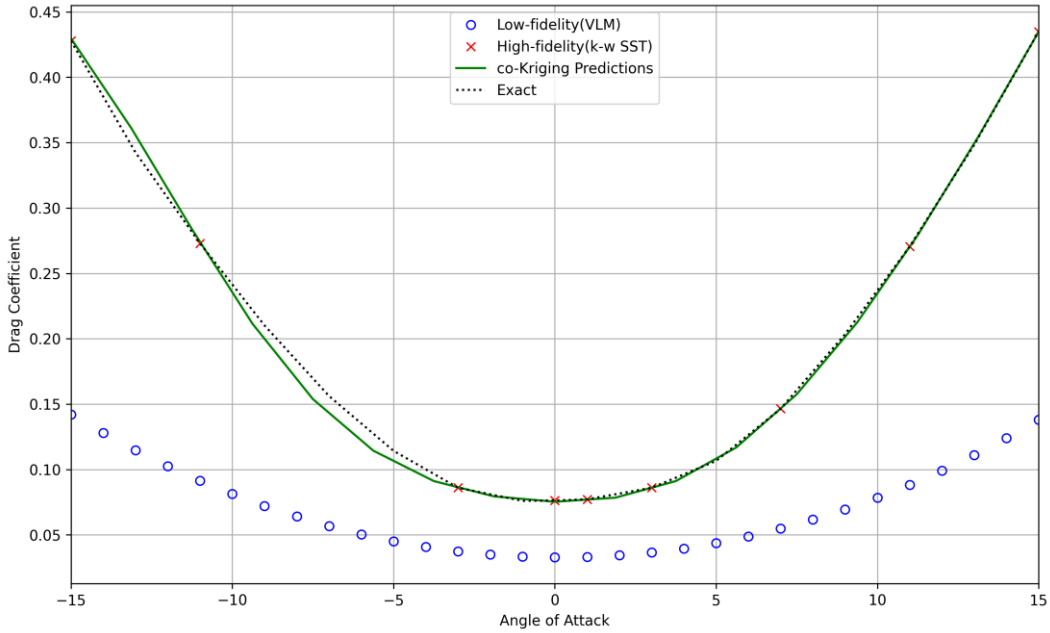

Figure 4.11. co-Kriging drag coefficient estimate using 31 low-fidelity and 9 high-fidelity data corresponding to test case 3

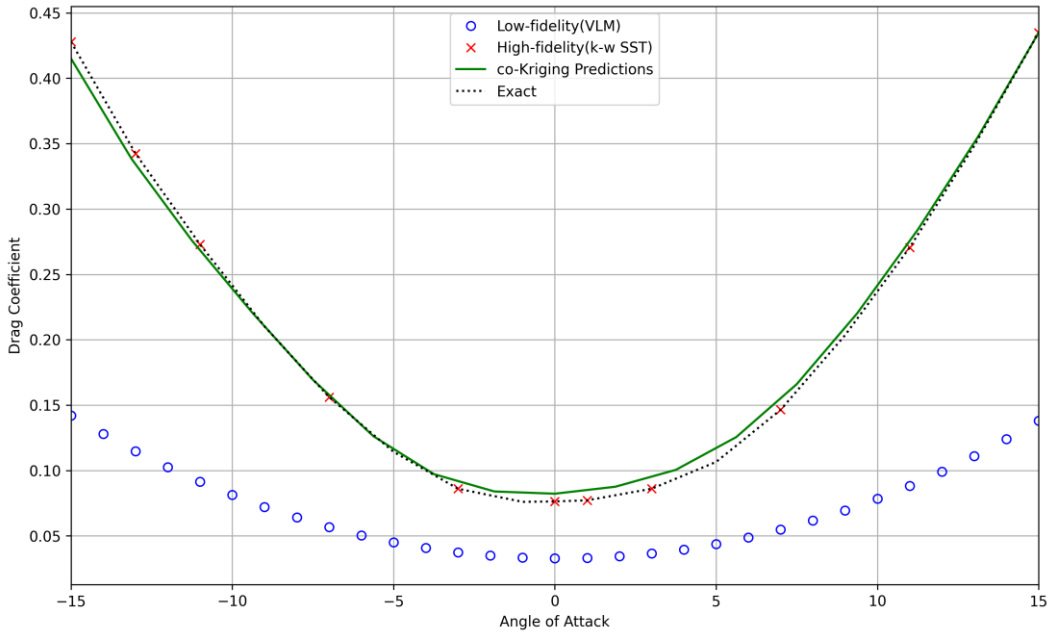

Figure 4.12. co-Kriging drag coefficient estimate using 31 low-fidelity and 11 high-fidelity data corresponding to test case 4

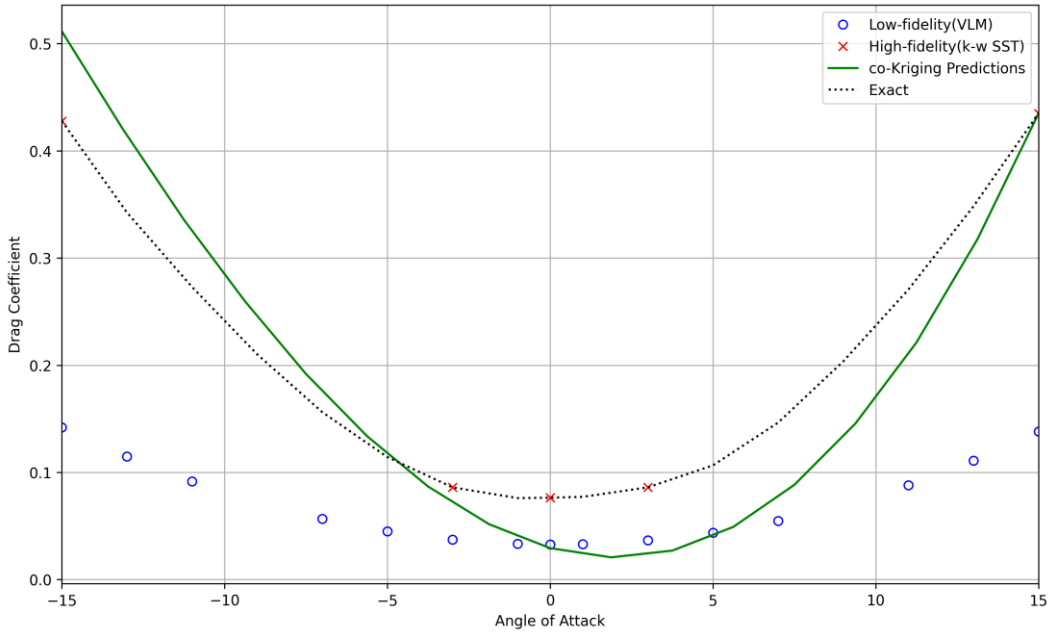

Figure 4.13. co-Kriging drag coefficient estimate using 15 low-fidelity and 5 high-fidelity data corresponding to test case 5

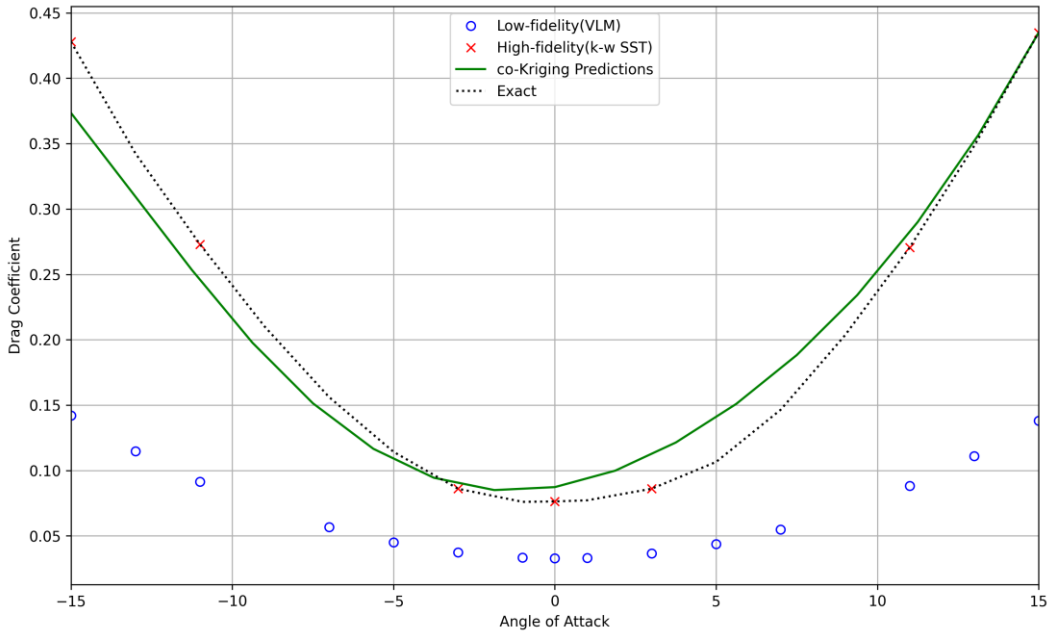

Figure 4.14. co-Kriging drag coefficient estimate using 15 low-fidelity and 7 high-fidelity data corresponding to test case 6

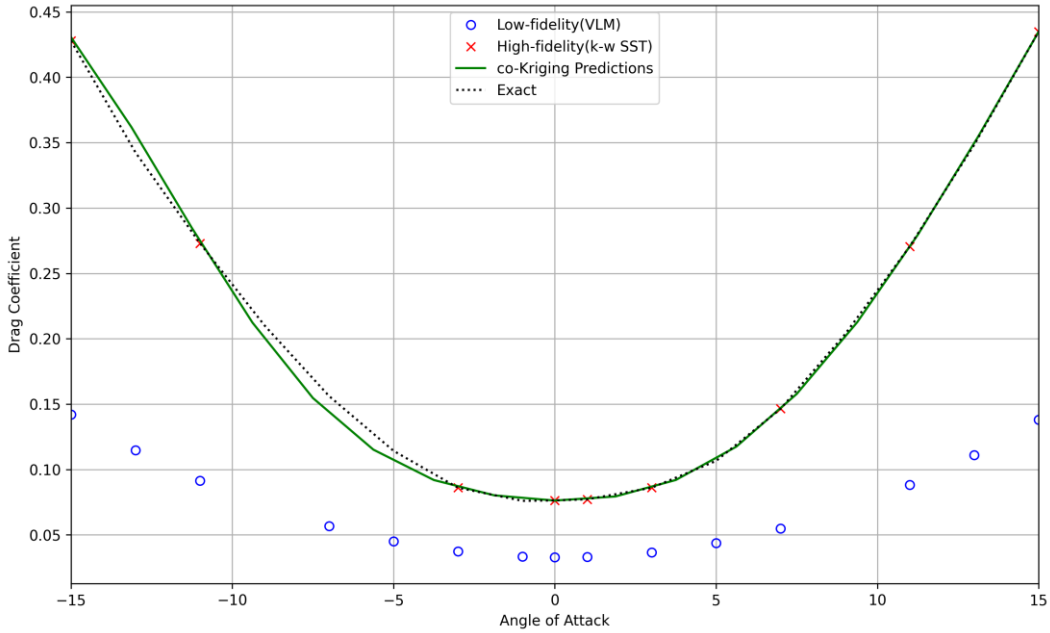

Figure 4.15. co-Kriging drag coefficient estimate using 15 low-fidelity and 9 high-fidelity data corresponding to test case 7

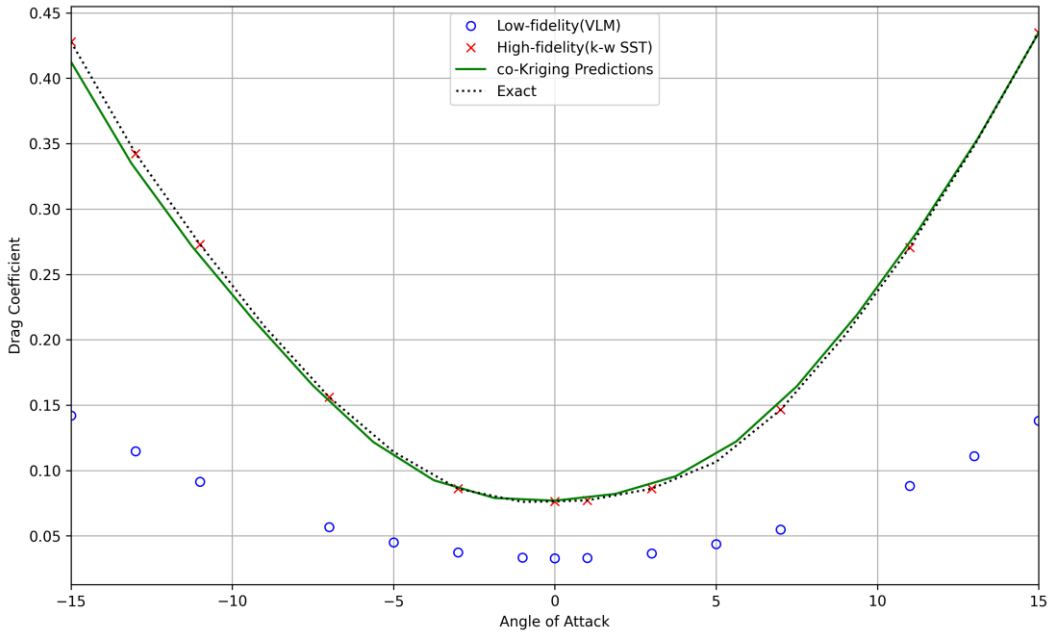

Figure 4.16. co-Kriging drag coefficient estimate using 15 low-fidelity and 11 high-fidelity data corresponding to test case 8

Table 4.4. Error values for co-Kriging method drag coefficient estimation

Test Case Number	Mean Square Error (MSE)	Data Configuration
1	0,5329403060096	31 Low and 5 High Fidelity Data
2	0,0001759825547	31 Low and 7 High Fidelity Data
3	0,0000561745000	31 Low and 9 High Fidelity Data
4	0,0001420552727	31 Low and 11 High Fidelity Data

Table 4.5. Error values for co-Kriging method drag coefficient estimation

Test Case Number	Mean Square Error (MSE)	Data Configuration
1	0,002584725	15 Low and 5 High Fidelity Data
2	0,000677397	15 Low and 7 High Fidelity Data
3	0,0000629348	15 Low and 9 High Fidelity Data
4	0,00009638280	15 Low and 11 High Fidelity Data

There are 8 test-cases in the drag coefficient estimation process with the Co-Kriging data fusion method. For the first 4 test cases with 31 low-fidelity data, the number of high-fidelity data increases. The predictions generally improve as the number of high fidelity data increases. Here, the model with 31 low-fidelity and 4 high-fidelity models offers the best result. In test-cases 5,6,7 and 8, which were created using 15 low-fidelity data, it was observed that with the increase in the number of high-fidelity data, the predicted data started to overlap with the actual data and the exact error values decreased, except for the model number 8.

4.1.3. co-Kriging method prediction to obtain pitch moment coefficient

Test-cases were applied to estimate the pitch moment coefficient of the model using the Co-Kriging method and the results are shown below.

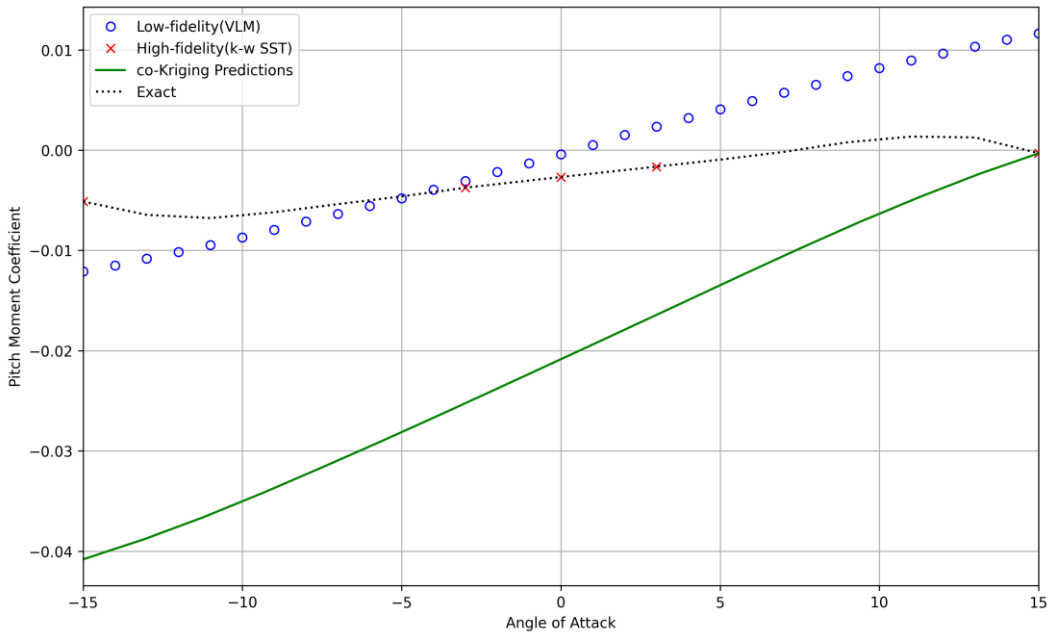

Figure 4.17. co-Kriging pitch moment coefficient estimate using 31 low-fidelity and 5 high-fidelity data corresponding to test case 1

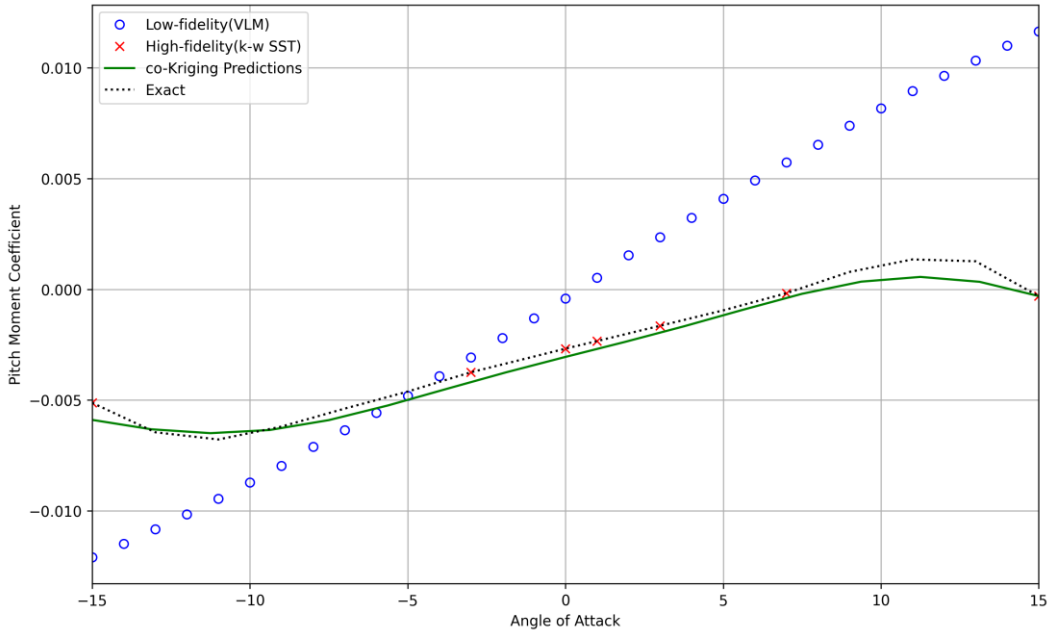

Figure 4.18. co-Kriging pitch moment coefficient estimate using 31 low-fidelity and 7 high-fidelity data corresponding to test case 2

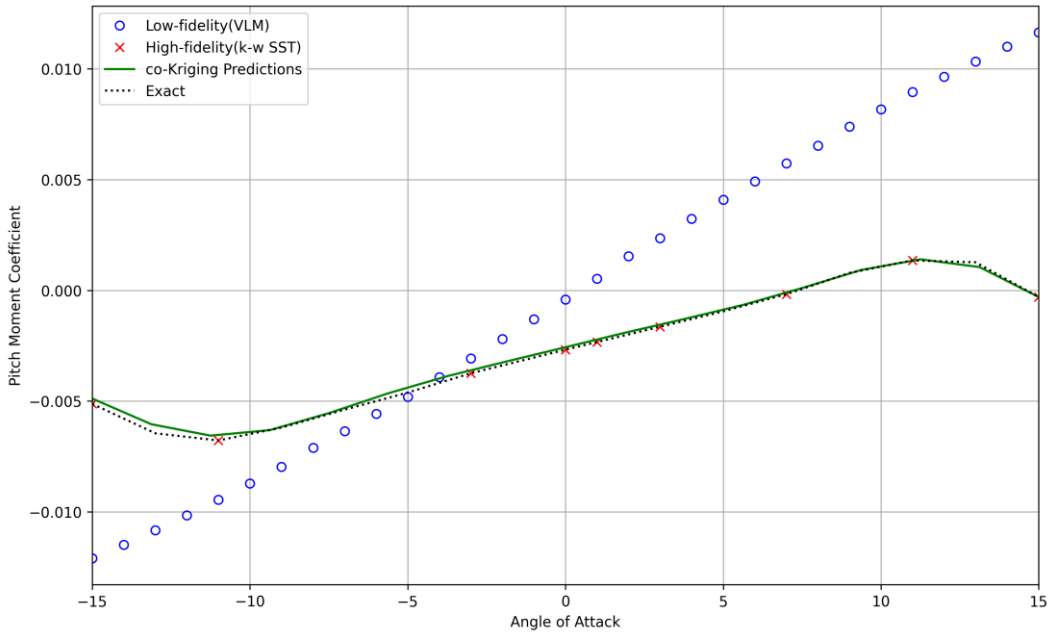

Figure 4.19. co-Kriging pitch moment coefficient estimate using 31 low-fidelity and 9 high-fidelity data corresponding to test case 3

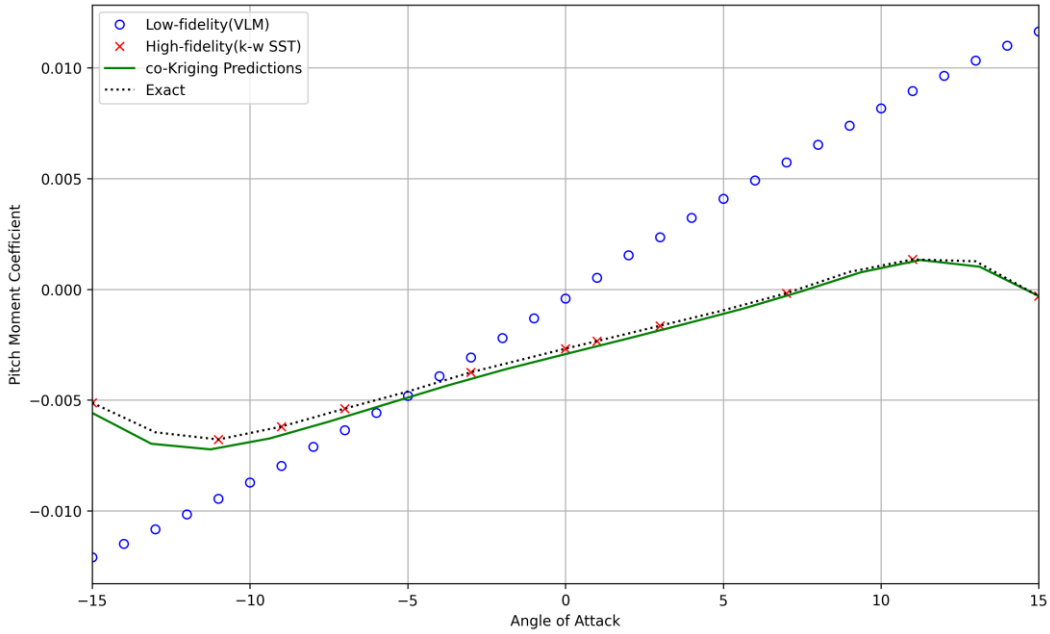

Figure 4.20. co-Kriging pitch moment coefficient estimate using 31 low-fidelity and 11 high-fidelity data corresponding to test case 4

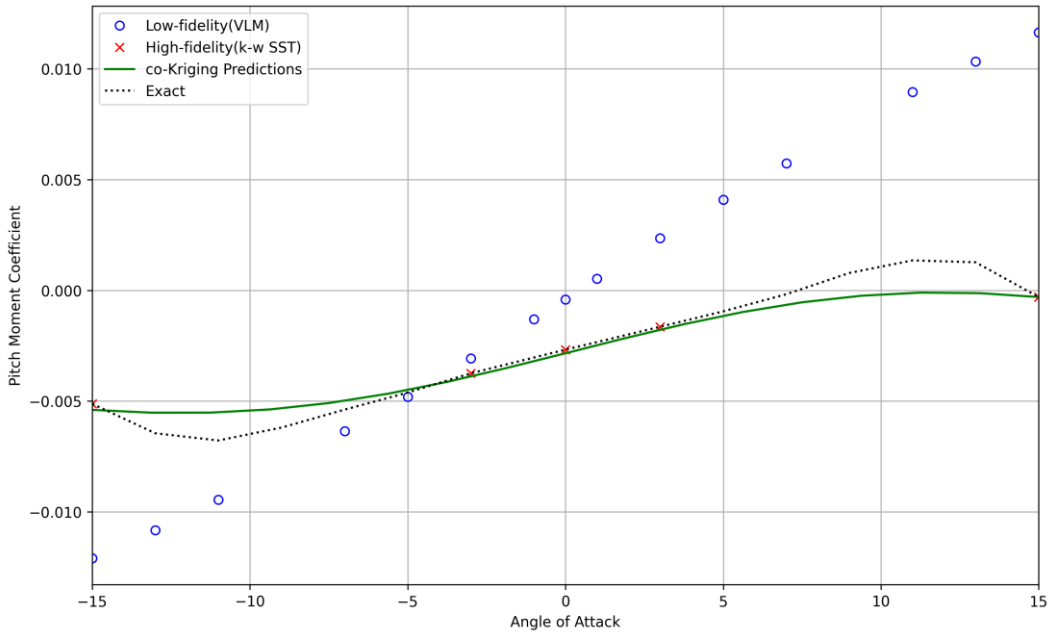

Figure 4.21. co-Kriging pitch moment coefficient estimate using 15 low-fidelity and 5 high-fidelity data corresponding to test case 5

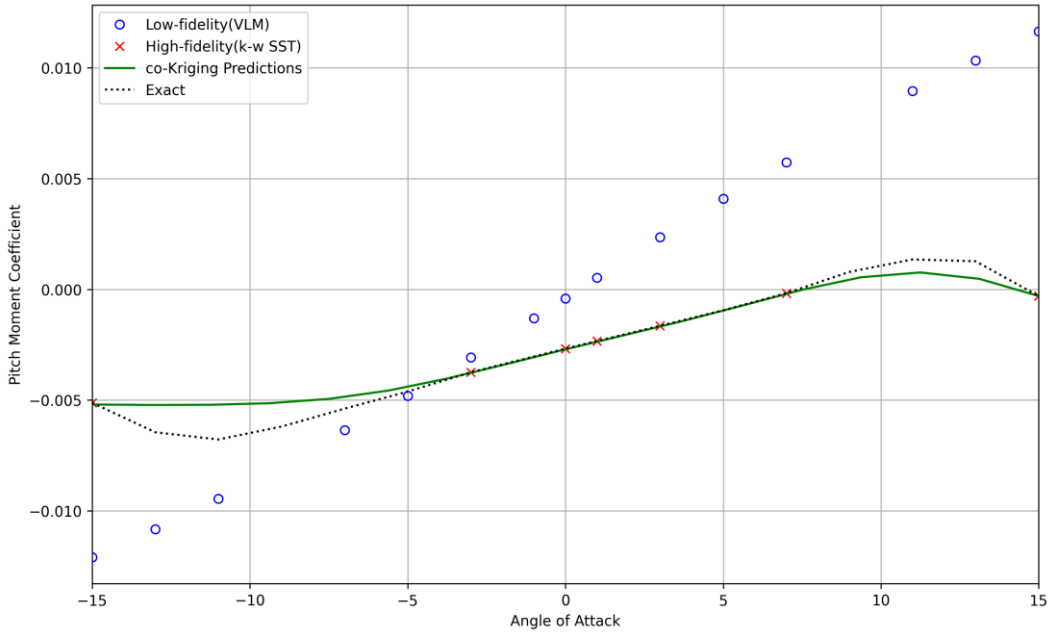

Figure 4.22. co-Kriging pitch moment coefficient estimate using 15 low-fidelity and 7 high-fidelity data corresponding to test case 6

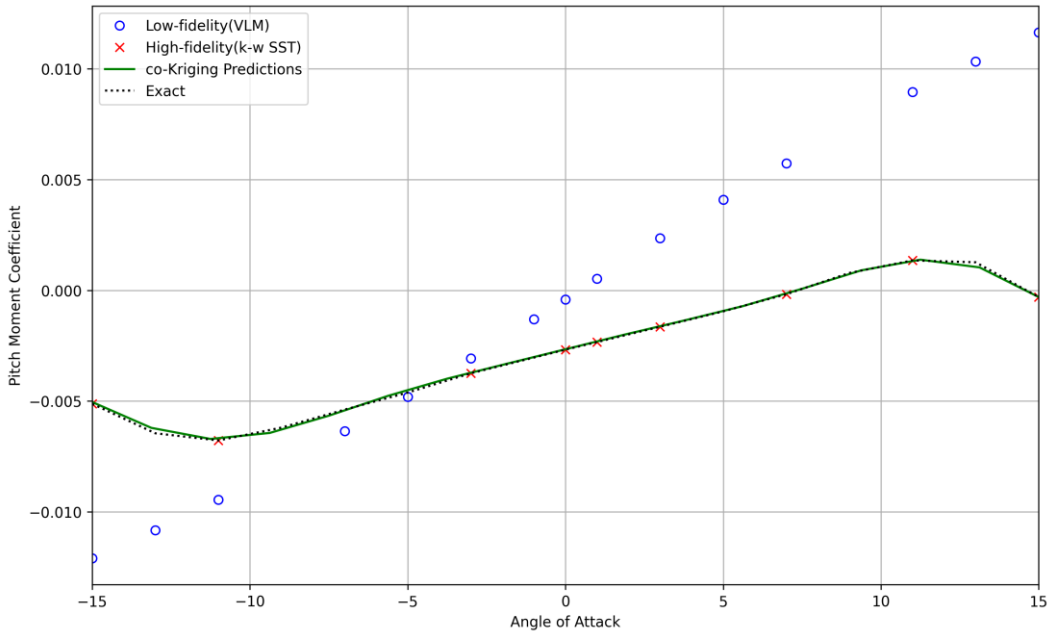

Figure 4.23. co-Kriging pitch moment coefficient estimate using 15 low-fidelity and 9 high-fidelity data corresponding to test case 7

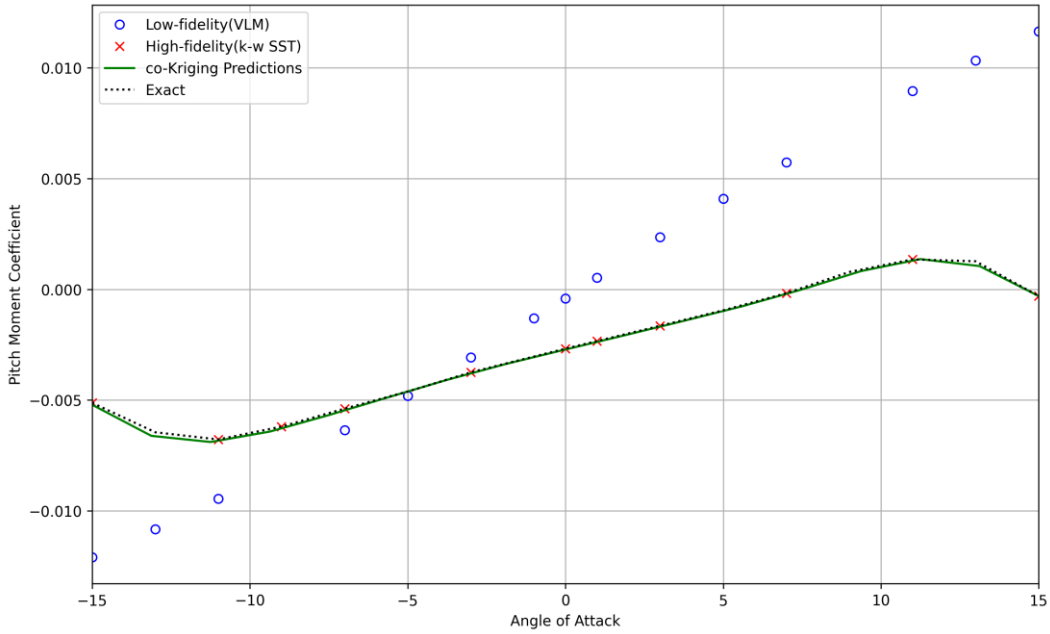

Figure 4.24. co-Kriging pitch moment coefficient estimate using 15 low-fidelity and 11 high-fidelity data corresponding to test case 8

Table 4.6. Error values for co-Kriging method pitch moment coefficient estimation

Test Case Number	Mean Square Error (MSE)	Data Configuration
1	0,000430959	31 Low and 5 High Fidelity Data
2	0,0000002501729	31 Low and 7 High Fidelity Data
3	0,0000000525619	31 Low and 9 High Fidelity Data
4	0,0000001432055	31 Low and 11 High Fidelity Data

Table 4.7. Error values for co-Kriging method pitch moment coefficient estimation

Test Case Number	Mean Square Error (MSE)	Data Configuration
1	0,0000005283470	15 Low and 5 High Fidelity Data
2	0,000000394926000	15 Low and 7 High Fidelity Data
3	0,0000000437	15 Low and 9 High Fidelity Data
4	0,00000004187	15 Low and 11 High Fidelity Data

When the models for the pitch moment coefficient prediction of the Co-Kriging data fusion method are examined, the correlation of the data is poor because there is no agreement and similarity between the data taken from OpenVSP and ANSYS Fleunt. Therefore, the prediction ability of the data fusion method is poor in test-cases with a small number of high fidelity data, while it improves when the number of high fidelity data increases and at the same time when the number of low fidelity data decreases. Test case 4 showed the best and most consistent results, while the other tests show significant results. The reason for the large

amount of data and time required to estimate the pitch moment coefficient is due to the poor correlation between low and high fidelity data.

Table 4.8. Efficiency and mse comparison of each parameter for co-Kriging data fusion method

Parameter	Test case number	Co-Kriging prediction time (s)	Time required to obtain the data used in test case (s)	Time required to obtain the all data (s)	Efficiency (%)	MSE
C_l	1	1,2	612 590	2 080 800	70,55987	0,55956519
C_l	2	1,1	857 390	2 080 800	58,79517	0,01451498
C_l	3	1,1	1 102 190	2 080 800	47,03046	0,00292268
C_l	4	1,2	1 346 990	2 080 800	35,26576	0,00264852
C_l	5	1,2	612 286	2 080 800	70,57448	0,002924136
C_l	6	1,2	857 086	2 080 800	58,80978	0,00273631
C_l	7	1,2	1 101 886	2 080 800	47,04507	0,00285235
C_l	8	1,2	1 346 686	2 080 800	35,28036	0,00103612
C_d	1	1,2	612 590	2 080 800	70,55987	0,53294030
C_d	2	1,3	857 390	2 080 800	58,79516	0,00017598
C_d	3	1,2	1 102 190	2 080 800	47,03046	0,00005617
C_d	4	1,2	1 346 990	2 080 800	35,26575	0,00014205
C_d	5	1,3	612 286	2 080 800	70,57448	0,002584725
C_d	6	1,3	857 086	2 080 800	58,80977	0,000677397
C_d	7	1,4	1 101 886	2 080 800	47,04506	0,000062934
C_d	8	1,3	1 346 686	2 080 800	35,28036	0,000096382
C_m	1	1,4	612 590	2 080 800	70,55986	0,000430959
C_m	2	1,4	857 390	2 080 800	58,79515	0,0000002501
C_m	3	1,5	1 102 190	2 080 800	47,03044	0,0000000525
C_m	4	1,4	1 346 990	2 080 800	35,26574	0,0000001432
C_m	5	1,4	612 286	2 080 800	70,57447	0,000000528
C_m	6	1,4	857 086	2 080 800	58,80976	0,0000003949
C_m	7	1,4	1 101 886	2 080 800	47,04506	0,0000000437
C_m	8	1,4	1 346 686	2 080 800	35,28035	0,0000000418

Looking at Table 4.8, when the efficiency values are analyzed for all parameters, the maximum efficiency for the estimation of lift, drag and pitch moment coefficient is theoretically 70.55% in test cases 1 and 5. However, when the mse rates are analyzed, the lowest error values are not in test cases 1 and 5. The lowest error value values were observed in test case 8 for lift coefficient, test case 8 for drag coefficient and test case 8 for pitch moment coefficient. When the efficiency and error value values are analyzed together, it will be possible to determine which test case is better.

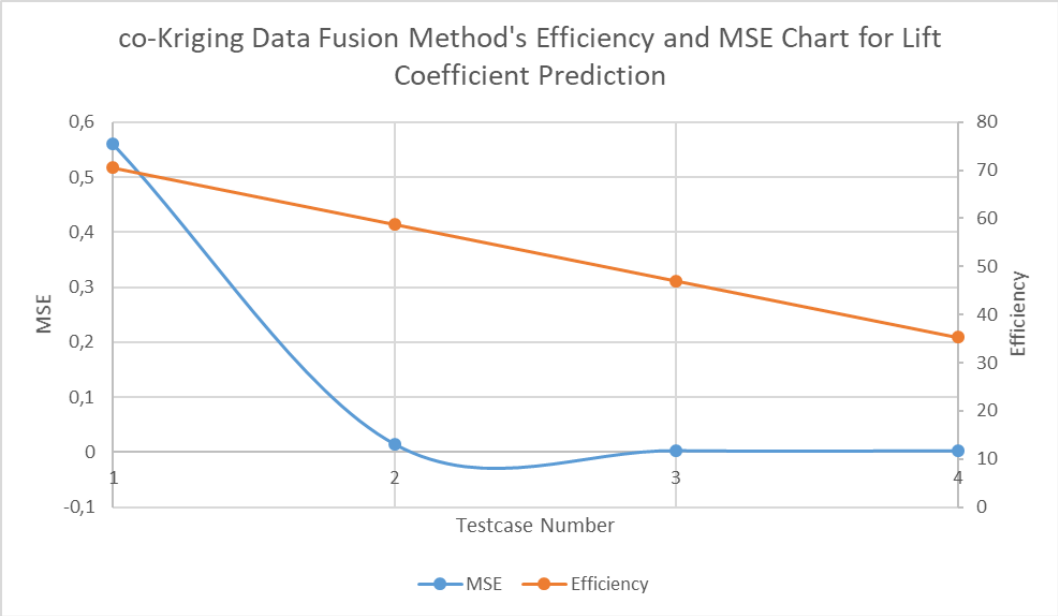

Figure 4.25. Comparison of efficiency and MSE for co-Kriging data fusion method lift coefficient estimation for the first four testcases

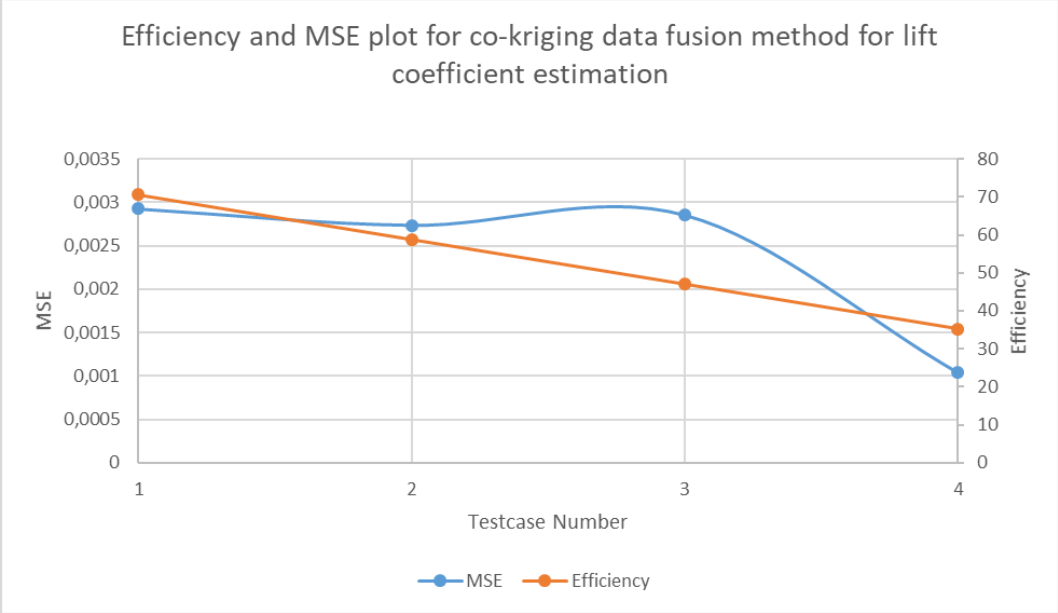

Figure 4.26. Comparison of efficiency and MSE for co-Kriging data fusion method lift coefficient estimation for the second four testcases

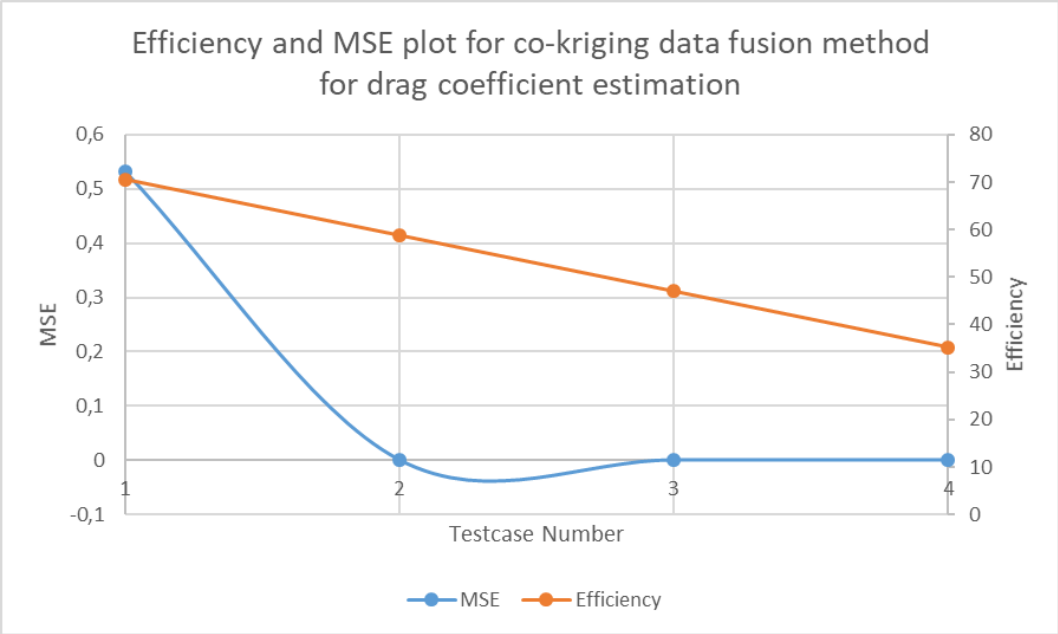

Figure 4.27. Comparison of efficiency and MSE for co-Kriging data fusion method drag coefficient estimation for the first four testcases

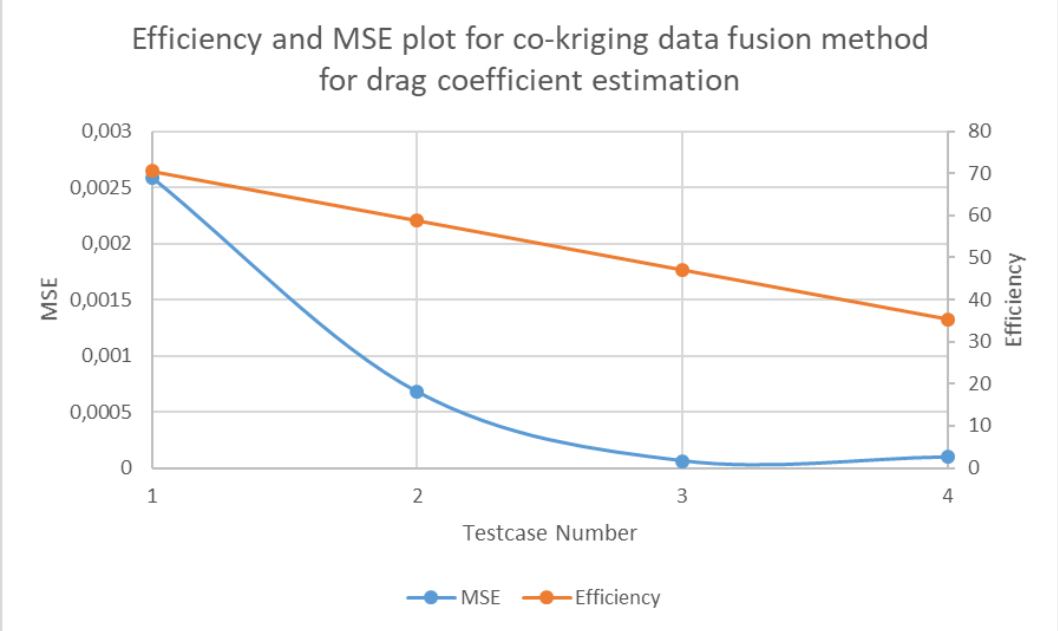

Figure 4.28. Comparison of efficiency and MSE for co-Kriging data fusion method drag coefficient estimation for the second four testcases

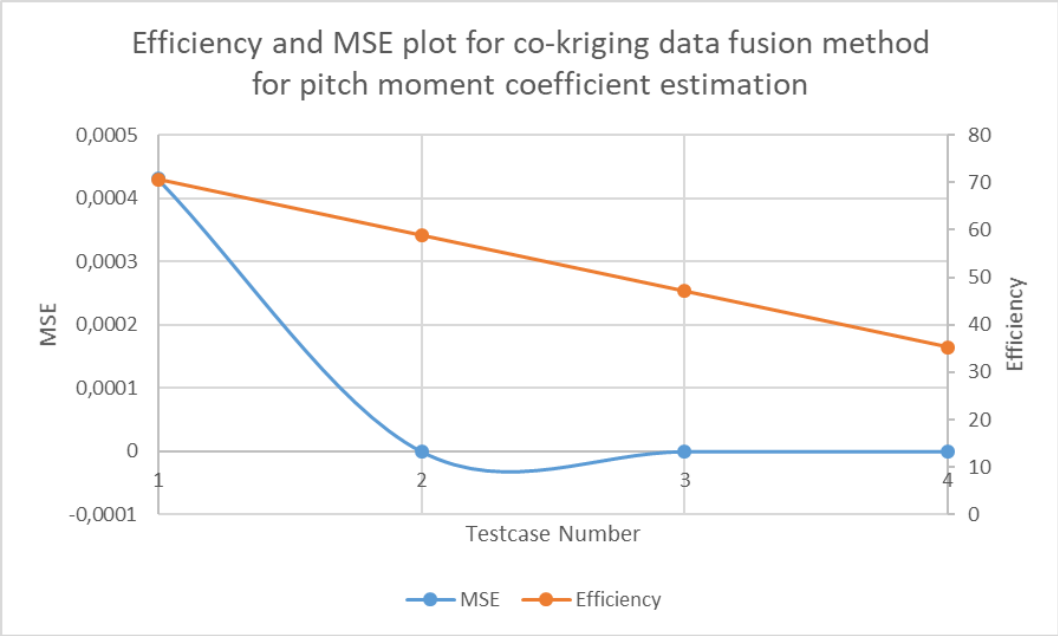

Figure 4.29. Comparison of efficiency and MSE for co-Kriging data fusion method pitch moment coefficient estimation for the first four testcases

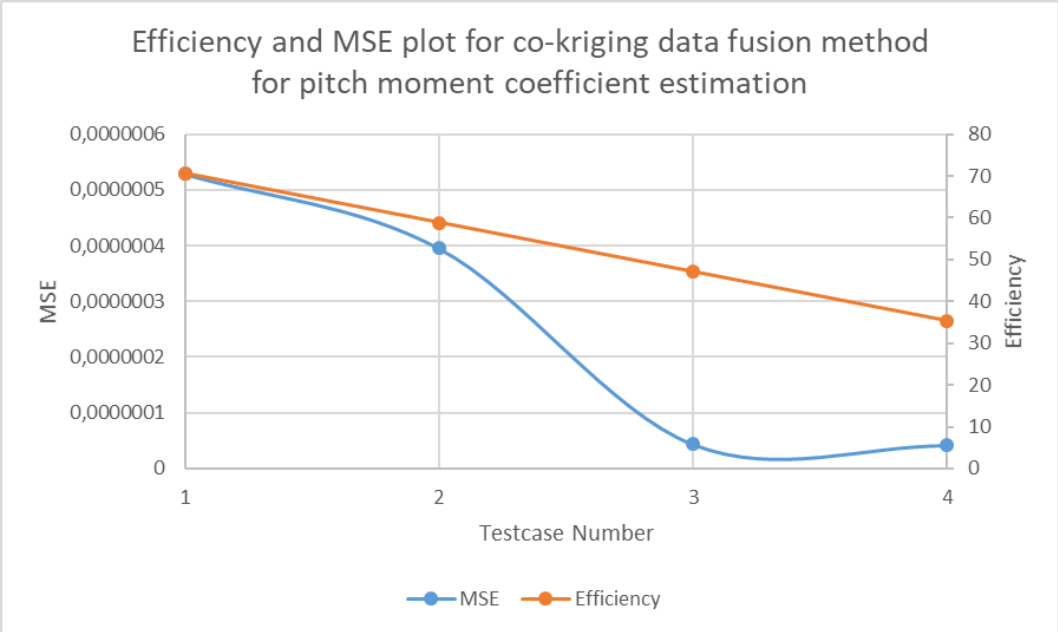

Figure 4.30. Comparison of efficiency and MSE for co-Kriging data fusion method pitch moment coefficient estimation for the second four testcases

As shown in Figure 4.26 and 4.27, when the error value and efficiency values are compared, the most suitable test-case for the lift coefficient is 8. The efficiency value is high and at the same time the error value is low compared to the other testcases. In Figure 4.28 and 4.29, the best case for drag coefficient estimation is test case 8. For pitch moment estimation, the test case number 8 is shown in Figure 4.29 and 4.30, which has high efficiency but low error value.

4.2. Multi-Fidelity Gaussian Process Regression Data Fusion Method

In this data fusion method, two different data sources were used. First, low and high fidelity data were combined. Fewer high fidelity data and more low fidelity data are used and data fusion is performed. The data obtained as a result of the fusion will have higher fidelity than the low fidelity data. For this purpose, the performance of the data fusion process was examined by using different numbers and fidelity types of data. Radial Basis Function (RBF) was used as the kernel function for the multi-fidelity GPR method. Accordingly, the test-case prepared to measure the performance of the multi-fidelity GPR method is shown in Table 4.1. The data fusion process according to the test cases in Table 4.1 is listed below for lift, drag and moment coefficients.

4.2.1. Multi-fidelity GPR method prediction to obtain lift coefficient

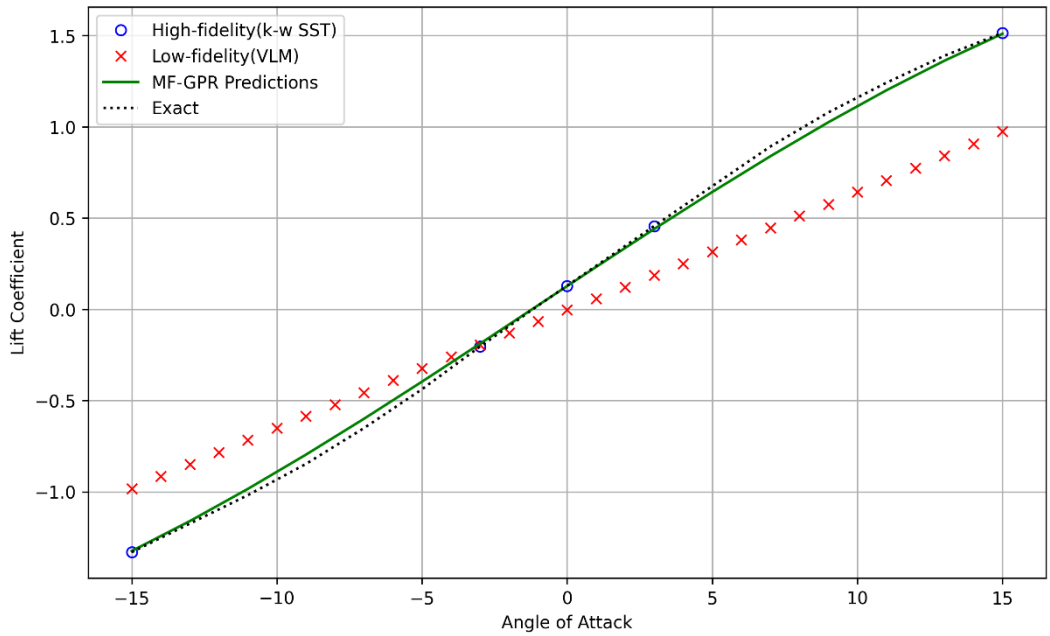

Figure 4.31. Multi-fidelity Gaussian Process Regression lift coefficient estimate using 31 low-fidelity and 5 high-fidelity data corresponding to test case 1

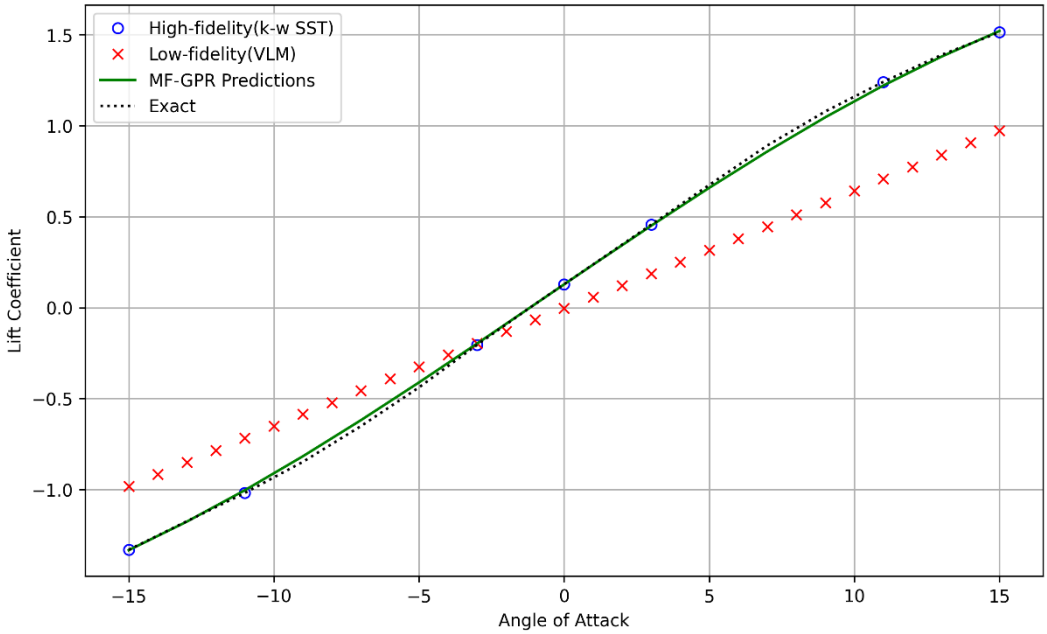

Figure 4.32. Multi-fidelity Gaussian Process Regression lift coefficient estimate using 31 low-fidelity and 7 high-fidelity data corresponding to test case 2

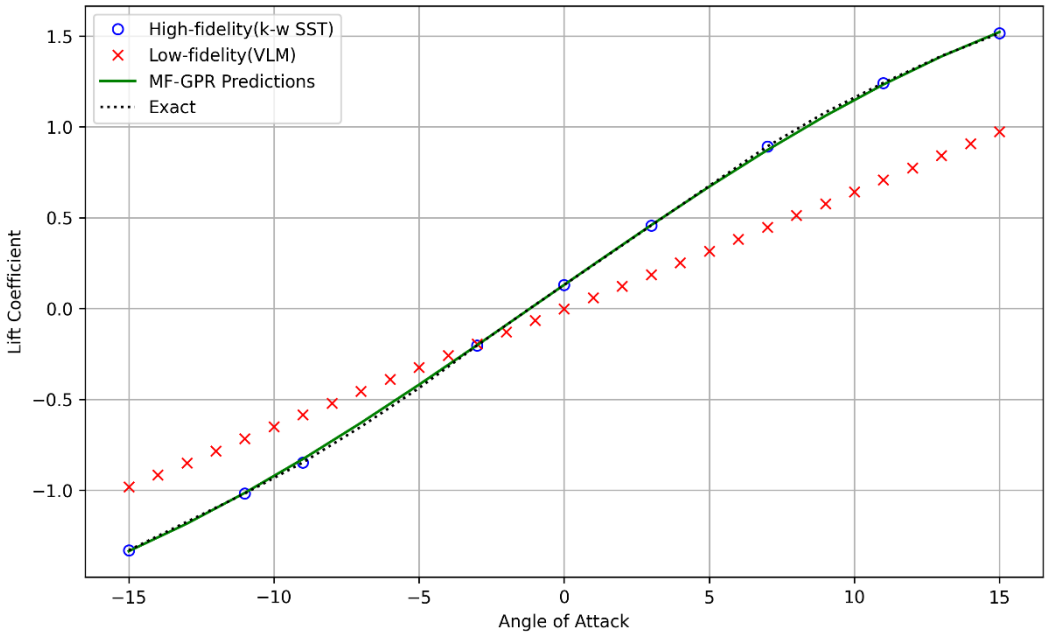

Figure 4.33. Multi-fidelity Gaussian Process Regression lift coefficient estimate using 31 low-fidelity and 9 high-fidelity data corresponding to test case 3

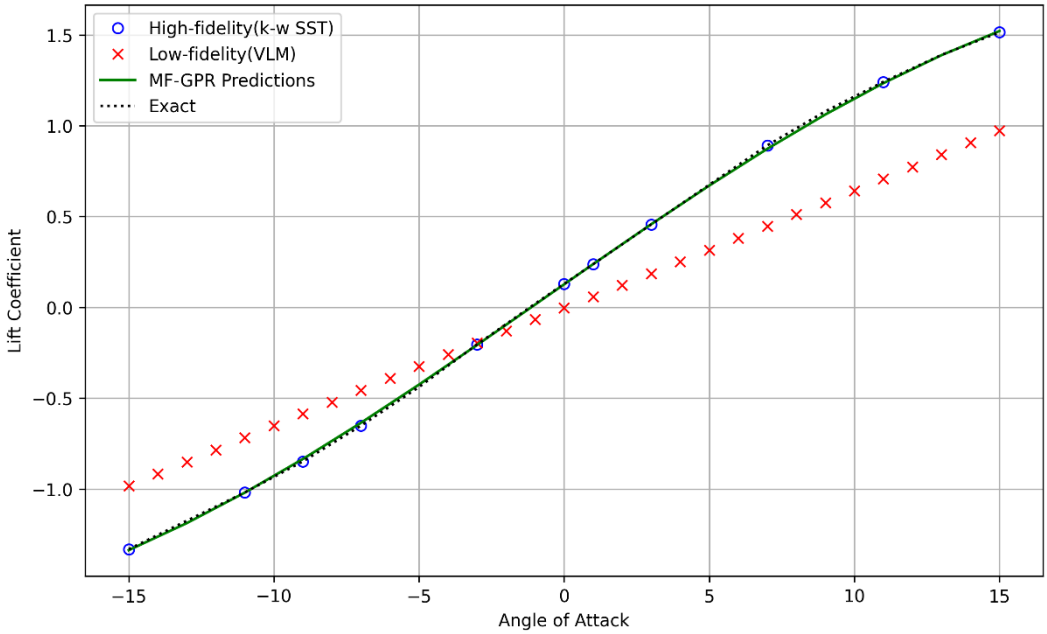

Figure 4.34. Multi-fidelity Gaussian Process Regression lift coefficient estimate using 31 low-fidelity and 11 high-fidelity data corresponding to test case 4

The predictions obtained when the number of low-fidelity data was reduced from 31 to 15 are listed below.

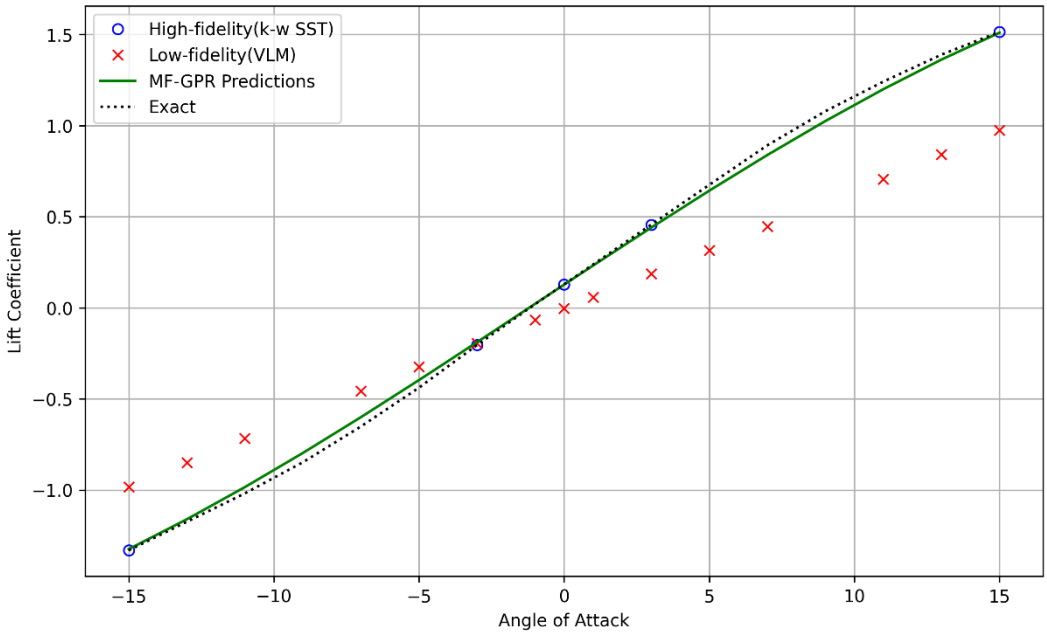

Figure 4.35. Multi-fidelity Gaussian Process Regression lift coefficient estimate using 15 low-fidelity and 5 high-fidelity data corresponding to test case 5

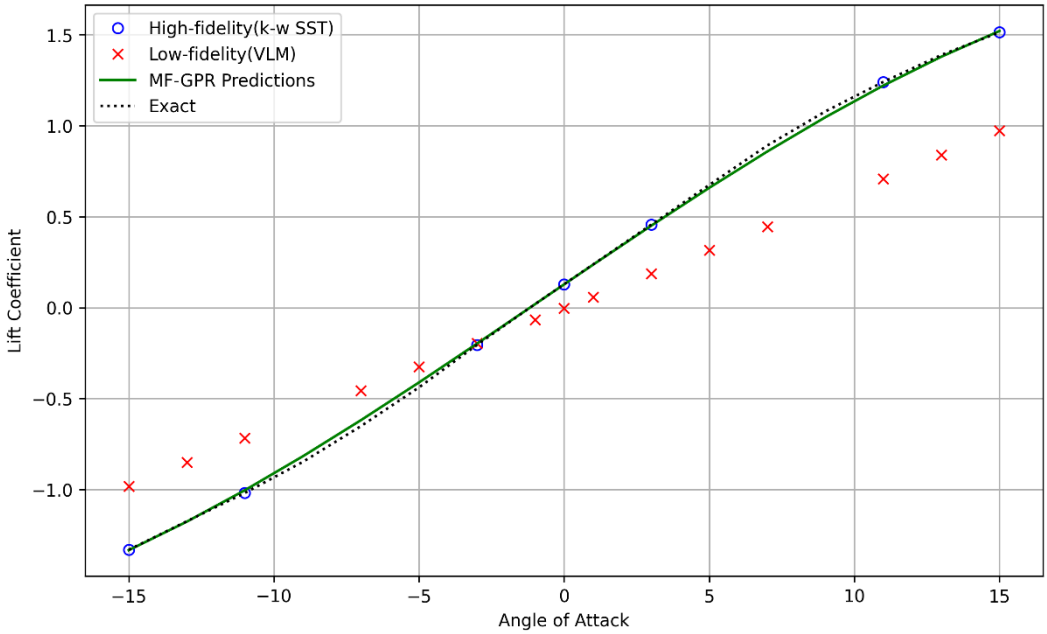

Figure 4.36. Multi-fidelity Gaussian Process Regression lift coefficient estimate using 15 low-fidelity and 7 high-fidelity data corresponding to test case 6

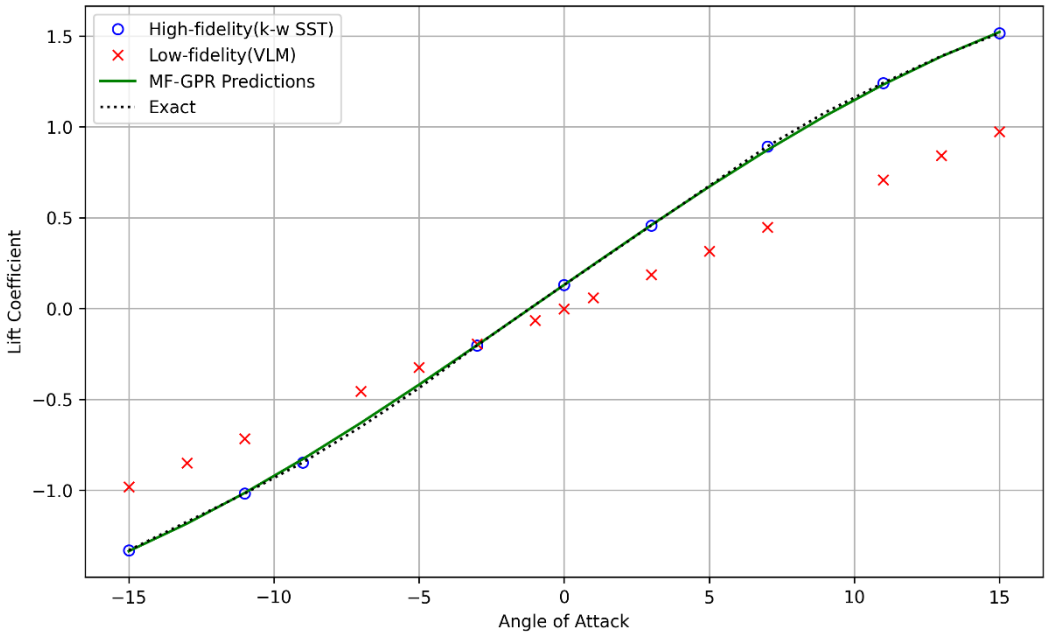

Figure 4.37. Multi-fidelity Gaussian Process Regression lift coefficient estimate using 15 low-fidelity and 9 high-fidelity data corresponding to test case 7

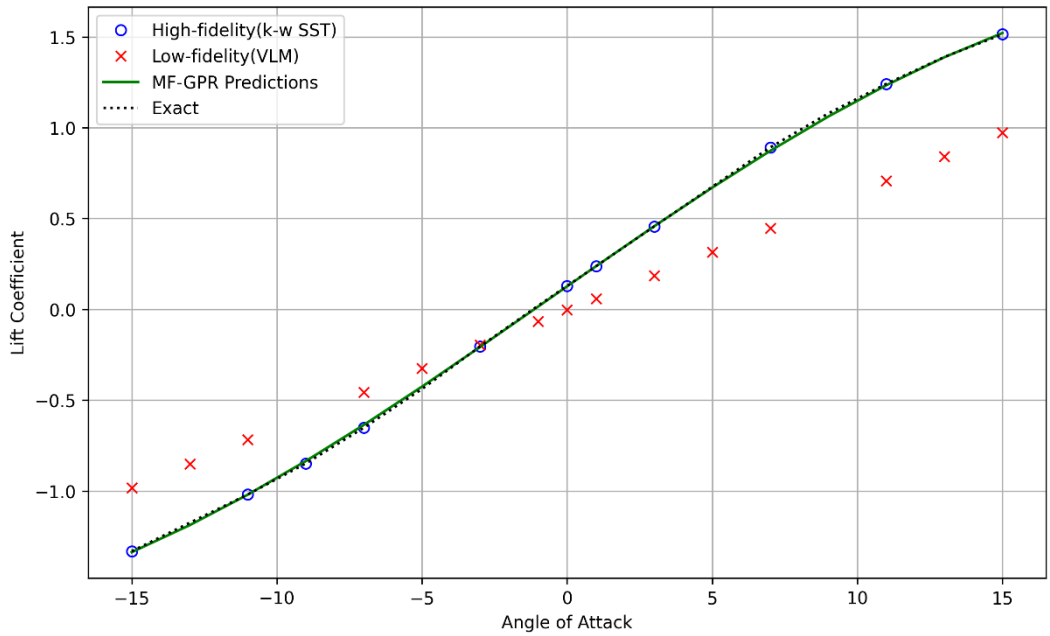

Figure 4.38. Multi-fidelity Gaussian Process Regression lift coefficient estimate using 15 low-fidelity and 11 high-fidelity data corresponding to test case 8

Table 4.9. Multi-fidelity GPR method lift coefficient estimation error value

Test Case Number	Mean Square Error (MSE)	Data Configuration
1	0,0010664820552	31 Low and 5 High Fidelity Data
2	0,0003515745474	31 Low and 7 High Fidelity Data
3	0,0001326546781	31 Low and 9 High Fidelity Data
4	0,0000952156600	31 Low and 11 High Fidelity Data

Table 4.10. Multi-fidelity GPR method lift coefficient estimation error value

Test Case Number	Mean Square Error (MSE)	Data Configuration
1	0,001066482	15 Low and 5 High Fidelity Data
2	0,000351575	15 Low and 7 High Fidelity Data
3	0,000132655	15 Low and 9 High Fidelity Data
4	0,000095256	15 Low and 11 High Fidelity Data

There are 8 test-cases in the lift coefficient estimation process with Multi-fidelity Gaussian Process Regression data fusion method. For the first 4 test cases with 31 low-fidelity data, the number of high- fidelity data increases. The predictions generally improve as the number of high fidelity data increases. Here, the model with 31 low- fidelity and 11 high- fidelity models offers the best result. However, test-case 4 is the most efficient model in terms of efficiency as the other models give very close results.

4.2.2. Multi-fidelity GPR method prediction to obtain drag coefficient

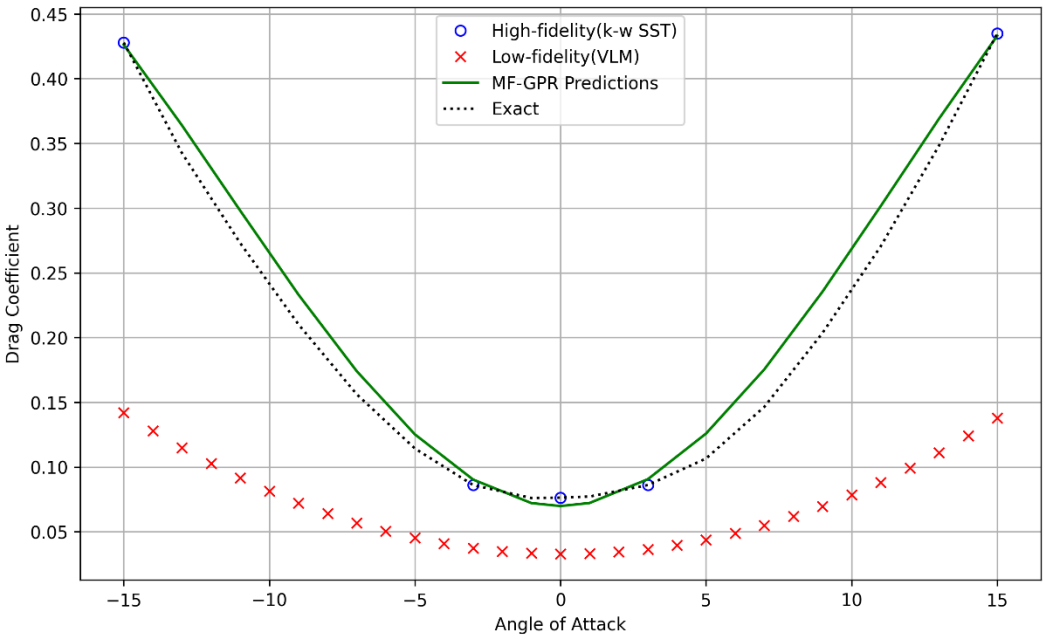

Figure 4.39. Multi-fidelity Gaussian Process Regression drag coefficient estimate using 31 low-fidelity and 5 high-fidelity data corresponding to test case 1

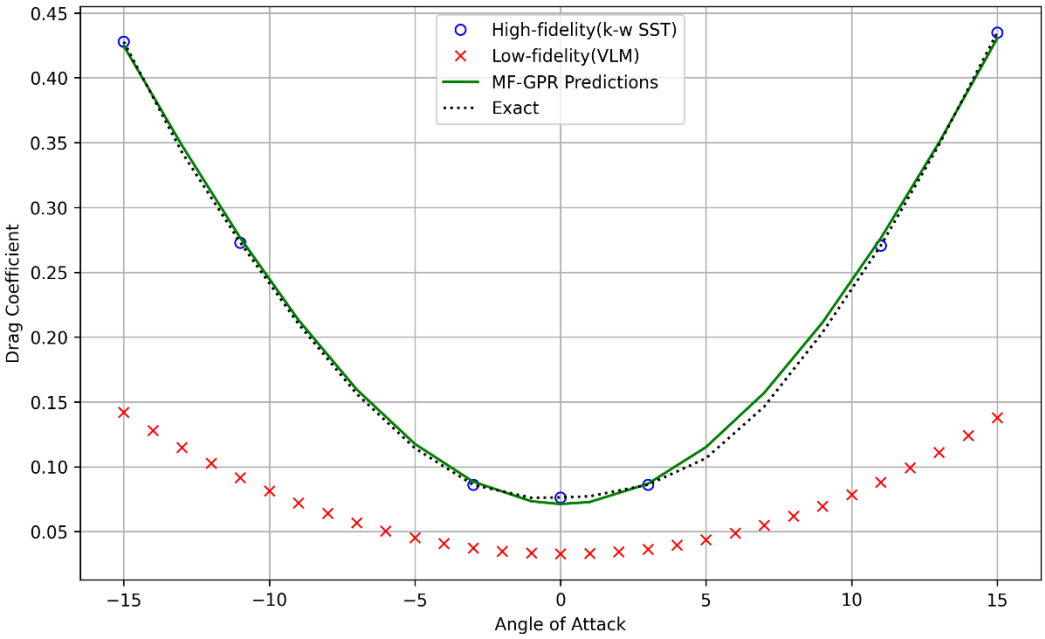

Figure 4.40. Multi-fidelity Gaussian Process Regression drag coefficient estimate using 31 low-fidelity and 7 high-fidelity data corresponding to test case 2

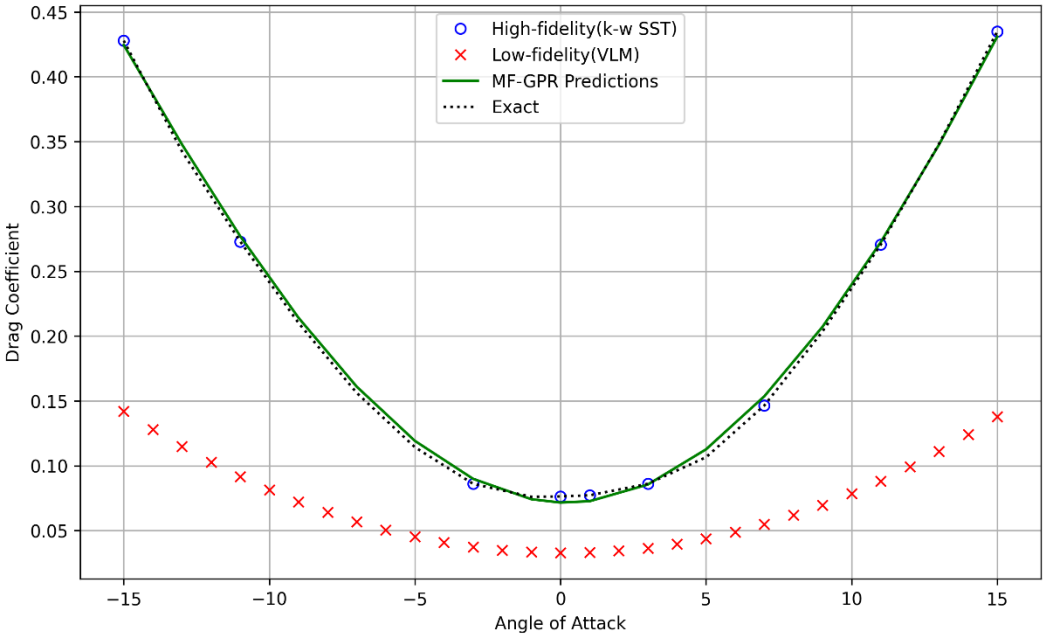

Figure 4.41. Multi-fidelity Gaussian Process Regression drag coefficient estimate using 31 low-fidelity and 9 high-fidelity data corresponding to test case 3

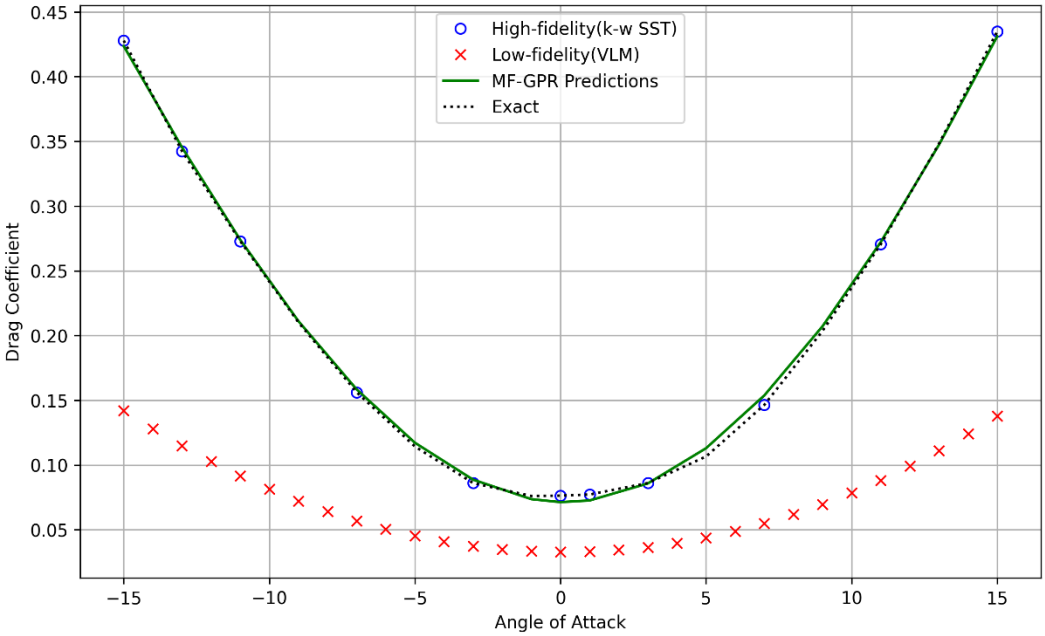

Figure 4.42. Multi-fidelity Gaussian Process Regression drag coefficient estimate using 31 low-fidelity and 11 high-fidelity data corresponding to test case 4

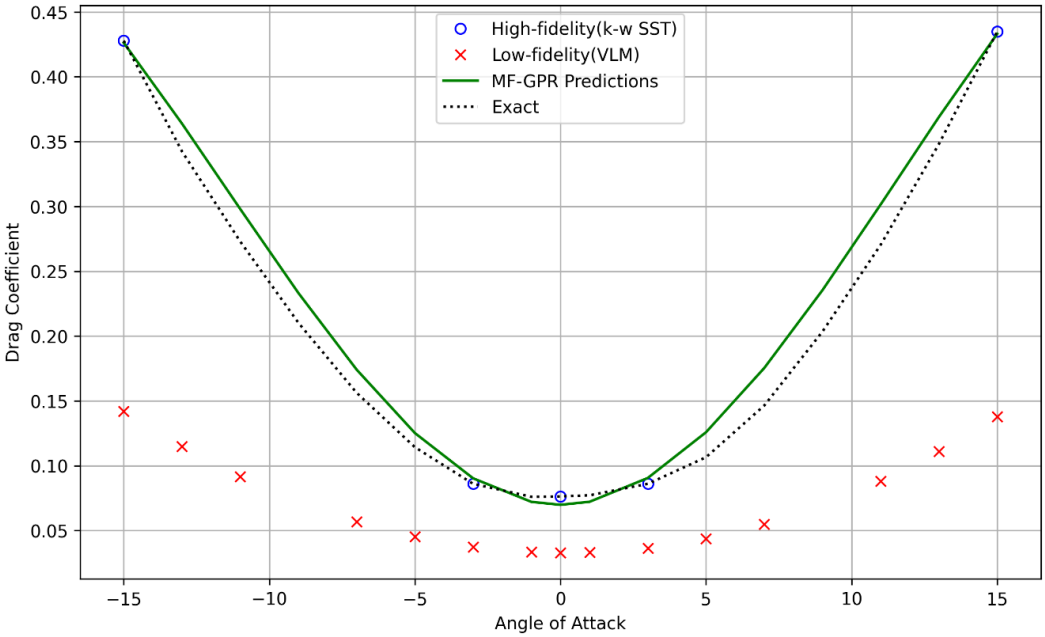

Figure 4.43. Multi-fidelity Gaussian Process Regression drag coefficient estimate using 15 low-fidelity and 5 high-fidelity data corresponding to test case 5

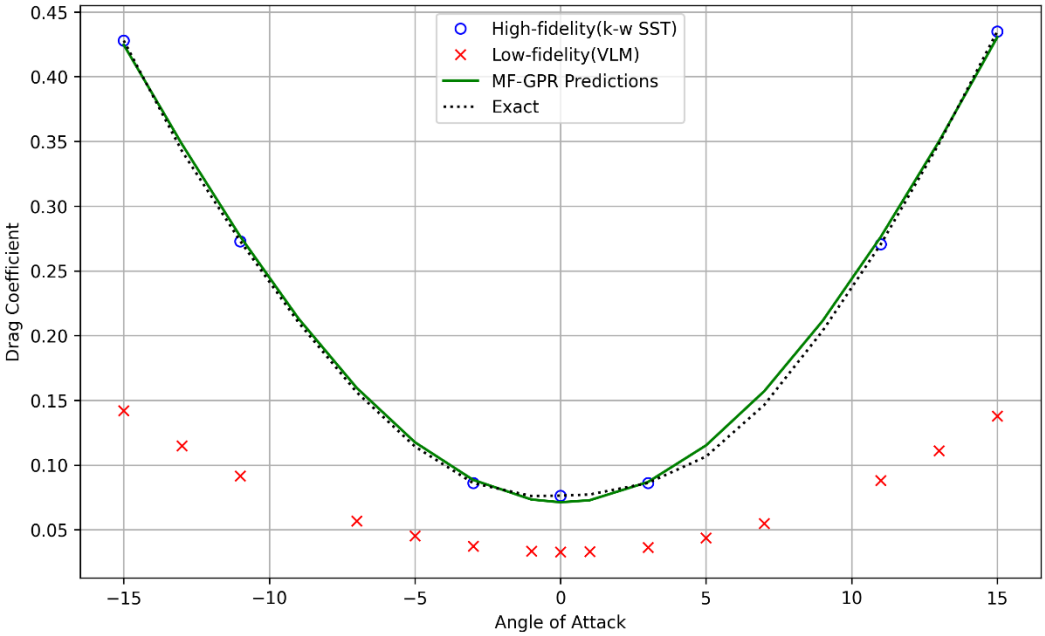

Figure 4.44. Multi-fidelity Gaussian Process Regression drag coefficient estimate using 15 low-fidelity and 7 high-fidelity data corresponding to test case 6

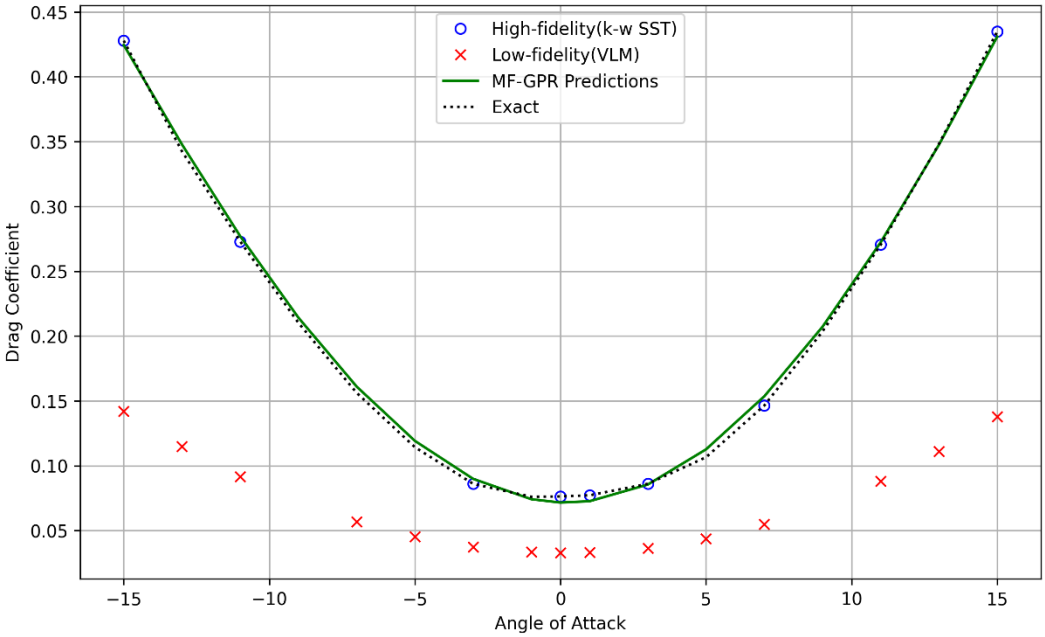

Figure 4.45. Multi-fidelity Gaussian Process Regression drag coefficient estimate using 15 low-fidelity and 9 high-fidelity data corresponding to test case 7

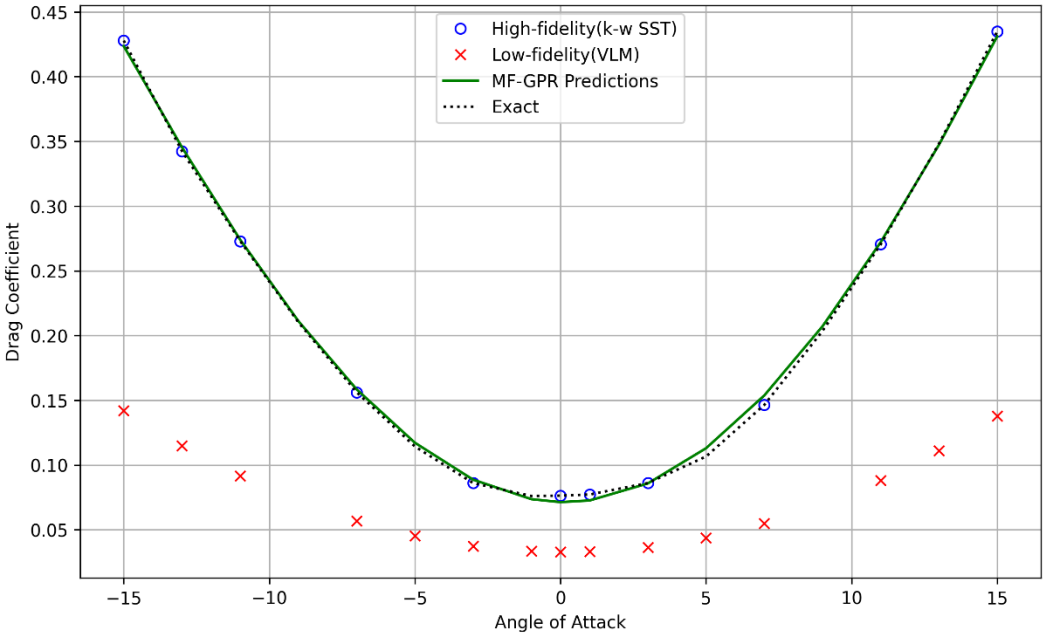

Figure 4.46. Multi-fidelity Gaussian Process Regression drag coefficient estimate using 15 low-fidelity and 11 high-fidelity data corresponding to test case 8

Table 4.11. Multi-fidelity GPR method drag coefficient estimation error value

Test Case Number	Mean Square Error (MSE)	Data Configuration
1	0,0003417207759	31 Low and 5 High Fidelity Data
2	0,0000261927050	31 Low and 7 High Fidelity Data
3	0,0000177449330	31 Low and 9 High Fidelity Data
4	0,0000133269291	31 Low and 11 High Fidelity Data

Table 4.12. Multi-fidelity GPR method drag coefficient estimation error value

Test Case Number	Mean Square Error (MSE)	Data Configuration
1	0,000341721	15 Low and 5 High Fidelity Data
2	0,000026192706	15 Low and 7 High Fidelity Data
3	0,000017744933	15 Low and 9 High Fidelity Data
4	0,0000133269292	15 Low and 11 High Fidelity Data

The drag coefficient was estimated using MF-GPR and the performance of the model was measured by varying the amount of low and high fidelity data. Here, for the test cases using 31 low-fidelity data, increasing the number of high-fidelity data facilitated the model to make better predictions. When we decrease the number of low-fidelity data in the model, the prediction performance of the model is not affected much and the prediction performance increases with the increase in the number of high-fidelity data.

4.2.3. Multi-fidelity GPR method prediction to obtain pitch moment coefficient

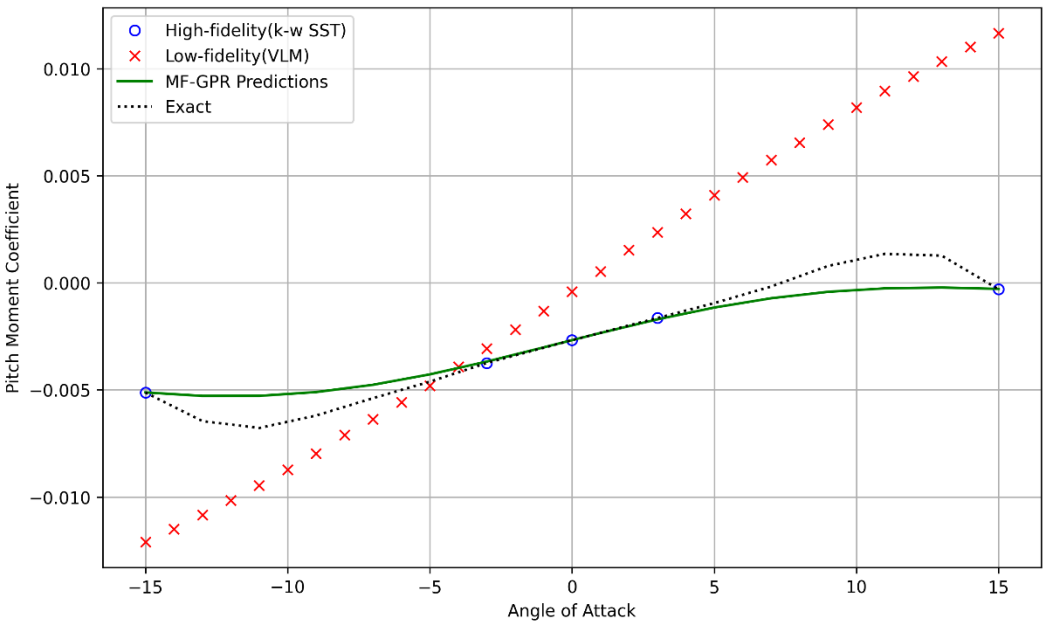

Figure 4.47. Multi -fidelity Gaussian Process Regression pitch moment coefficient estimate using 31 low-fidelity and 5 high-fidelity data corresponding to test case 1

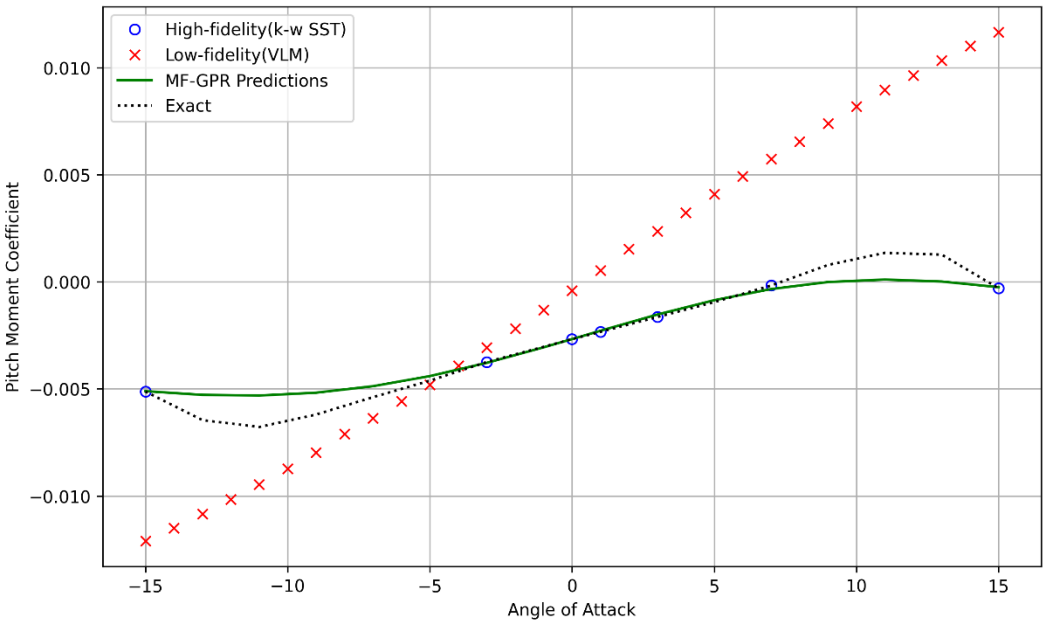

Figure 4.48. Multi-fidelity Gaussian Process Regression pitch moment coefficient estimate using 31 low-fidelity and 7 high-fidelity data corresponding to test case 2

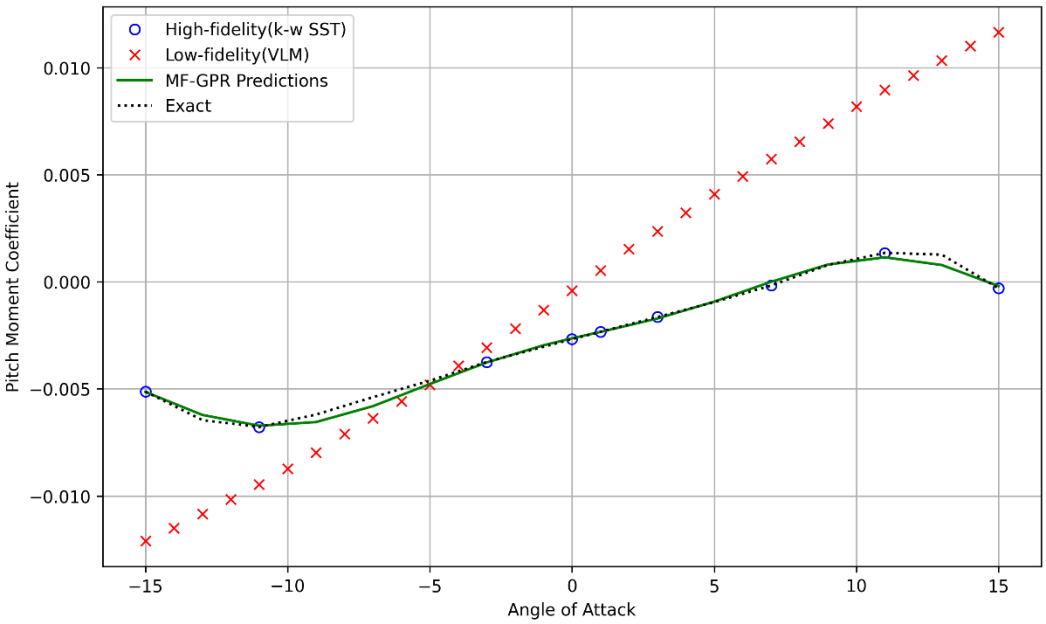

Figure 4.49. Multi-fidelity Gaussian Process Regression pitch moment coefficient estimate using 31 low-fidelity and 9 high-fidelity data corresponding to test case 3

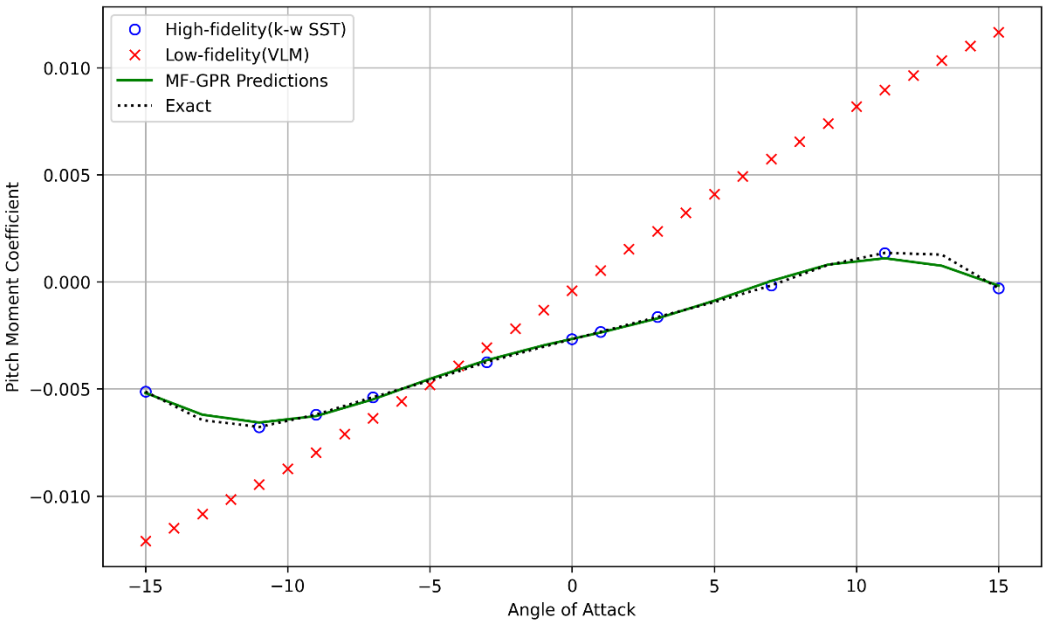

Figure 4.50. Multi-fidelity Gaussian Process Regression pitch moment coefficient estimate using 31 low-fidelity and 11 high-fidelity data corresponding to test case 4

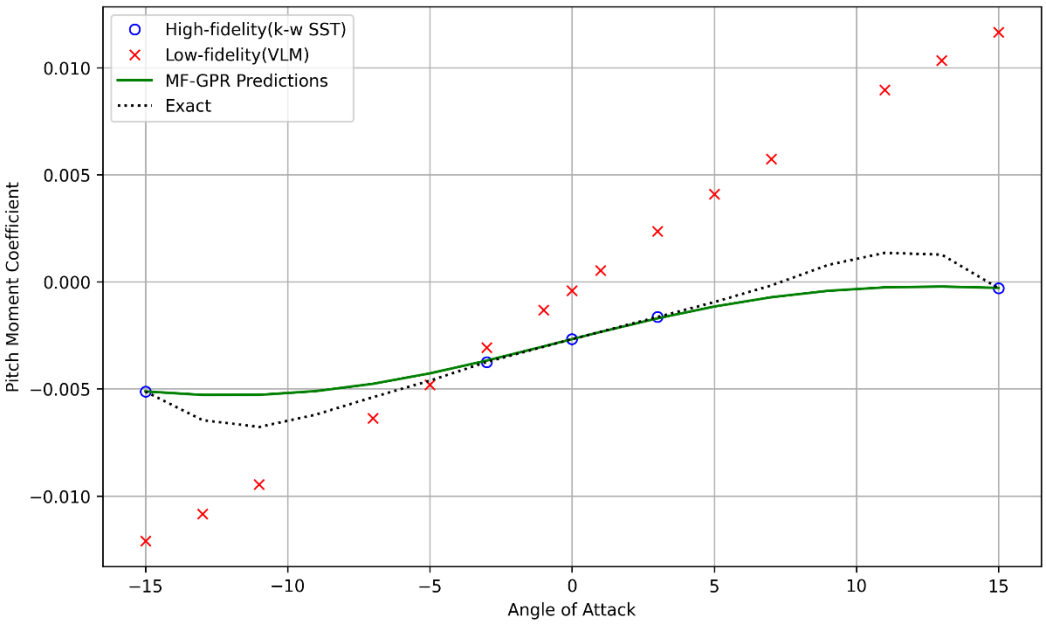

Figure 4.51. Multi-fidelity Gaussian Process Regression pitch moment coefficient estimate using 15 low-fidelity and 5 high-fidelity data corresponding to test case 5

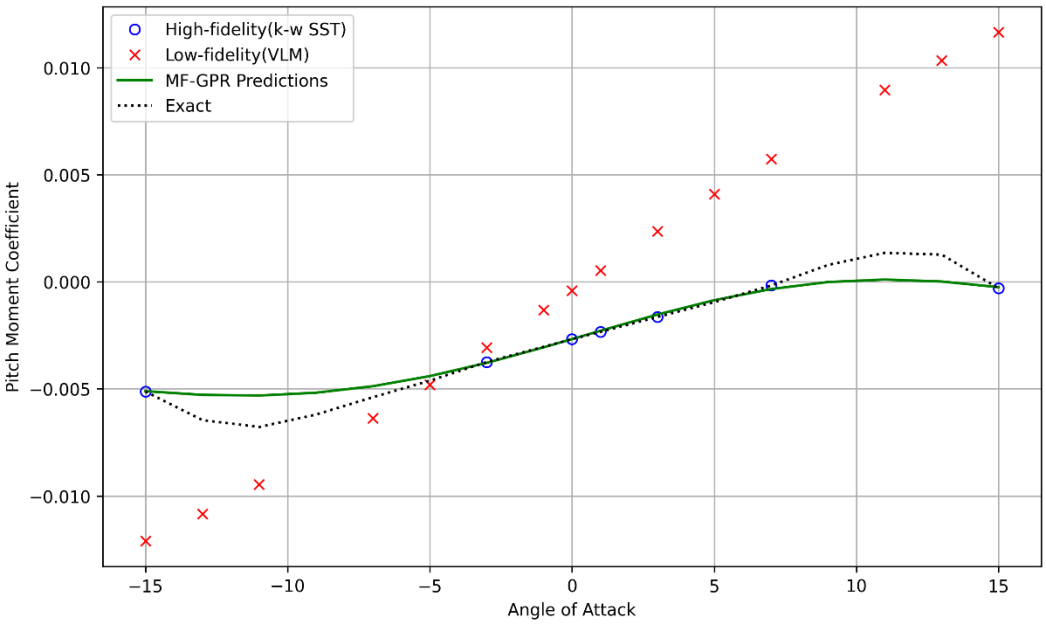

Figure 4.52. Multi-fidelity Gaussian Process Regression pitch moment coefficient estimate using 15 low-fidelity and 7 high-fidelity data corresponding to test case 6

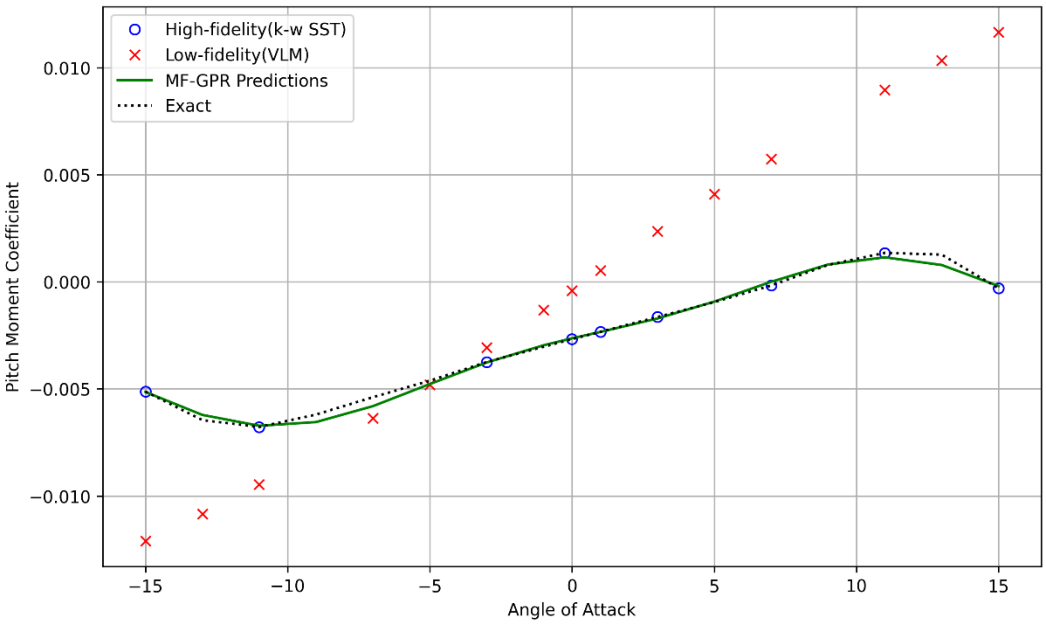

Figure 4.53. Multi-fidelity Gaussian Process Regression pitch moment coefficient estimate using 15 low-fidelity and 9 high-fidelity data corresponding to test case 7

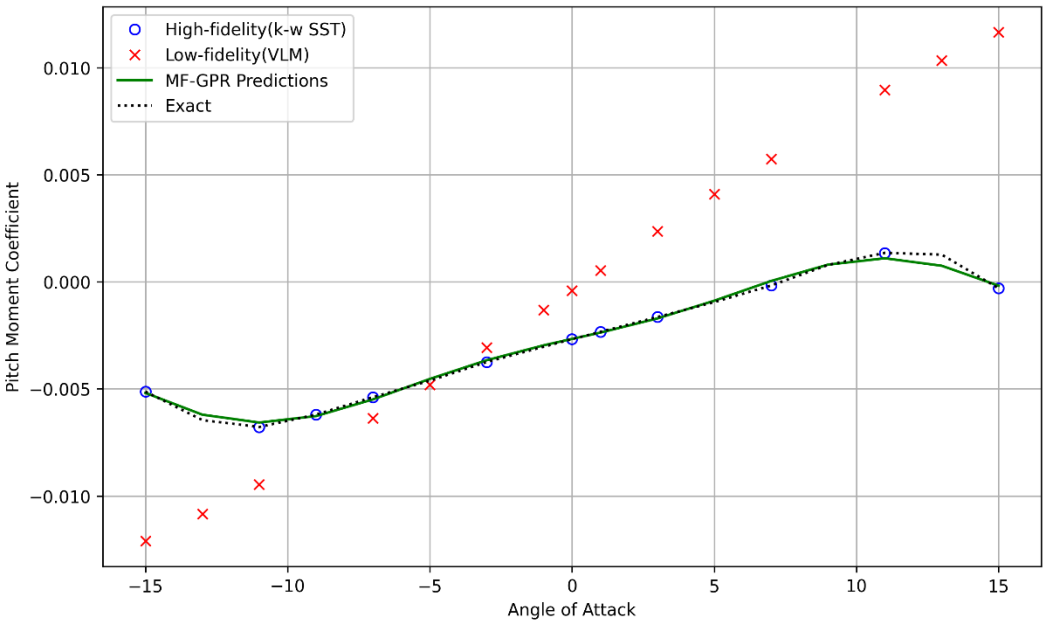

Figure 4.54. Multi-fidelity Gaussian Process Regression pitch moment coefficient estimate using 15 low-fidelity and 11 high-fidelity data corresponding to test case 8

The pitch moment coefficient was estimated using MF-GPR and the performance of the model was measured by varying the amount of low and high fidelity data. it is concluded that the prediction performance improves with increasing the number of high-fidelity data. When we decrease the number of low-fidelity data in the model, the data training performance does not change noticeably. However, in tests where the number of high-fidelity data is low, increasing the number of low-fidelity data is important for GPR method prediction.

Table 4.13. Multi-fidelity GPR method pitch moment coefficient estimation error value

Test Case Number	Mean Square Error (MSE)	Data Configuration
1	0,0000007038420	31 Low and 5 High Fidelity Data
2	0,0000000666647	31 Low and 7 High Fidelity Data
3	0,0000000512180	31 Low and 9 High Fidelity Data
4	0,0000000323295	31 Low and 11 High Fidelity Data

Table 4.14. Multi-fidelity GPR method pitch moment coefficient estimation error value

Test Case Number	Mean Square Error (MSE)	Data Configuration
1	0,0000007038421	15 Low and 5 High Fidelity Data
2	0,000000051266	15 Low and 7 High Fidelity Data
3	0,000000042180	15 Low and 9 High Fidelity Data
4	0,0000000323295	15 Low and 11 High Fidelity Data

Table 4.15. Efficiency and mse comparison of each parameter for multi-fidelity Gaussian Process Regression Data Fusion Method

Parameter	Test case number	MF-GPR prediction time (s)	Time required to obtain the data used in test case (s)	Time required to obtain the all data (s)	Efficiency (%)	MSE
C_l	1	4,6	612 593	2 080 800	70,55975	0,001066482
C_l	2	4,8	857 392	2 080 800	58,795	0,000351574
C_l	3	3,0	1 102 193	2 080 800	47,03036	0,000132654
C_l	4	3,4	1 346 992	2 080 800	35,26564	0,000095215
C_l	5	4,8	612 288	2 080 800	70,53436	0,001066482
C_l	6	3,9	857 088	2 080 800	58,8096	0,000351575
C_l	7	4,0	1 101 889	2 080 800	47,04495	0,000132655
C_l	8	5,0	1 346 688	2 080 800	35,28019	0,000095256
C_d	1	4,0	612 592	2 080 800	70,55977	0,000341720
C_d	2	3,0	857 392	2 080 800	58,79505	0,000026192
C_d	3	3,7	1 102 193	2 080 800	47,03035	0,000017744
C_d	4	4,2	1 346 992	2 080 800	35,26566	0,000013326
C_d	5	4,8	612 289	2 080 800	70,53436	0,000341721
C_d	6	3,8	857 088	2 080 800	58,8096	0,000026192
C_d	7	3,9	1 101 889	2 080 800	47,04492	0,000017744
C_d	8	4,0	1 346 688	2 080 800	35,28023	0,000013326
C_m	1	3,2	612 592	2 080 800	70,55973	0,000000703
C_m	2	3,3	857 392	2 080 800	58,79506	0,000000066
C_m	3	4,5	1 102 193	2 080 800	47,03035	0,000000051
C_m	4	3,4	1 346 993	2 080 800	35,26563	0,000000032
C_m	5	3,4	612 288	2 080 800	70,57438	0,000000703
C_m	6	4,9	857 089	2 080 800	58,80966	0,000000051
C_m	7	4,0	1 101 888	2 080 800	47,04493	0,00000004
C_m	8	4,5	1 346 689	2 080 800	35,28023	0,000000032

All test results are listed in Table 4.15. Looking at the table, when the efficiency values are examined in the tests performed for all parameters, the maximum efficiency for the estimation of lift, drag and pitch moment coefficient is theoretically seen in test cases 1 and 5 with 70.55%. However, when the mse rates are analyzed, the lowest error value are not in test cases 1 and 5. The error values are lowest in test case 4 for lift coefficient, in test cases 4 and 8 for drag coefficient and all values are approximately the same for pitch moment coefficient. However, high efficiency alone is not desirable. At the same time, where efficiency is high, the error value should be low. Figures 4.55, 4.56, 4.57, 4.58, 4.59 and 4.60 show the efficiency versus error value for three different aerodynamic parameters.

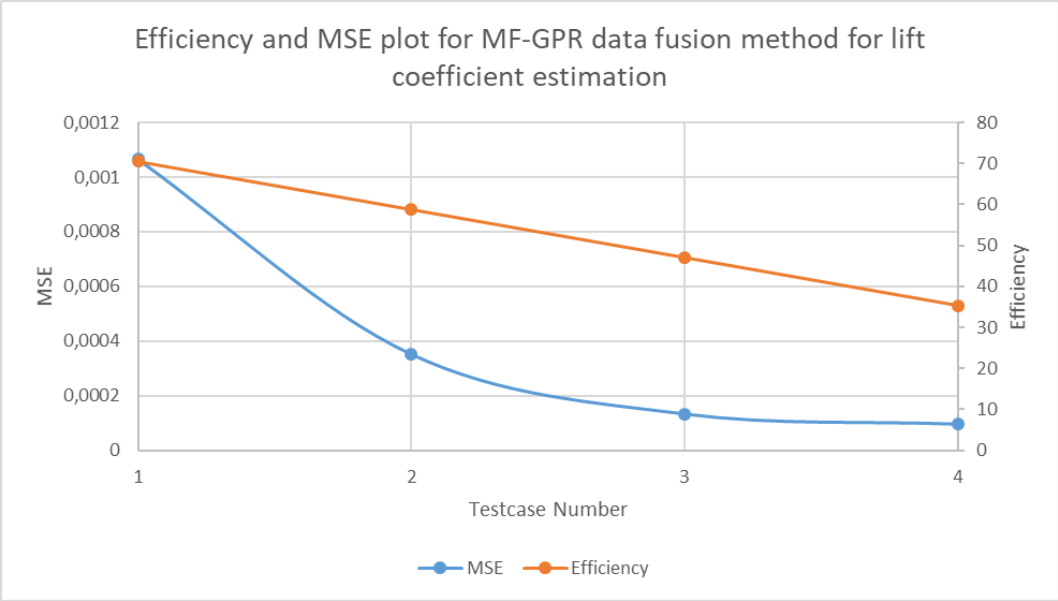

Figure 4.55. Multi-fidelity Gaussian Process Regression method efficiency and MSE comparison for lift coefficient estimation for the first four testcases

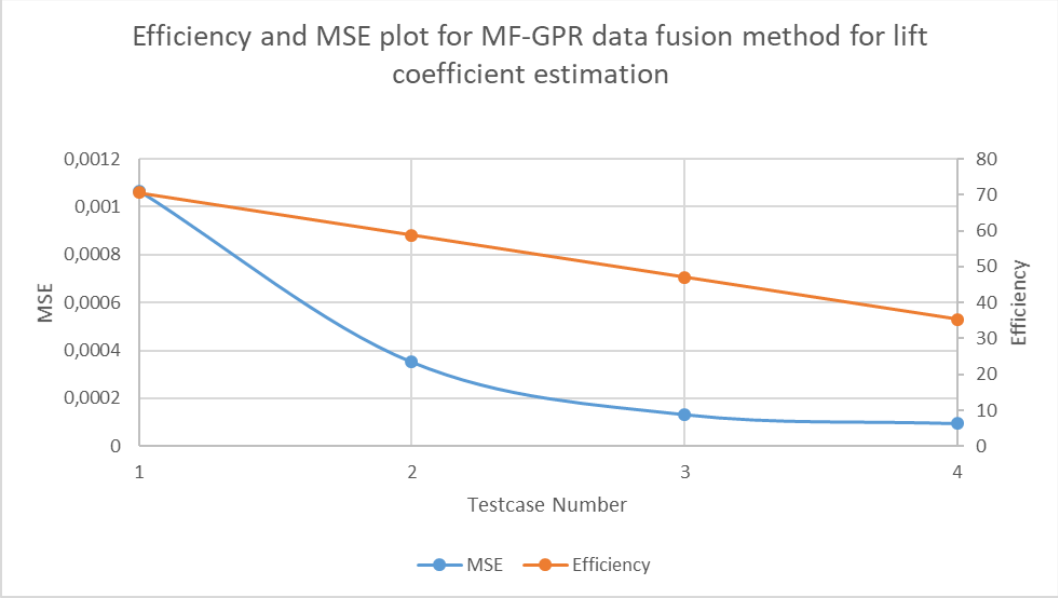

Figure 4.56. Multi-fidelity Gaussian Process Regression method efficiency and MSE comparison for lift coefficient estimation for the second four testcases

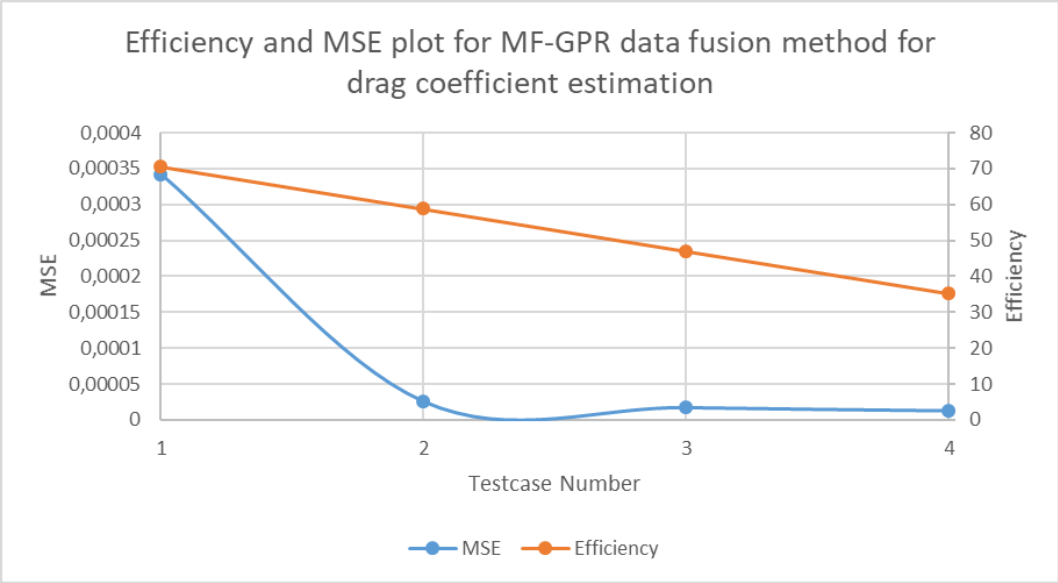

Figure 4.57. Multi-fidelity Gaussian Process Regression method efficiency and MSE comparison for drag coefficient estimation for the first four testcases

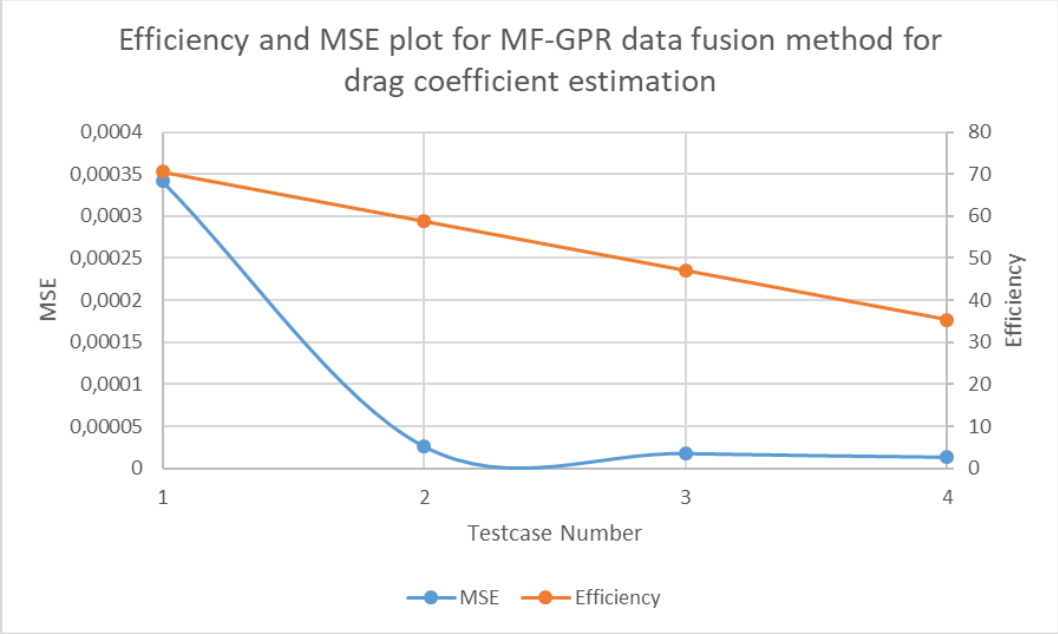

Figure 4.58. Multi-fidelity Gaussian Process Regression method efficiency and MSE comparison for drag coefficient estimation for the second four testcases

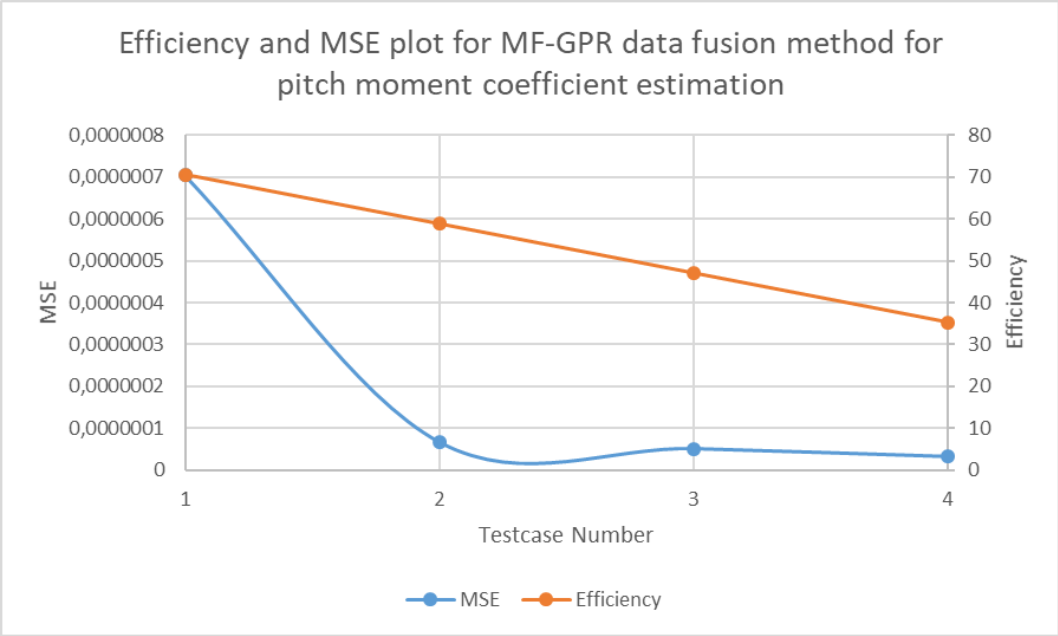

Figure 4.59. Multi-fidelity Gaussian Process Regression method efficiency and MSE comparison for pitch moment coefficient estimation for the first four testcases

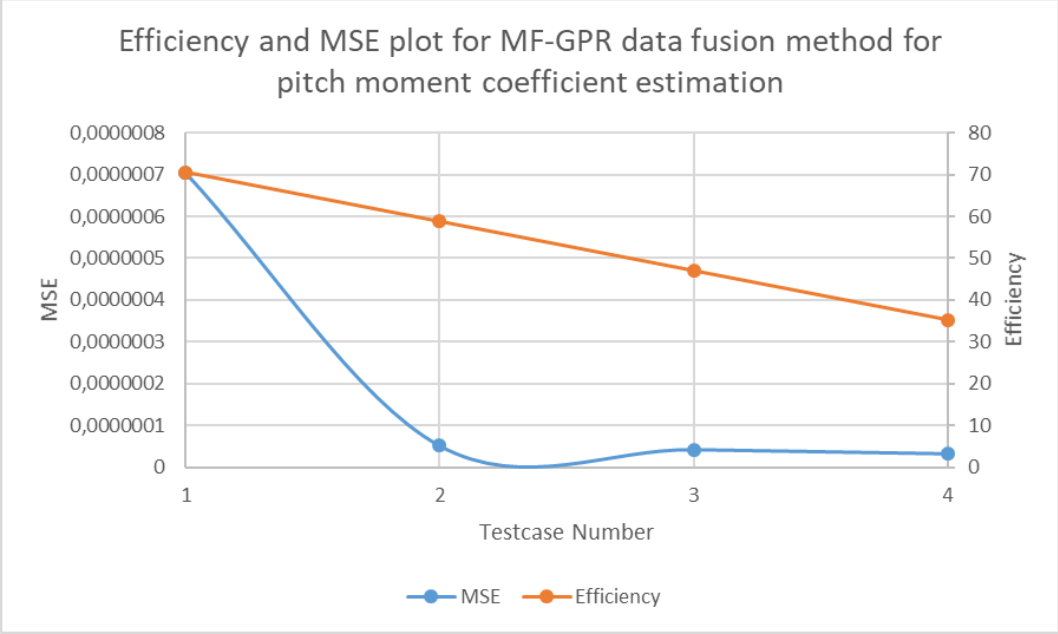

Figure 4.60. Multi-fidelity Gaussian Process Regression method efficiency and MSE comparison for pitch moment coefficient estimation for the second four testcases

Figure 4.55 and 4.56 shows that the most appropriate model for the MF-GPR method for the lift coefficient prediction is test case 3; Figure 4.57 and 4.58 shows that test case 2 for drag coefficient and Figure 4.59 and 4.60 shows that test case 2 for pitch moment coefficient showed the best performance in the MSE comparison according to efficiency.

4.3. Multi-Fidelity Neural Network Data Fusion Method

In this method, data fusion was performed using data with two different fidelities data sources. In the data fusion process using artificial neural networks, Tanh function was used as the activation function. The neural network consists of 4 hidden layers and each layer has 16 neurons. The lift, drag and pitch moment coefficients were estimated with multi-fidelity neural networks. The results are listed below. Using the test cases in Table 4.1, the performance and prediction ability of the multi-fidelity neural networks were measured using different numbers of low and high fidelity data.

4.3.1. Multi-fidelity neural network method prediction to obtain lift coefficient

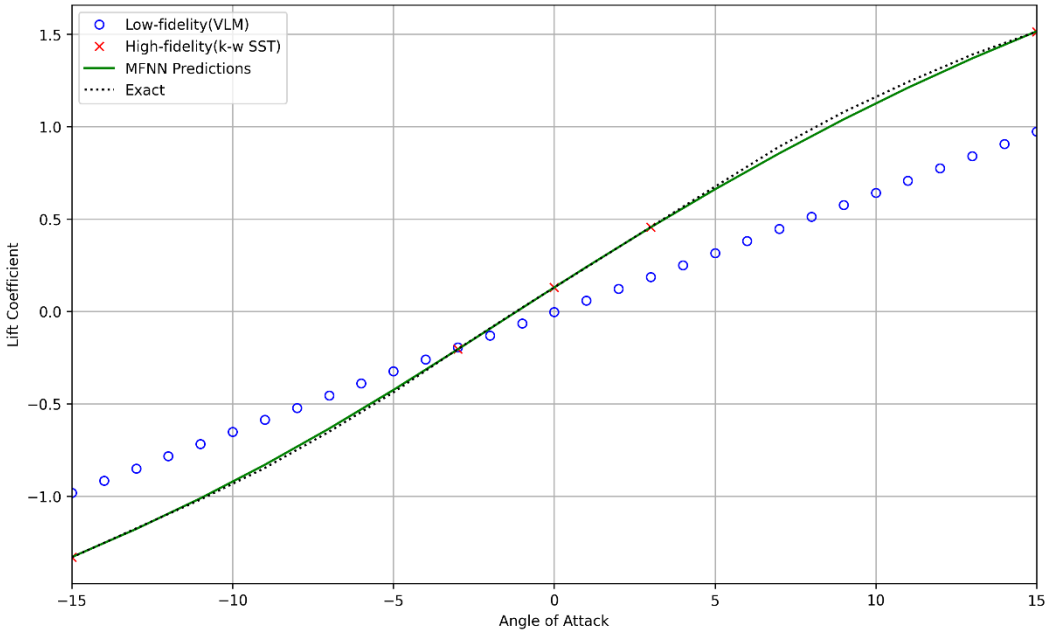

Figure 4.61. Multi-fidelity Neural Network lift coefficient estimate using 31 low-fidelity and 5 high-fidelity data corresponding to test case 1

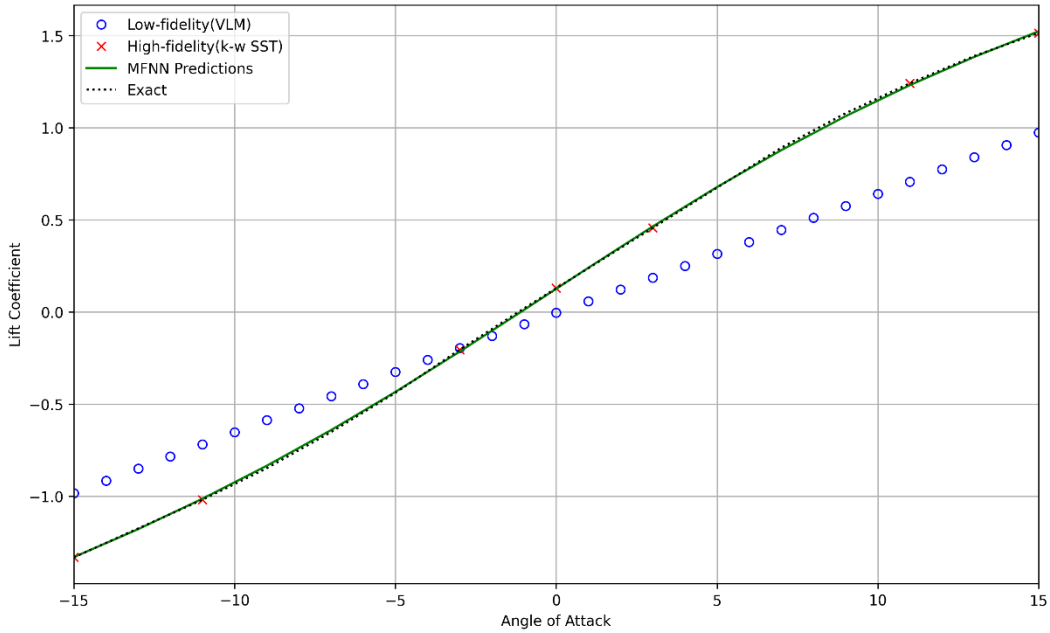

Figure 4.62. Multi-fidelity Neural Network lift coefficient estimate using 31 low-fidelity and 7 high-fidelity data corresponding to test case 2

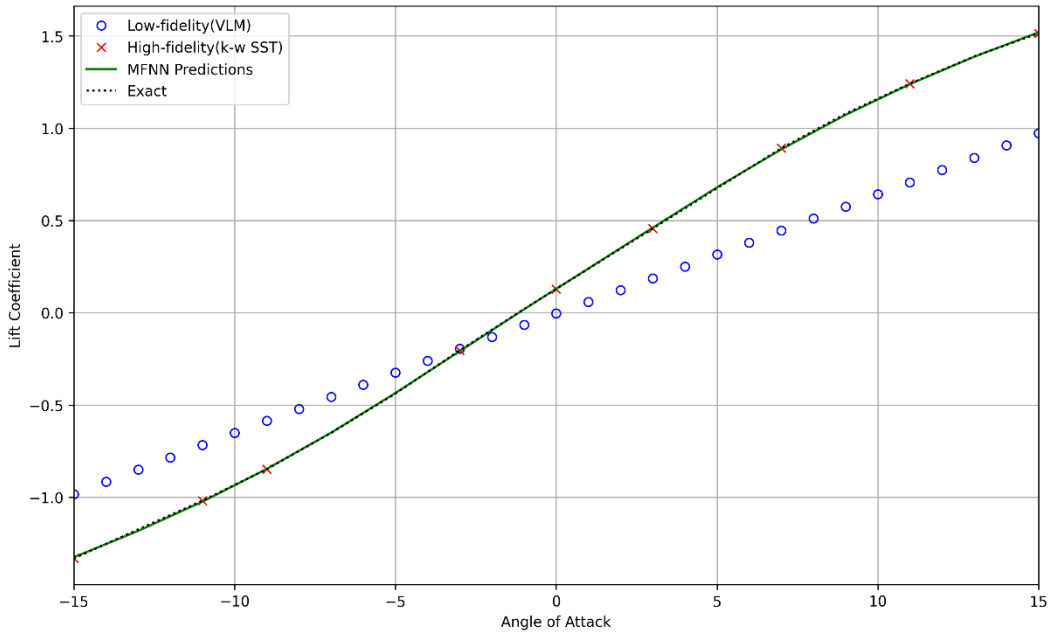

Figure 4.63. Multi-fidelity Neural Network lift coefficient estimate using 31 low-fidelity and 9 high-fidelity data corresponding to test case 3

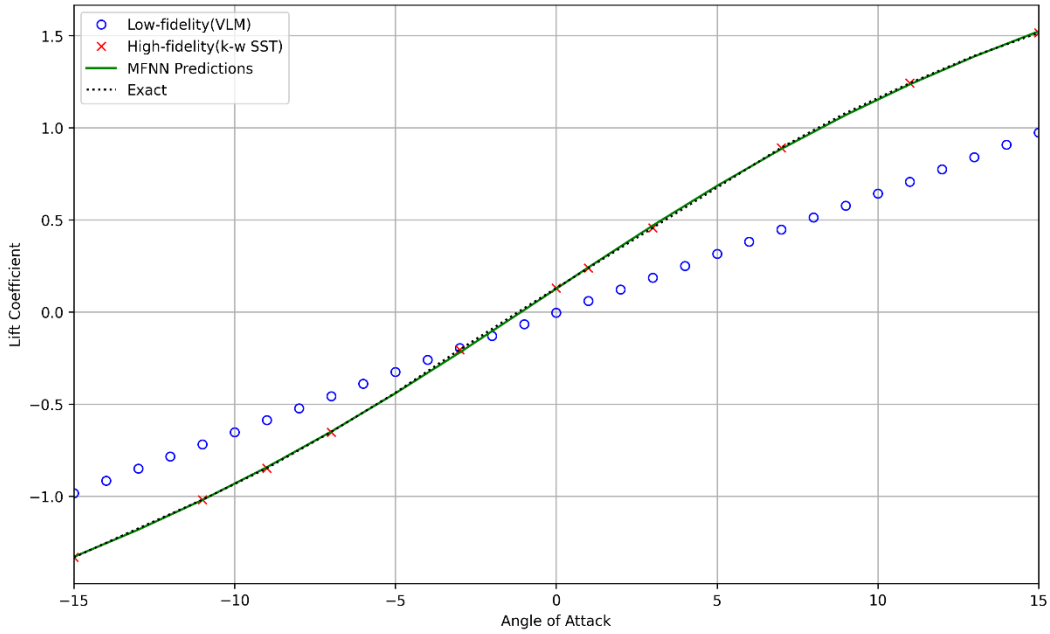

Figure 4.64. Multi-fidelity Neural Network lift coefficient estimate using 31 low-fidelity and 11 high-fidelity data corresponding to test case 4

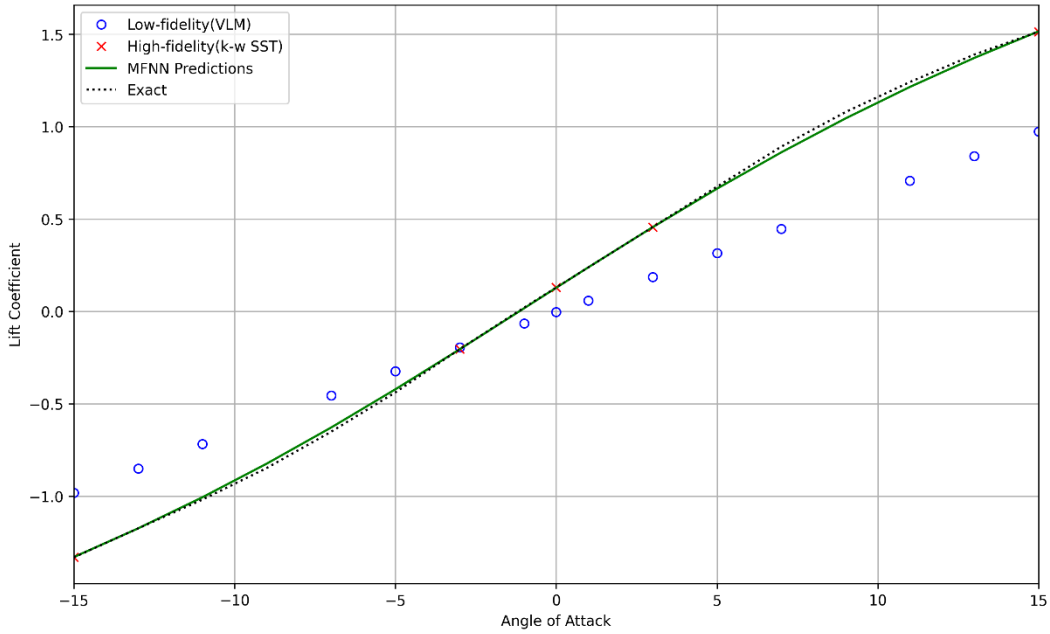

Figure 4.65. Multi-fidelity Neural Network lift coefficient estimate using 15 low-fidelity and 5 high-fidelity data corresponding to test case 5

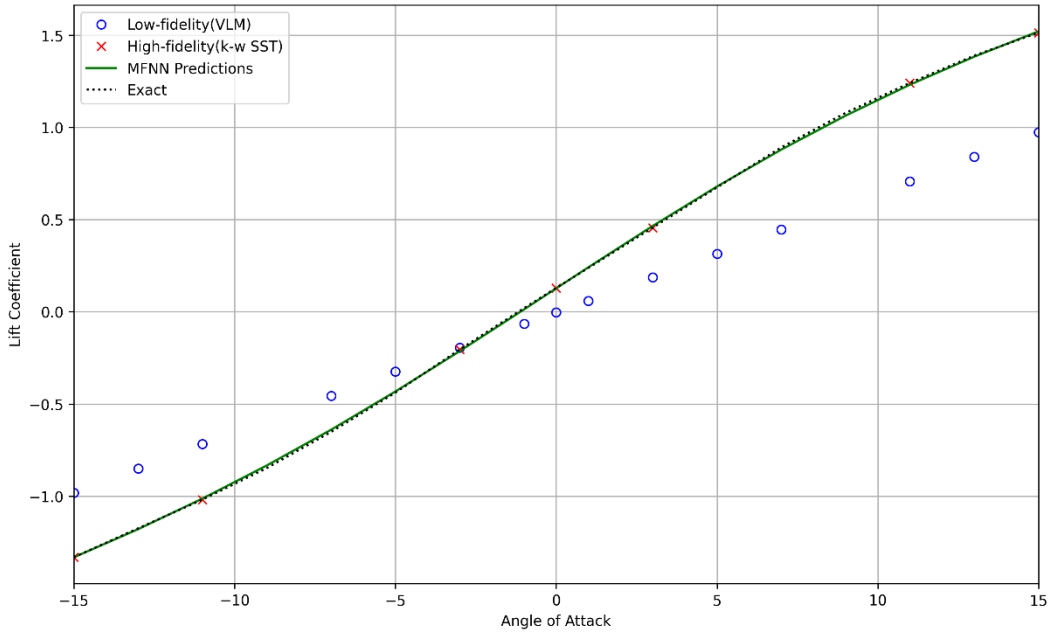

Figure 4.66. Multi-fidelity Neural Network lift coefficient estimate using 15 low-fidelity and 7 high-fidelity data corresponding to test case 6

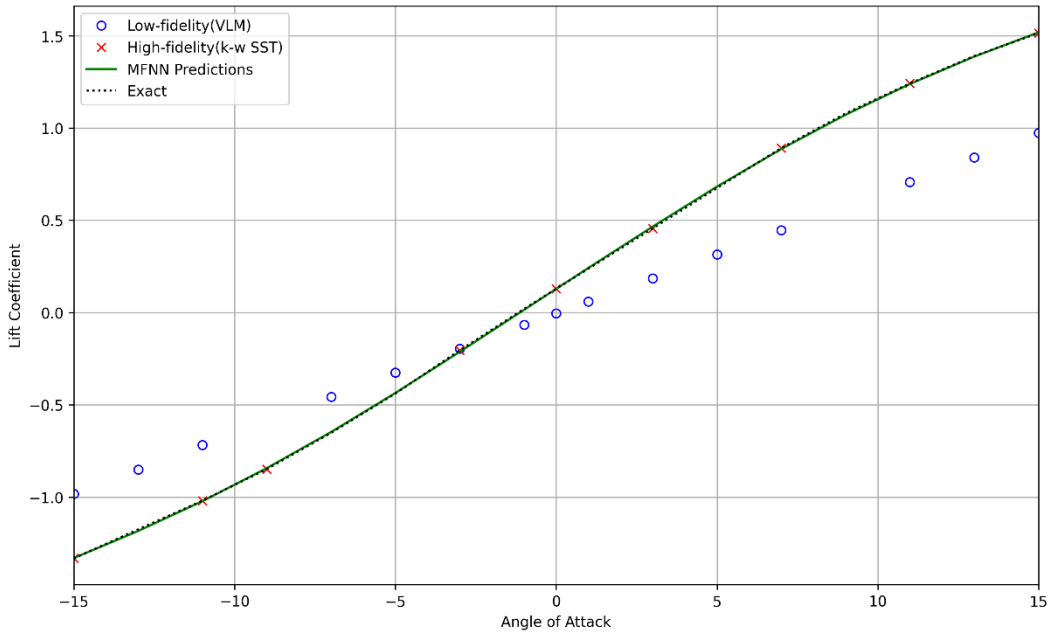

Figure 4.67. Multi-fidelity Neural Network lift coefficient estimate using 15 low-fidelity and 9 high-fidelity data corresponding to test case 7

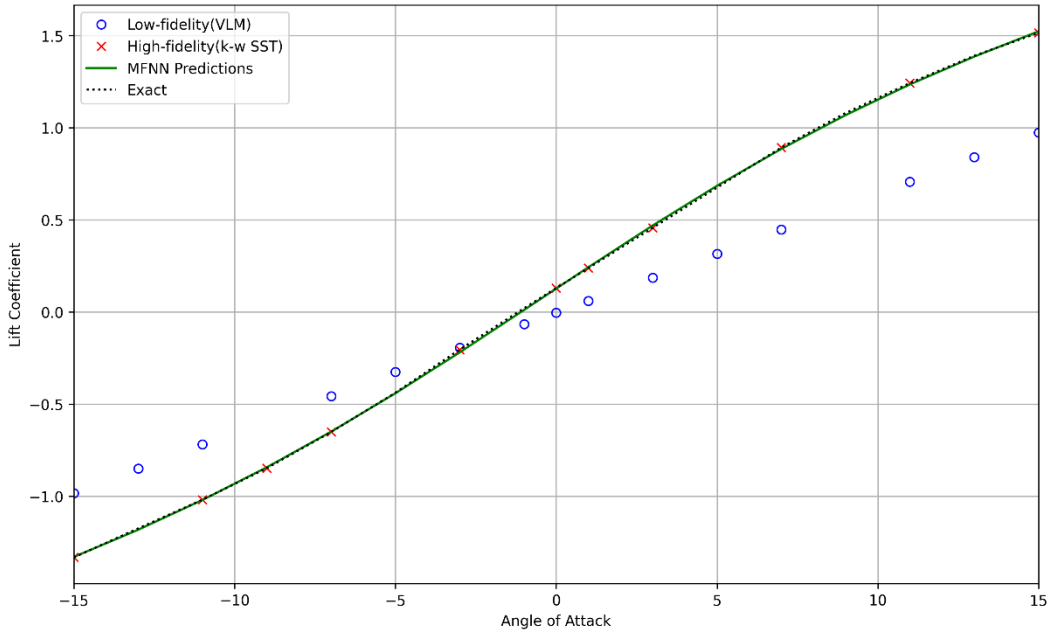

Figure 4.68. Multi-fidelity Neural Network lift coefficient estimate using 15 low-fidelity and 11 high-fidelity data corresponding to test case 8

Table 4.16. Multi-fidelity Neural Network method lift coefficient estimation error values

Test Case Number	Mean Square Error (MSE)	Data Configuration
1	0,0003125145278	31 Low and 5 High Fidelity Data
2	0,0000749648176	31 Low and 7 High Fidelity Data
3	0,0000190920679	31 Low and 9 High Fidelity Data
4	0,0000017175090	31 Low and 11 High Fidelity Data

Table 4.17. Multi-fidelity Neural Network method lift coefficient estimation error values

Test Case Number	Mean Square Error (MSE)	Data Configuration
1	0,000283599	15 Low and 5 High Fidelity Data
2	0,00007206277	15 Low and 7 High Fidelity Data
3	0,00003010605	15 Low and 9 High Fidelity Data
4	0,0000184705	15 Low and 11 High Fidelity Data

A multi-fidelity neural network model was used to predict the lift coefficient and the performance of the model for lift coefficient prediction was determined using 8 different test cases. According to the results, the test cases with low fidelity data showed high performance and very low error values compared to the high fidelity data set. However, the error values increases as the number of high fidelity data increases. This is due to the incorrect positioning of high fidelity data in the data set. Therefore, neural networks cannot provide the necessary training. When the number of low-fidelity data is reduced and the number of high- fidelity data is gradually increased, the model makes good predictions. In addition, the

lowest error values is observed in test-case 4 and 8 and the performance of the other models decreases with the increase in the number of high fidelity data.

4.3.2. Multi-fidelity neural network method prediction to obtain drag coefficient

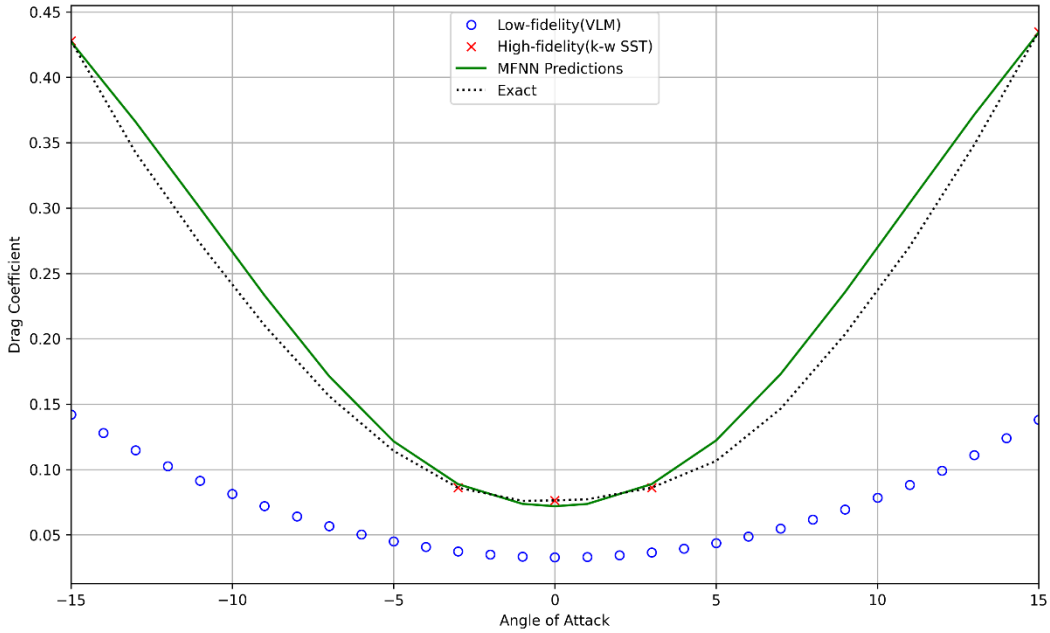

Figure 4.69. Multi-fidelity Neural Network drag coefficient estimate using 31 low-fidelity and 5 high-fidelity data corresponding to test case 1

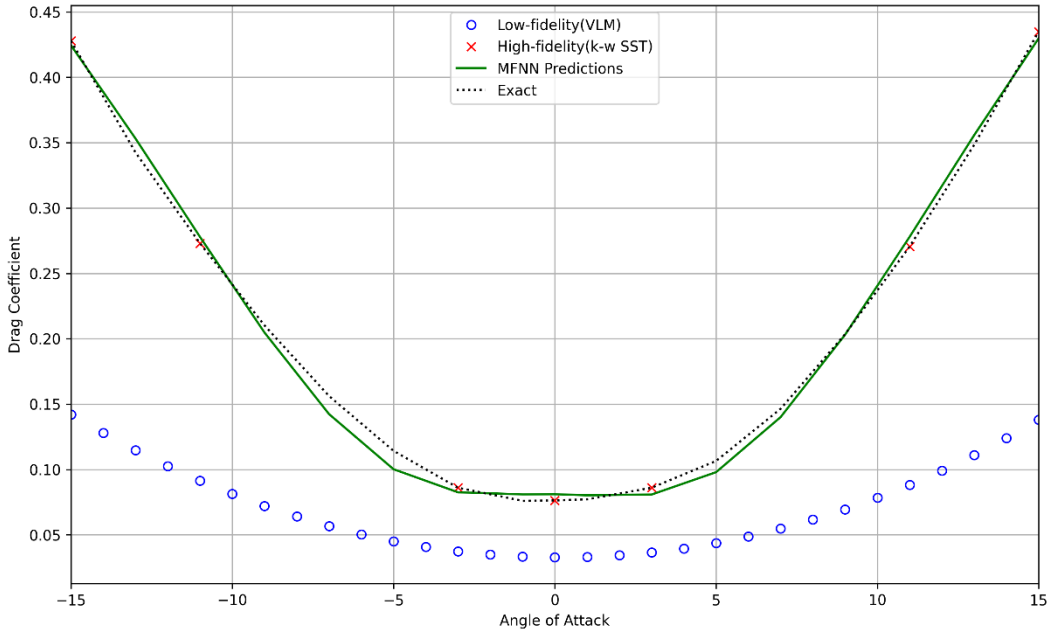

Figure 4.70. Multi-fidelity Neural Network drag coefficient estimate using 31 low-fidelity and 7 high-fidelity data corresponding to test case 2

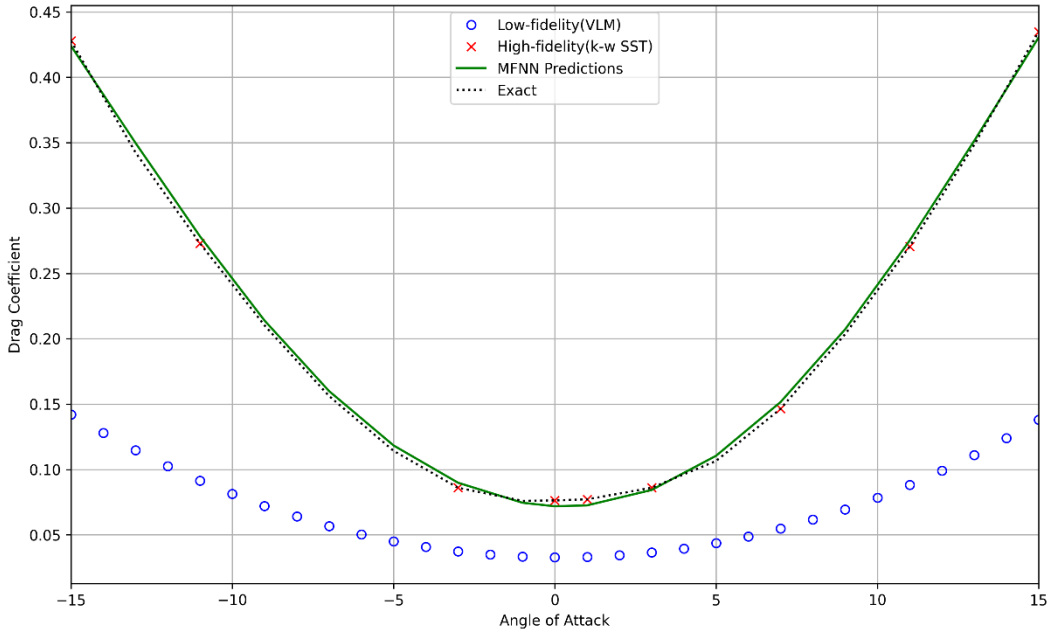

Figure 4.71. Multi-fidelity Neural Network drag coefficient estimate using 31 low-fidelity and 9 high-fidelity data corresponding to test case 3

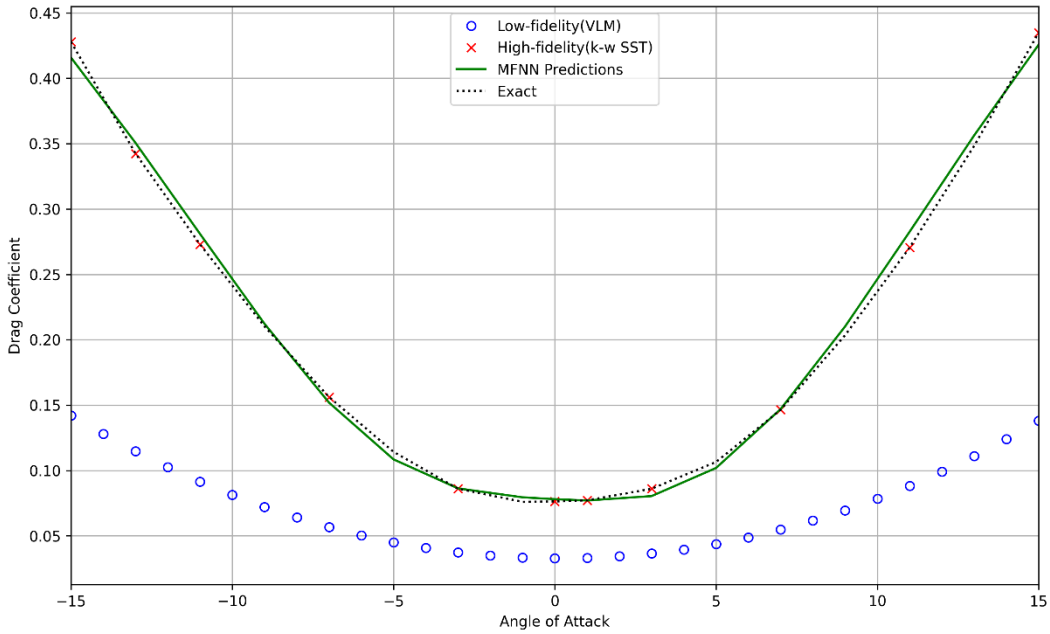

Figure 4.72. Multi-fidelity Neural Network drag coefficient estimate using 31 low-fidelity and 11 high-fidelity data corresponding to test case 4

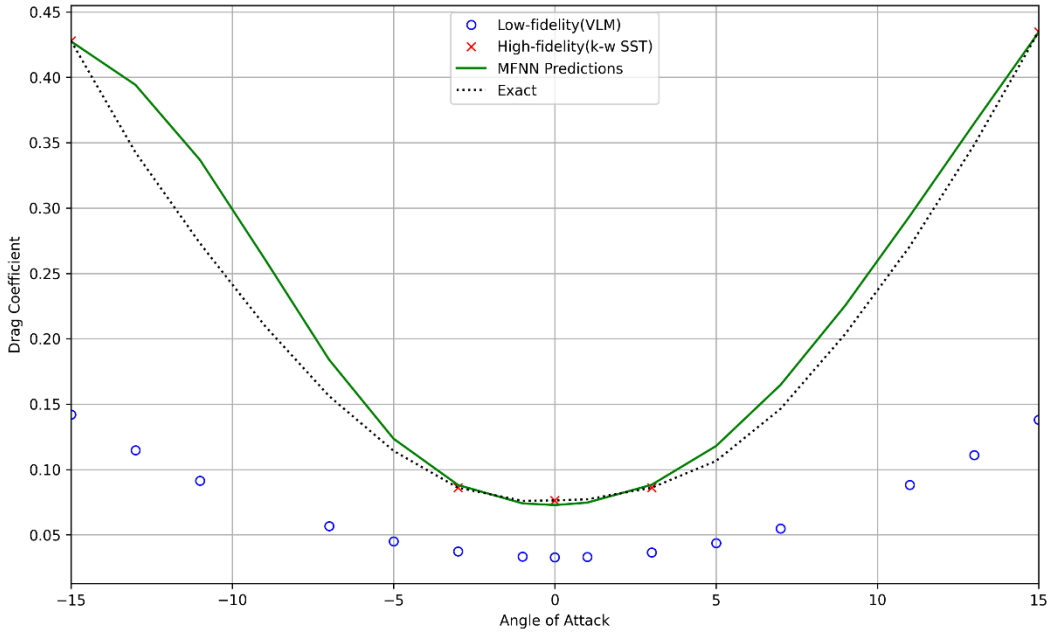

Figure 4.73. Multi-fidelity Neural Network drag coefficient estimate using 15 low-fidelity and 5 high-fidelity data corresponding to test case 5

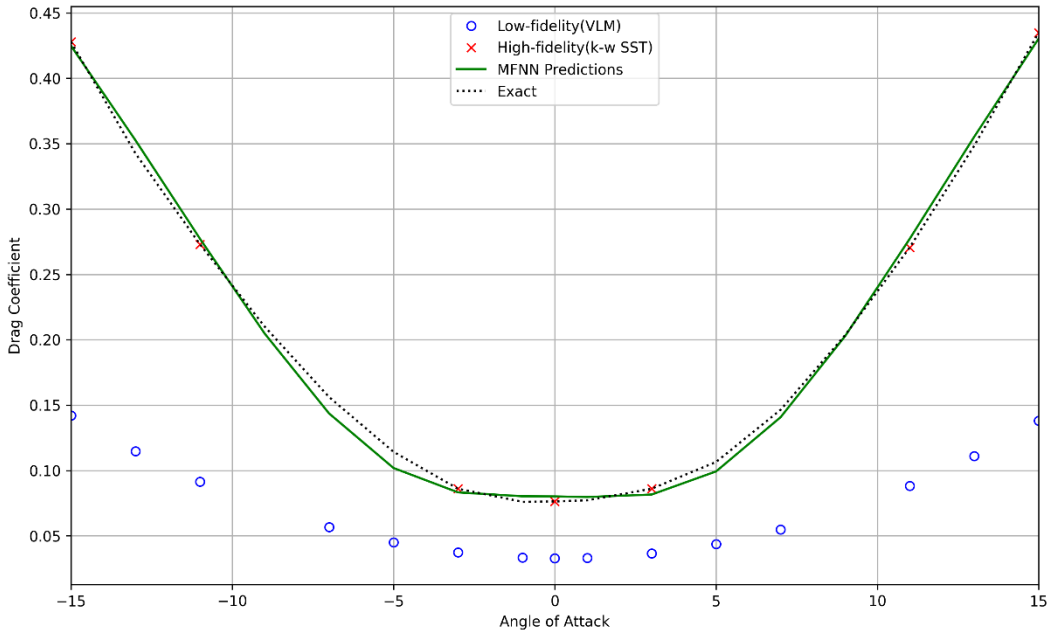

Figure 4.74. Multi-fidelity Neural Network drag coefficient estimate using 15 low-fidelity and 7 high-fidelity data corresponding to test case 6

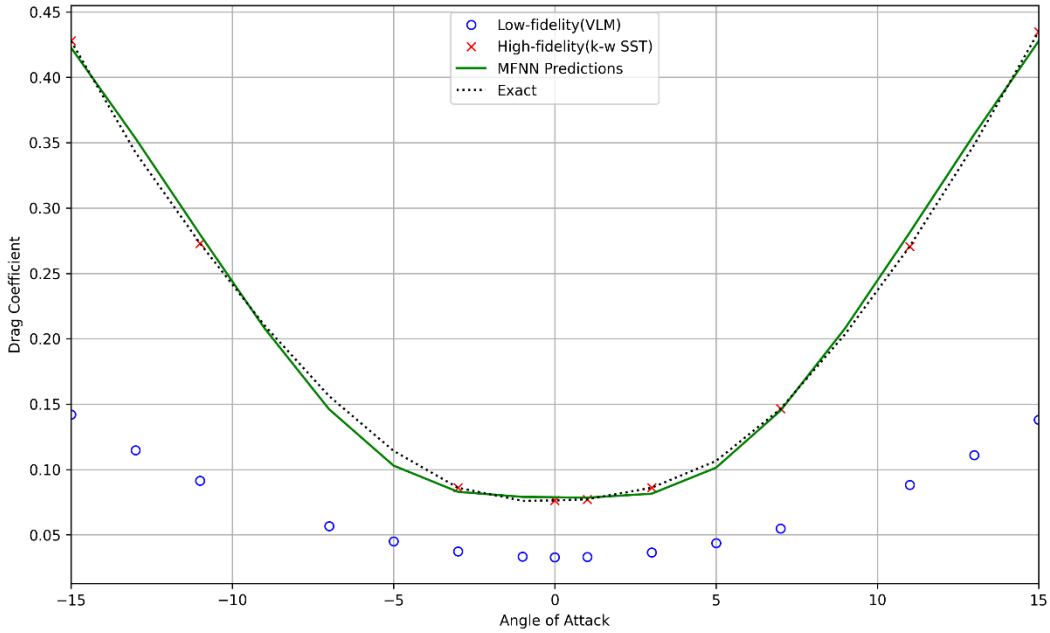

Figure 4.75. Multi-fidelity Neural Network drag coefficient estimate using 15 low-fidelity and 9 high-fidelity data corresponding to test case 7

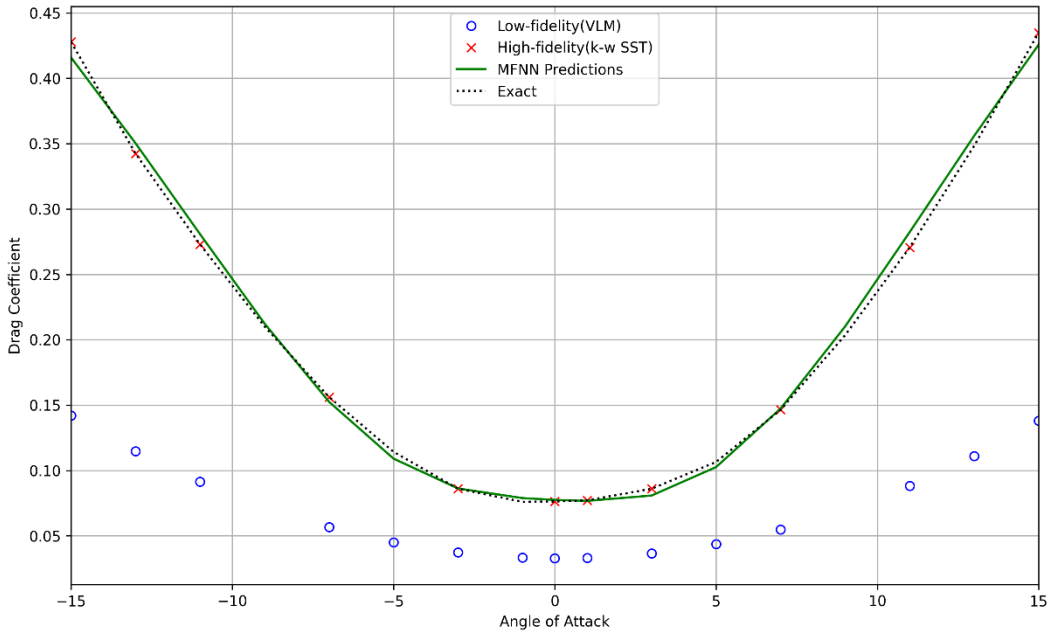

Figure 4.76. Multi-fidelity Neural Network drag coefficient estimate using 15 low-fidelity and 11 high-fidelity data corresponding to test case 8

Table 4.18. Multi-fidelity Neural Network method drag coefficient estimation error values

Test Case Number	Mean Square Error (MSE)	Data Configuration
1	0,0003393378389	31 Low and 5 High Fidelity Data
2	0,0000538826616	31 Low and 7 High Fidelity Data
3	0,0000182073000	31 Low and 9 High Fidelity Data
4	0,0000233888000	31 Low and 11 High Fidelity Data

Table 4.19. Multi-fidelity Neural Network method drag coefficient estimation error values

Test Case Number	Mean Square Error (MSE)	Data Configuration
1	0,000705705	15 Low and 5 High Fidelity Data
2	0,0000430052800	15 Low and 7 High Fidelity Data
3	0,00004403600	15 Low and 9 High Fidelity Data
4	0,0000405681	15 Low and 11 High Fidelity Data

The drag coefficient estimation was performed with a multi-fidelity neural network model and the performance of the model for drag coefficient estimation was determined using 8 different test cases. According to the results, the test cases with low fidelity data showed high performance and very low error values compared to the high fidelity data set. However, the error values increases as the number of high fidelity data increases. This is due to the incorrect positioning of high fidelity data in the data set. Therefore, neural networks cannot provide the necessary training. When the number of low-fidelity data is reduced and the number of high-fidelity data is gradually increased, the model makes good predictions. In addition, the lowest error values is observed in test-case 4 and 8 and the performance of the other models decreases with the increase in the number of high fidelity data.

4.3.2. Multi-fidelity neural network method prediction to obtain pitch moment coefficient

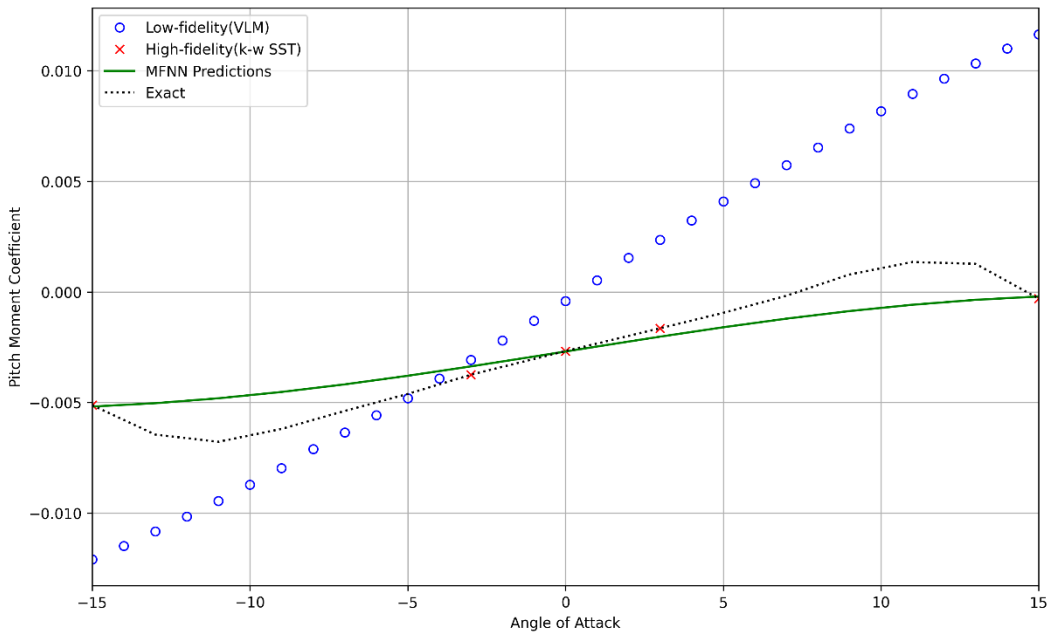

Figure 4.77. Multi-fidelity Neural Network pitch moment coefficient estimate using 31 low-fidelity and 5 high-fidelity data corresponding to test case 1

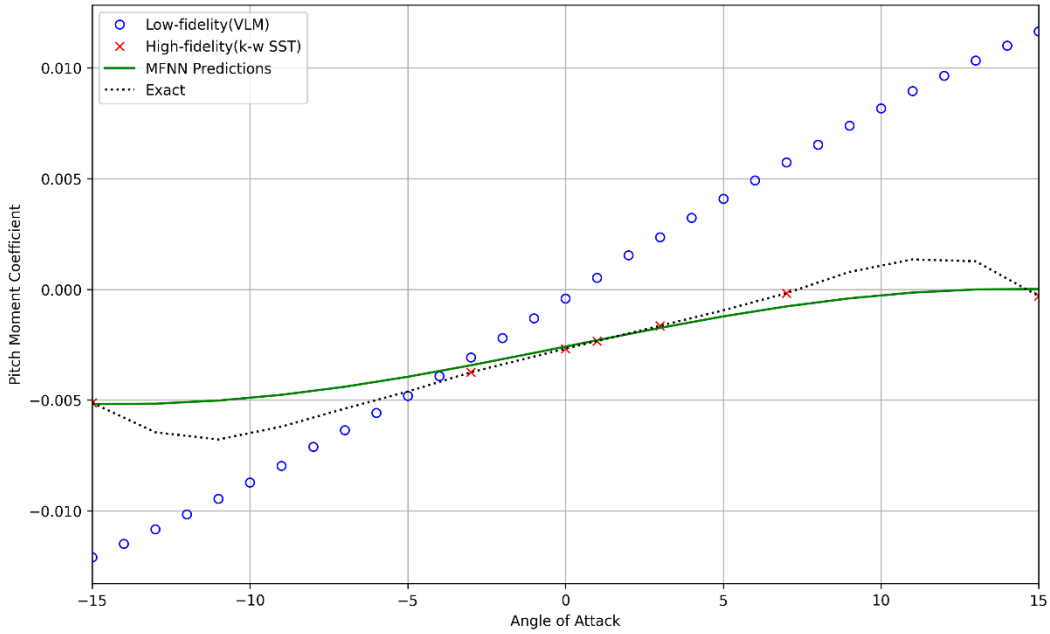

Figure 4.78. Multi-fidelity Neural Network pitch moment coefficient estimate using 31 low-fidelity and 7 high-fidelity data corresponding to test case 2

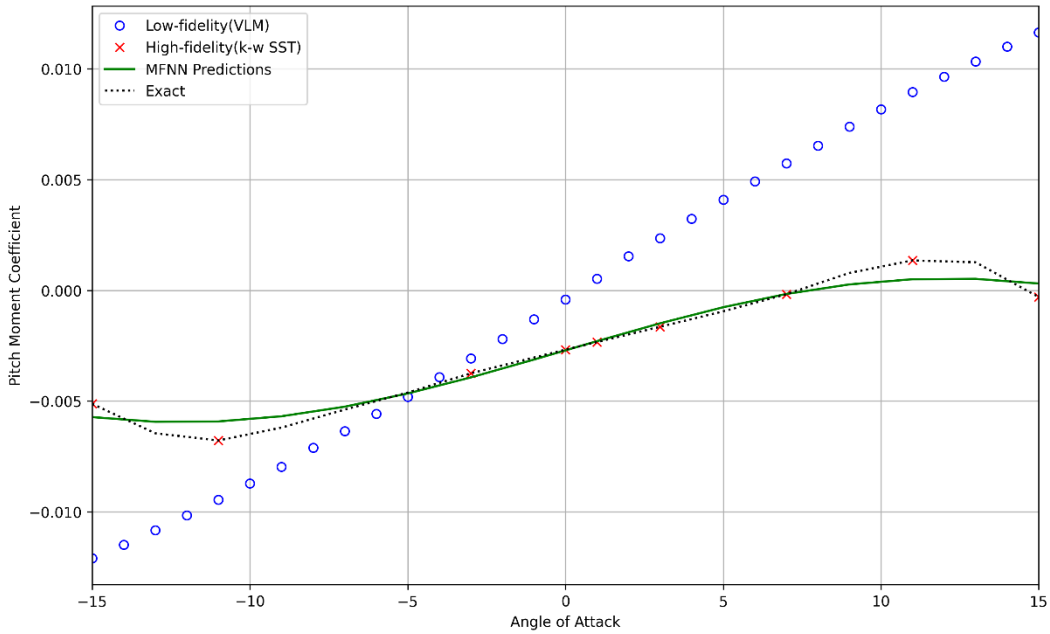

Figure 4.79. Multi-fidelity Neural Network pitch moment coefficient estimate using 31 low-fidelity and 9 high-fidelity data corresponding to test case 3

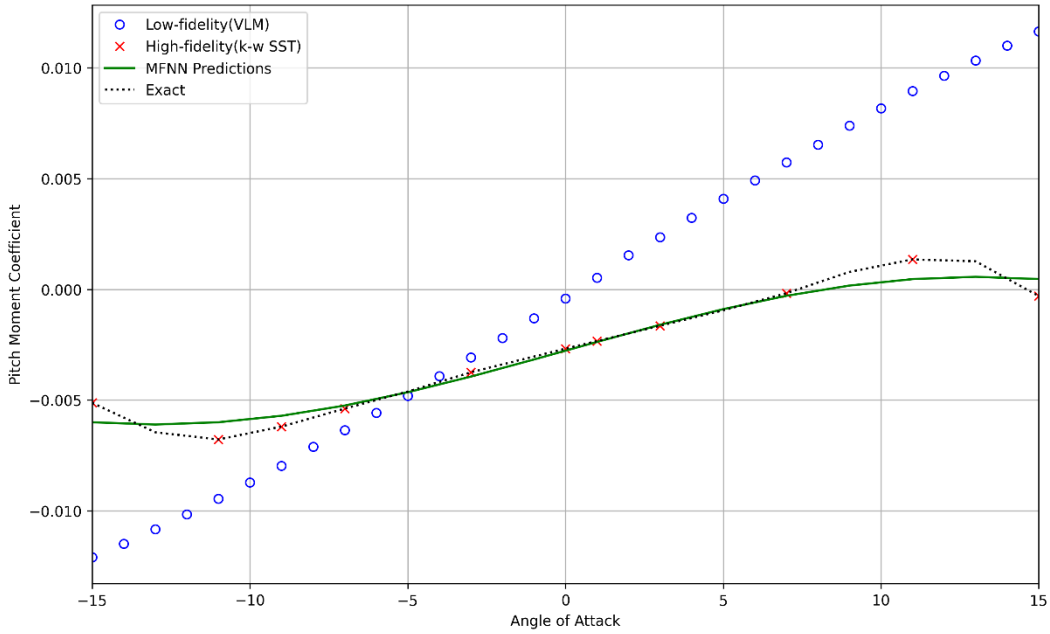

Figure 4.80. Multi-fidelity Neural Network pitch moment coefficient estimate using 31 low-fidelity and 11 high-fidelity data corresponding to test case 4

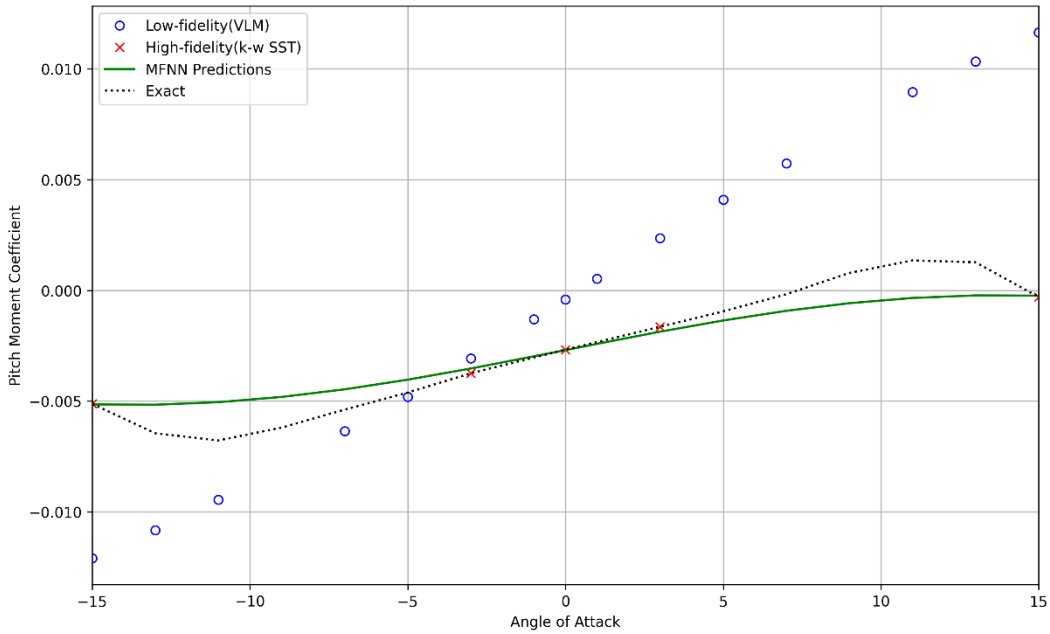

Figure 4.81. Multi-fidelity Neural Network pitch moment coefficient estimate using 15 low-fidelity and 5 high-fidelity data corresponding to test case 5

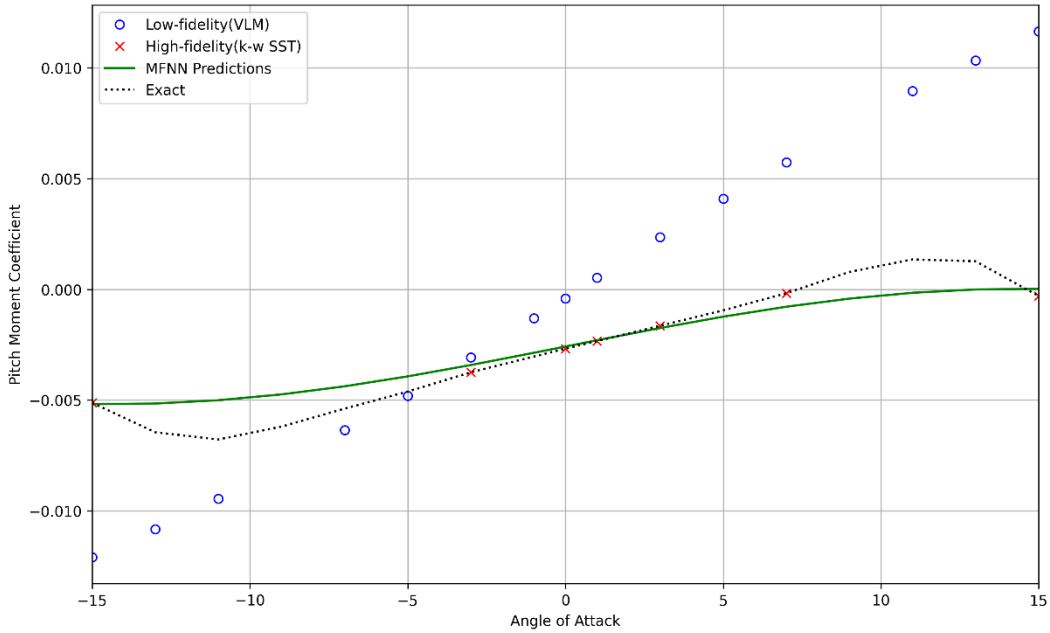

Figure 4.82. Multi-fidelity Neural Network pitch moment coefficient estimate using 15 low-fidelity and 7 high-fidelity data corresponding to test case 6

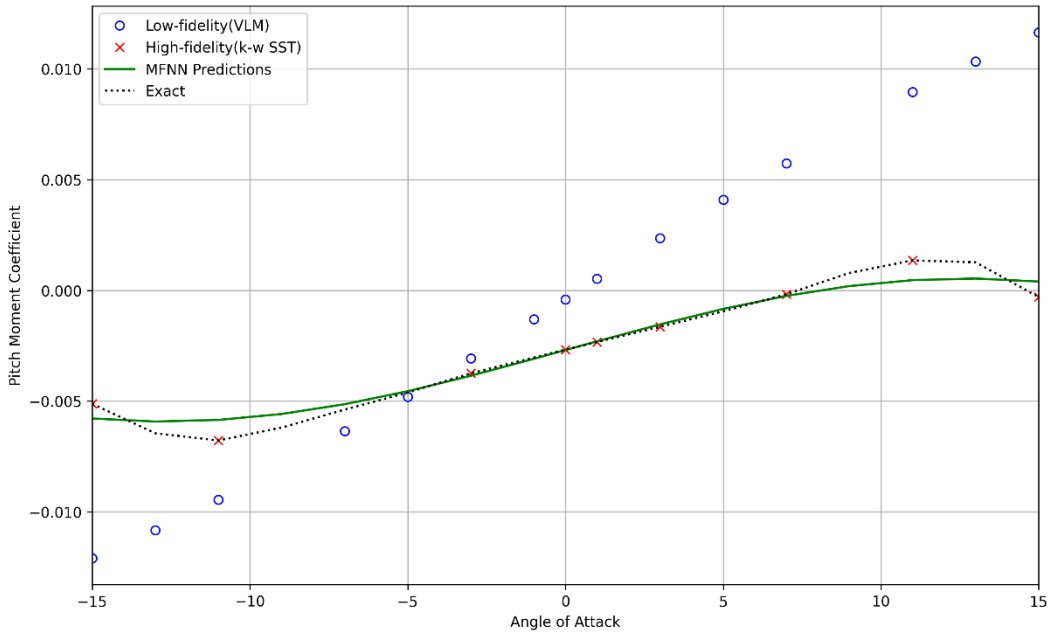

Figure 4.83. Multi-fidelity Neural Network pitch moment coefficient estimate using 15 low-fidelity and 9 high-fidelity data corresponding to test case 7

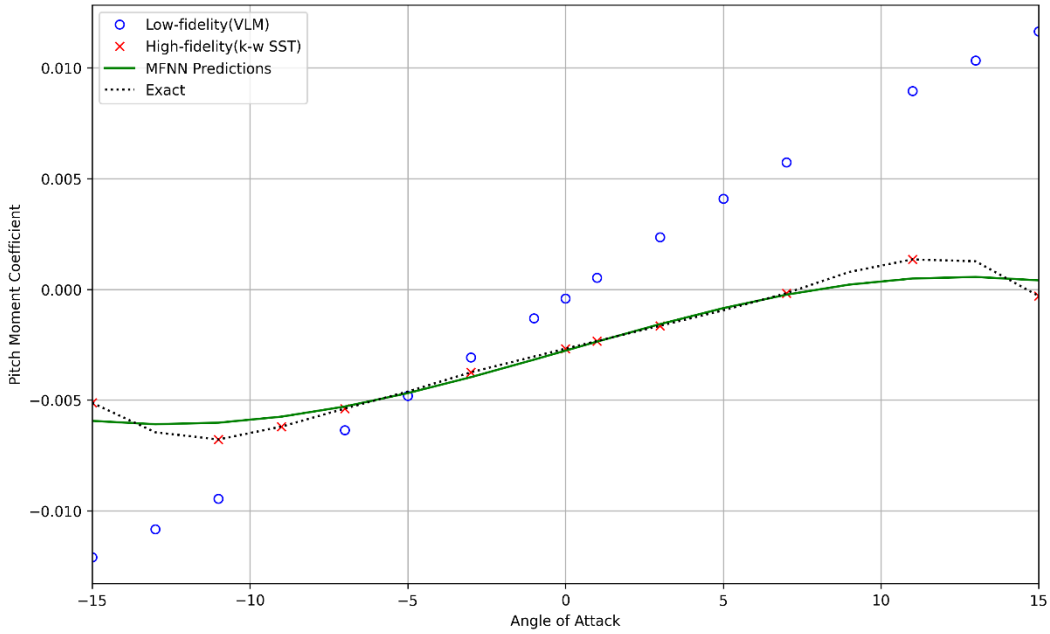

Figure 4.84. Multi-fidelity Neural Network pitch moment coefficient estimate using 15 low-fidelity and 11 high-fidelity data corresponding to test case 8

Table 4.20. Multi-fidelity Neural Network method pitch moment coefficient estimation error values

Test Case Number	Mean Square Error (MSE)	Data Configuration
1	0,0000012790737	31 Low and 5 High Fidelity Data
2	0,0000008340106	31 Low and 7 High Fidelity Data
3	0,0000002162221	31 Low and 9 High Fidelity Data
4	0,0000002406160	31 Low and 11 High Fidelity Data

Table 4.21. Multi-fidelity Neural Network method pitch moment coefficient estimation error values

Test Case Number	Mean Square Error (MSE)	Data Configuration
1	0,0000009154879944	15 Low and 5 High Fidelity Data
2	0,0000004518890	15 Low and 7 High Fidelity Data
3	0,00000024951	15 Low and 9 High Fidelity Data
4	0,0000002210	15 Low and 11 High Fidelity Data

In the multi fidelity neural network pitch moment coefficient prediction model, pitch moment values from two different sources were combined. Due to the large difference between the moment values, the mean square error values were low. Among the test cases, test cases 4 and 8 with the highest number of high fidelity data showed the best prediction performance. Due to the poor correlation value of the data, more data is needed to train the model. However, for a fair performance test, the model was trained with a maximum of 11 high fidelity data.

Table 4.22. Efficiency and mse comparison of each parameter for multi-fidelity neural network data fusion method

Parameter	Test case number	MFNN prediction time (s)	Time required to obtain the data used in test case (s)	Time required to obtain the all data (s)	Efficiency (%)	MSE
C_l	1	31,9	612 620	2 080 800	70,5584	0,000312514
C_l	2	34,1	857 423	2 080 800	58,7936	0,000074964
C_l	3	33,6	1 102 222	2 080 800	47,0289	0,000019092
C_l	4	39,9	1 347 028	2 080 800	35,2639	0,000001717
C_l	5	37,1	612 322	2 080 800	70,5728	0,000283599
C_l	6	33,2	857 118	2 080 800	58,8082	0,000072062
C_l	7	31,3	1 101 916	2 080 800	47,0436	0,000030106
C_l	8	34,6	1 346 719	2 080 800	35,2788	0,000018470
C_d	1	30,8	612 619	2 080 800	70,5584	0,000339337
C_d	2	33	857 422	2 080 800	58,7936	0,000053882
C_d	3	40,5	1 102 229	2 080 800	47,0286	0,000018207
C_d	4	35,8	1 347 024	2 080 800	35,2641	0,000023388
C_d	5	37,5	612 322	2 080 800	70,5727	0,000705705
C_d	6	30,2	857 115	2 080 800	58,8084	0,00004300
C_d	7	32,7	1 101 917	2 080 800	47,0436	0,00004403
C_d	8	38,9	1 346 723	2 080 800	35,2785	0,00004056
C_m	1	38,9	612 627	2 080 800	70,5581	0,000001279
C_m	2	35,1	857 424	2 080 800	58,7935	0,000000834
C_m	3	30,3	1 102 219	2 080 800	47,0291	0,000000216
C_m	4	34,8	1 347 023	2 080 800	35,2641	0,0000002406
C_m	5	32,9	612 317	2 080 800	70,5730	0,0000009154
C_m	6	38,6	857 123	2 080 800	58,8080	0,0000004518
C_m	7	39,6	1 101 924	2 080 800	47,0432	0,0000002495
C_m	8	40,0	1 346 725	2 080 800	35,2785	0,0000002210

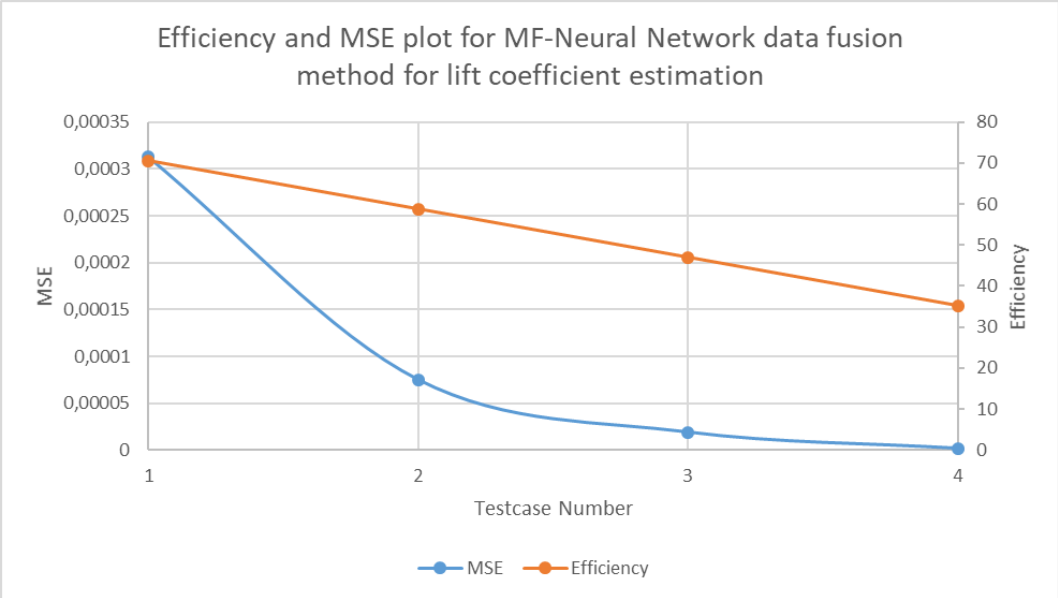

Figure 4.85. Efficiency and MSE comparison of Multi-fidelity Neural Network method for lift coefficient prediction for first four testcase

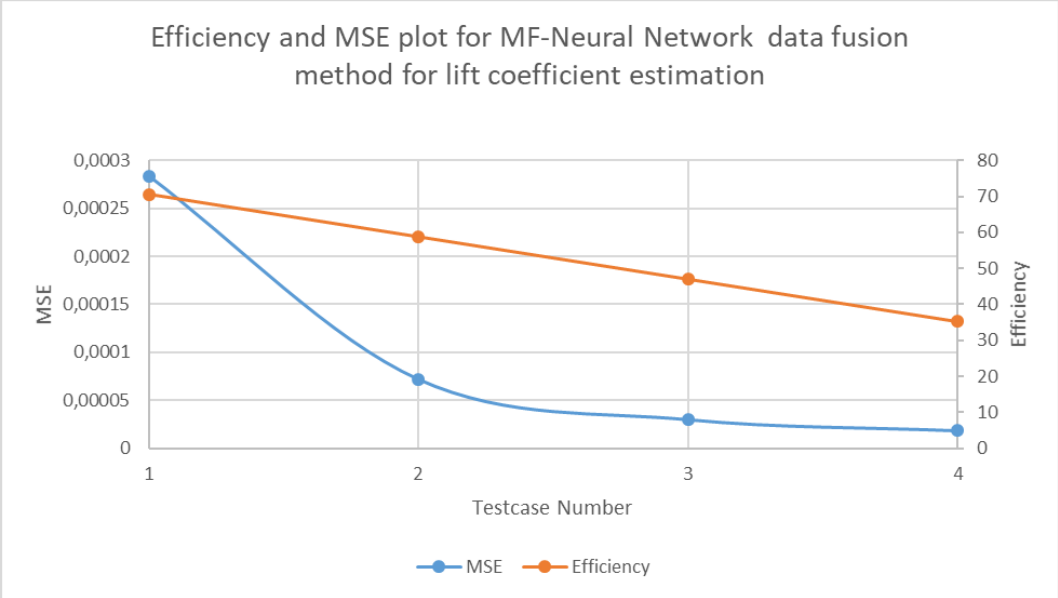

Figure 4.86. Efficiency and MSE comparison of Multi-fidelity Neural Network method for lift coefficient prediction for second four testcase

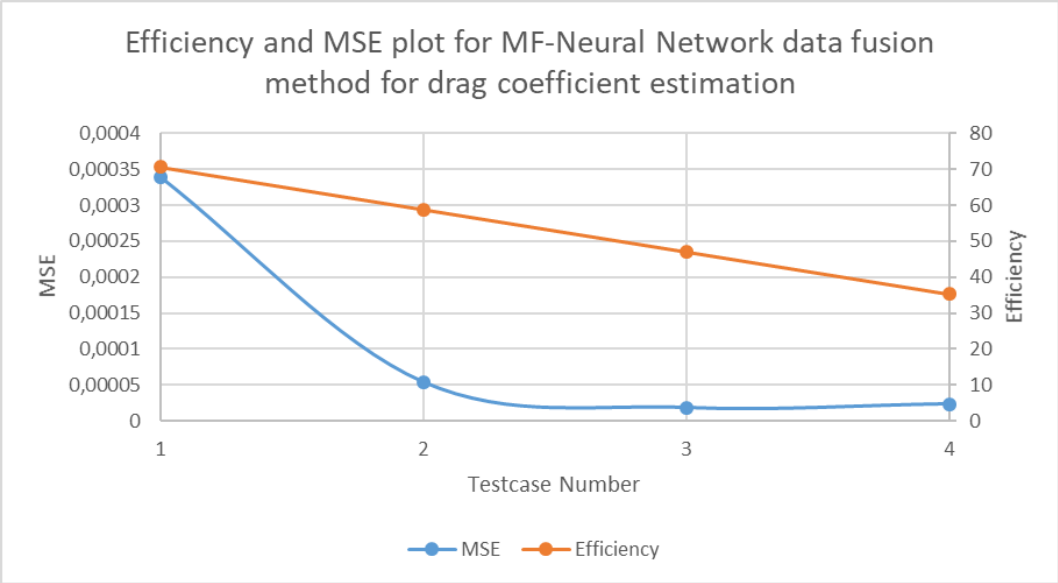

Figure 4.87. Efficiency and MSE comparison of Multi-fidelity Neural Network method for drag coefficient prediction for first four testcase

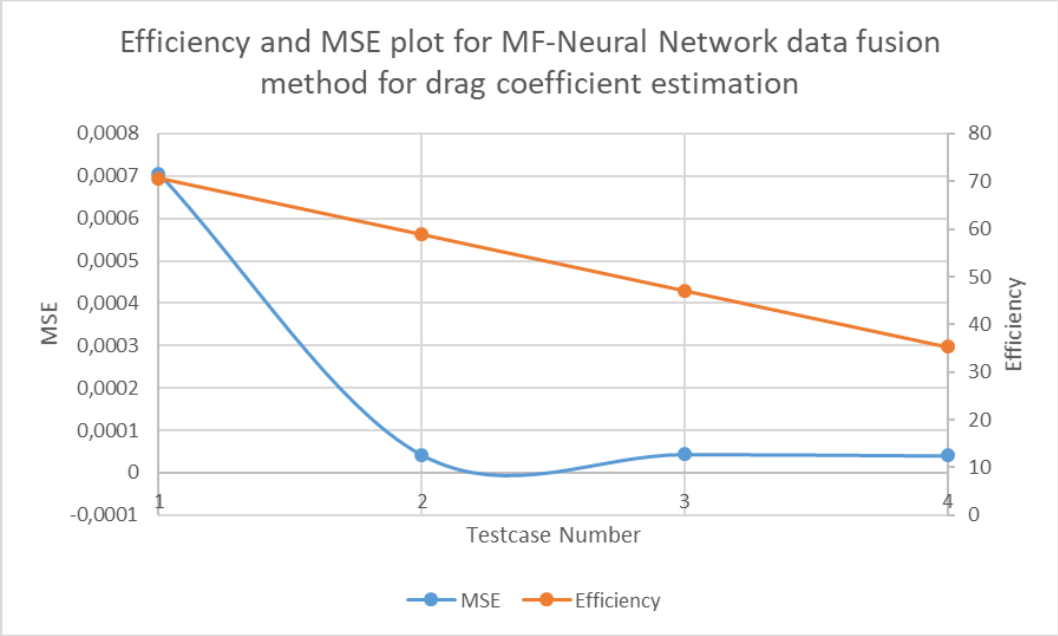

Figure 4.88. Efficiency and MSE comparison of Multi-fidelity Neural Network method for drag coefficient prediction for second four testcase

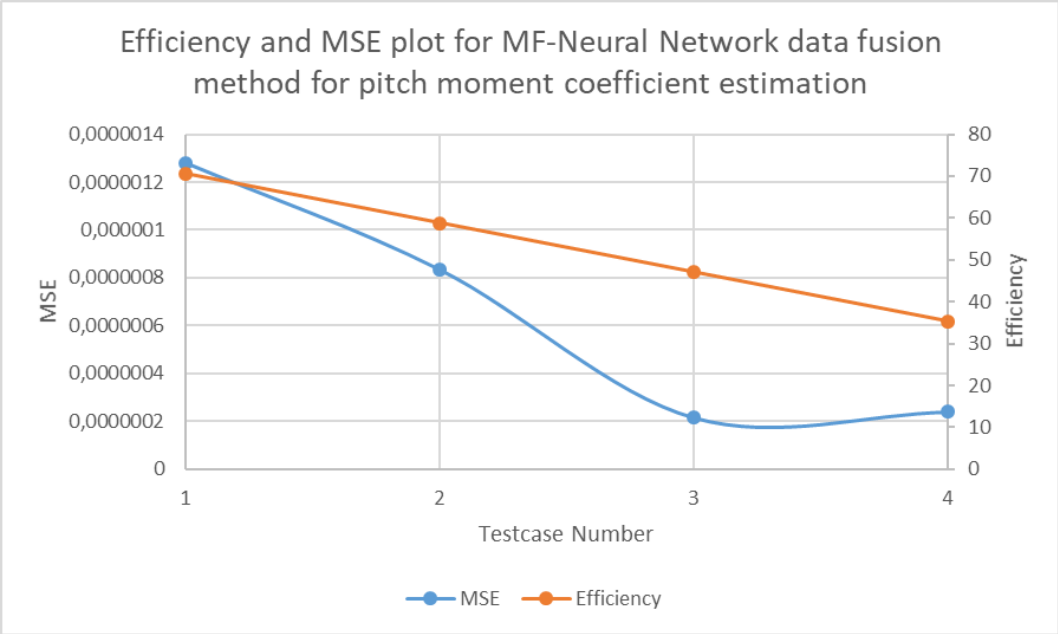

Figure 4.89. Efficiency and MSE comparison of Multi-fidelity Neural Network method for pitch moment coefficient prediction for first four testcase

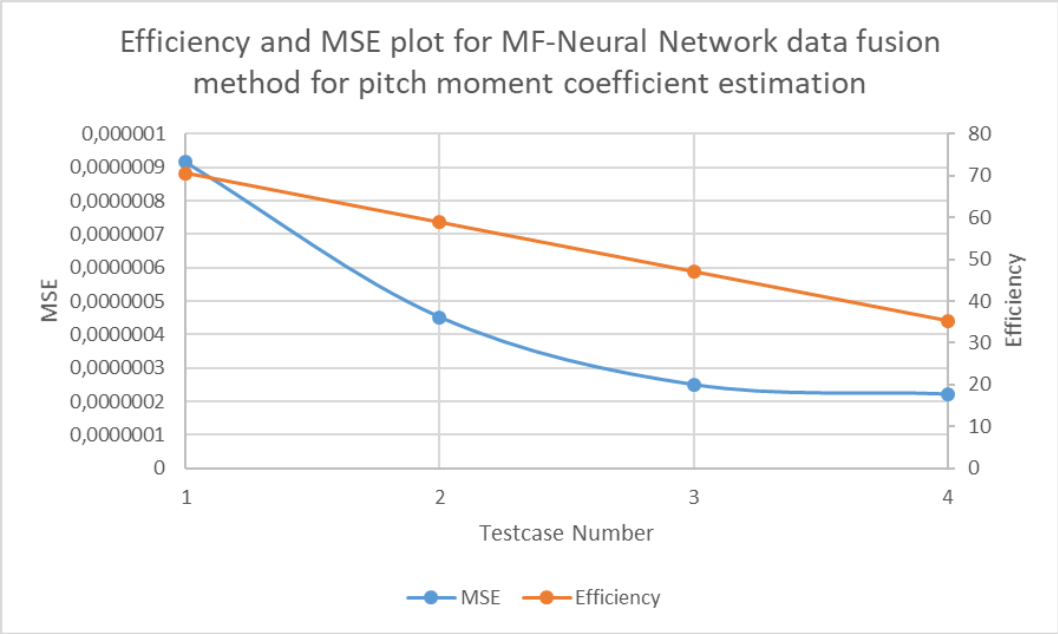

Figure 4.90. Efficiency and MSE comparison of Multi-fidelity Neural Network method for pitch moment coefficient prediction for second four testcase

In the data fusion study using multi-fidelity neural networks, predictions were made for lift, drag and pitch moment coefficients. A test case was created for each prediction and the efficiency and average error values were calculated for each of these test cases. A high theoretical efficiency means that the time required to build the model is less. High efficiency alone is not desirable. In addition, a low error values is related to how accurate the model is. Accordingly, the best test case for the estimation of the lift coefficient is number 4 and then

number 8 according to Figure 4.85 and 4.86. The best performing test case for drag coefficient prediction is number 3 and then number 6 according to Figure 4.87 and 4.88. According to Figure 4.89 and 4.90, the best performing test case for the estimation of the pitch moment coefficient is number 3 followed by number 6.

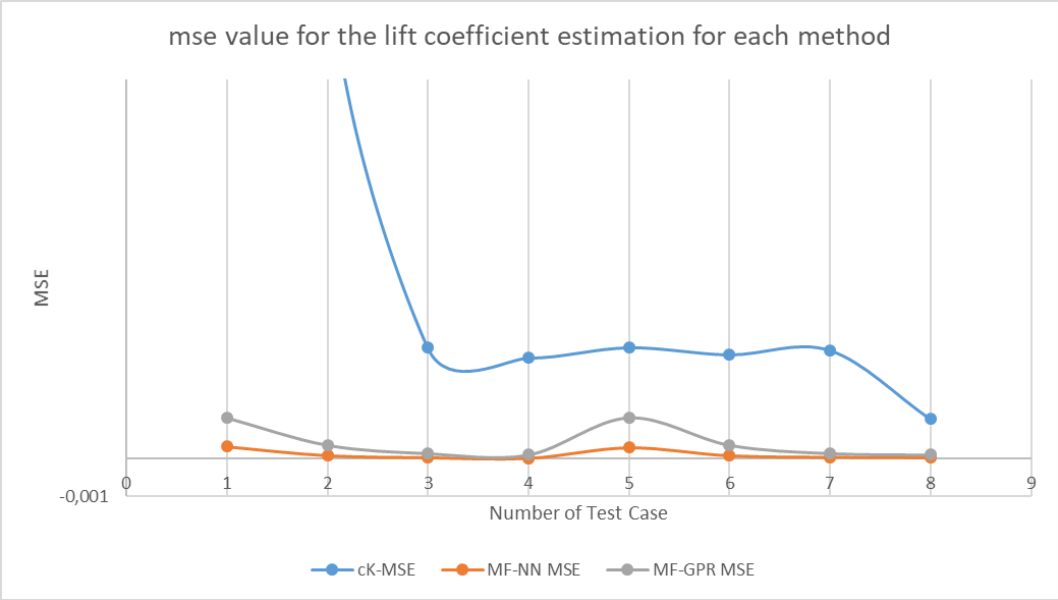

Figure 4.91. MSE comparison of three data fusion methods for lift coefficient predictions

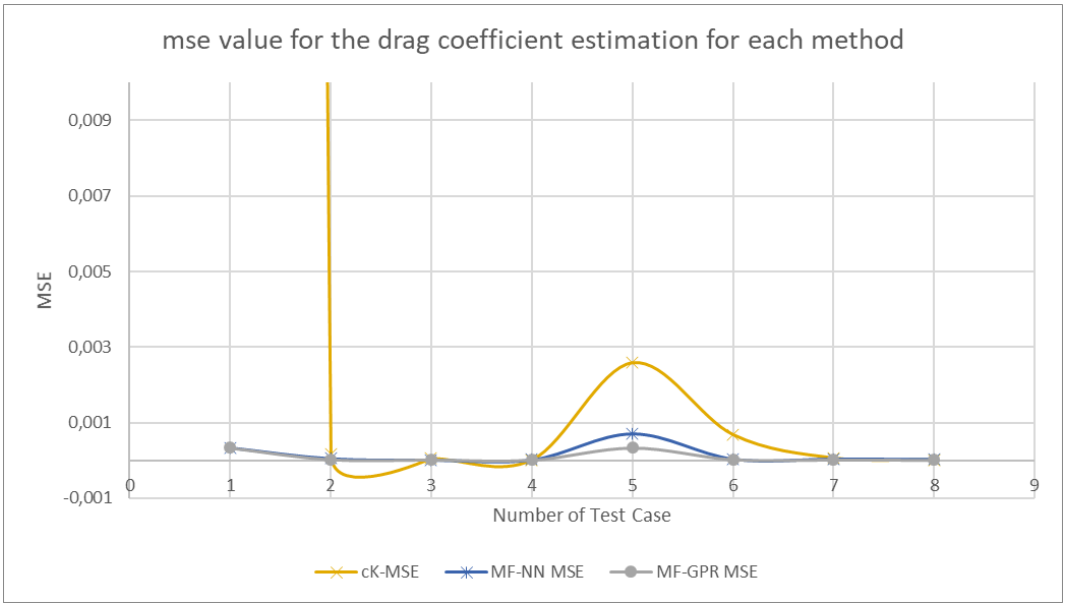

Figure 4.92. MSE comparison of three data fusion methods for drag coefficient predictions

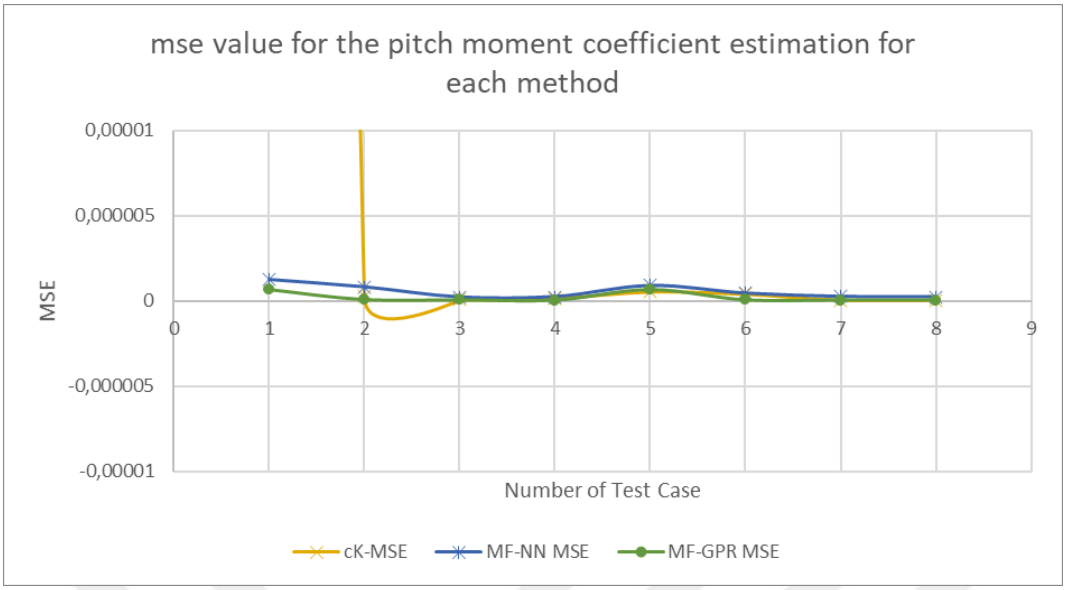

Figure 4.93. MSE comparison of three data fusion methods for pitch moment coefficient predictions

In the predictions for the lift coefficient, multi-fidelity neural networks showed the best performance when compared according to the error values of combining the three data. Except for test case 1 of the Co-Kriging method, the methods were able to show close results in all other test cases. When the error values for drag coefficient estimation are analyzed, some cases of the other methods outperformed the neural networks, but in general, the neural networks performed better.When the three methods for pitch moment coefficient estimation are analyzed, the multi-fidelity Gaussian Process Regression model has a higher error values than the other models. Except for the prediction made by the co-Kriging method in test case 1, the error values of the predictions made by neural networks and co-Kriging method are close to each other. As a result, the multi-fidelity neural network method was successful in predicting all three aerodynamic coefficients and showed low error values.

5. CONCLUSIONS

In this thesis, the number of datas have been used from different datasets which have low and high fidelity that belong to generic fighter aircraft. The aim of this thesis is to get high fidelity dataset by using some methods that are co-Kriging, multi fidelity Gaussian Process Regression and multi fidelity neural network. The data needed for these data fusion methods were obtained from different data sources. Low fidelity data were obtained using the Vortex-Lattice Method solver using OpenVSP software. High fidelity data was obtained using the k-ω SST solver in the ANSYS Fluent program. The high and low fidelity data were obtained by adjusting the performance and measurement limitations of the subsonic wind tunnel at Sivas University of Science and Technology as a reference. The data from both sources are classified as lift, drag and pitch moment coefficients. For each aerodynamic coefficient, there are 31 low-fidelity and 17 high-fidelity data, totaling 96 data. It takes 19 seconds to obtain one low-fidelity data and 34 hours to obtain one high-fidelity data. The data were subjected to data fusion using three different data fusion methods. To compare the performance of these methods, test cases with different numbers of data were created. With these test cases, the effects of increasing low and high fidelity data on the data fusion method predictions were examined. The MSE analysis and efficiency performance of each data fusion method were investigated.

In the tests conducted for the estimation of lift, drag and pitch moment coefficients using the Co-Kriging method, it was observed that the performance of the data fusion method generally improved with the increase in the number of high fidelity data. For the lift coefficient estimation, it was observed that the data fusion process using 31 low-fidelity data for the lift coefficient estimation largely matched the actual values when 9 high-fidelity data (test case 3) were used. When 11 high fidelity data (test case 4) were used, no significant change was observed. The worst prediction result was observed in testcase 1 with the least number of high fidelity data. When the number of low-fidelity data was increased to 15, the data became more meaningful as the ratio of low and high- fidelity data increased. The overlap with the actual values was observed when 11 high fidelity data (test case 4) were used. In the study for drag coefficient prediction, 31 low-fidelity data were used and it was observed that the prediction performance improved with the increase in the number of high-fidelity data. When the number of low-fidelity data was increased to 15, the prediction performance improved with the increase in the number of high-fidelity data. Test case 8 gave

the best performance for drag coefficient. In the tests for the pitch moment coefficient, when the number of low-fidelity data was set to 31 and 15 separately, it was determined that the prediction performance improved with the increase in the number of high-fidelity data and largely matched the actual values. Test case 8 gave the best result in the test. The locations of the data points used in the co-Kriging method and the relationship between the data points affect the performance of the co-Kriging method. Co-Kriging method is more sensitive than other methods.

In the lift, drag and pitch moment coefficient predictions using the multi-fidelity GPR method, the effect of increasing the number of high fidelity data on model performance was examined by using 31 and 15 low fidelity data. Accordingly, it is concluded that there is a continuous improvement in prediction performance with increasing data number in the tests using 31 low-fidelity data. When the number of low-fidelity data was 15, increasing the number of high-fidelity data improved the performance of the method and provided a large overlap with the real data. For the lift coefficient, test case 4 and test case 8 showed the best performance with very close results. The result did not change in the tests for drag coefficient estimation. In tests with 31 low-fidelity data, the model prediction performance improved as the number of high-fidelity data increased. With the number of low-fidelity data set to 15, it was observed that the data matched the real data as the number of high-fidelity data increased. The best prediction performance for the drag coefficient is again test case 4 and test case 8. In the tests for the prediction of the pitch moment coefficient, it was observed that when 31 and 15 low fidelity data were used, increasing the number of high fidelity data improved the prediction performance of the model. Test case 4 and test case 8 gave the best prediction for pitch moment coefficient. Therefore, the MF-GPR data fusion method performs data fusion by being less sensitive to the location of the data to be used and the optimization of their relationship with each other, such as co-Kriging. For this method, it is observed that the performance of the method increases with the increase in the number of data.

The performance of the Multi-fidelity Neural Network (MF-NN) method was examined in the lift, drag and pitch moment coefficient prediction tests. For the lift coefficient prediction using 31 low fidelity data, the MF-NN method improved the prediction performance with increasing high fidelity data. When the number of low fidelity data was 15, the prediction performance did not decrease with increasing high fidelity data. Test case 4 and test case 8

showed the best results. In the study for drag coefficient estimation, in the test cases with 5 high fidelity data (test cases 1 and 5), changing the number of low fidelity data affected the estimation performance and the test case with 31 low fidelity data gave a more favorable result. It was observed that the prediction performance of the method improved with increasing the number of high fidelity data. Here, test case 3 gave the best result. However, test case 4 and test case 3 showed very close values at 31 low fidelity. When 15 low fidelity data were used, 7, 9, 11 high fidelity data showed close results. In the tests for pitch moment coefficient prediction, it was observed that the predictions improved when the number of high fidelity data was increased while keeping 31 and 15 low fidelity data constant, but it was determined that more data was needed to learn the curve in the moment graph. In the tests for pitch moment coefficient, test case 4 and test case 8 showed the best results.

When all data fusion methods were compared, it was observed that all three methods gave successful results and the prediction results overlapped with the high fidelity data as the number of high fidelity data increased. It is observed that the Co-Kriging method has good performance for lift and moment coefficient predictions and poor performance for drag coefficient predictions; the MF-GPR method has good performance for all coefficients and the MF-NN method has good performance for lift and drag coefficients but poor performance for moment prediction. It is thought that more data is needed for MF-NN and the prediction performance will improve when these data are generated by Kriging method and the tests are performed again. In general, in the three data fusion processes, it is observed that although the prediction data seems to be the same with the decrease in the number of low-fidelity data, it is possible to improve the predictions by increasing the low-fidelity data when the number of high-fidelity data is low.

REFERENCES

1. He, Lei et al. “Multi-Fidelity Aerodynamic Data Fusion with a Deep Neural Network Modeling Method.” *Entropy (Basel, Switzerland)* vol. 22,9 1022. 12 Sep. 2020, doi:10.3390/e22091022

2. Meysam Mohammadi-Amin, Moein M. Entezari, Alireza Alikhani, An efficient surrogate-based framework for aerodynamic database development of manned reentry vehicles, *Advances in Space Research*, Volume 62, Issue 5, 2018, Pages 997-1014, ISSN 0273-1177, https://doi.org/10.1016/j.asr.2018.06.022.

3. Chun Tang, Ken Gee and Scott Lawrence. "Generation of Aerodynamic Data using a Design Of Experiment and Data Fusion Approach," *AIAA 2005-1137. 43rd AIAA Aerospace Sciences Meeting and Exhibit.* January 2005.

4. Huseyin B. Kurt, Murat Millidere, Fazil S. Gomec and Omur Ugur. "Multi-fidelity Aerodynamic Dataset Generation of a Fighter Aircraft," *AIAA 2021-0544. AIAA Scitech 2021 Forum.* January 2021.

5. Keane, Andy. (2003). Wing Optimization Using Design of Experiment, Response Surface, and Data Fusion Methods. *Journal of Aircraft.* 40. 741-750. 10.2514/2.3153.

6. Seyede Fatemeh Ghoreishi and Douglas L. Allaire. "Gaussian Process Regression for Bayesian Fusion of Multi-Fidelity Information Sources," *AIAA 2018-4176. 2018 Multidisciplinary Analysis and Optimization Conference.* June 2018.

7. Mehdi Ghoreyshi, Ken Badcok and Mark Woodgate. "Accelerating the Numerical Generation of Aerodynamic Models for Flight Simulation," *AIAA 2009-733. 47th AIAA Aerospace Sciences Meeting including The New Horizons Forum and Aerospace Exposition.* January 2009.

8. Pham Vinh, Kim Mukyeom, Tyan Maxim, Lee Jae-Woo. Numerical Experience with Variable-fidelity Metamodeling for Aerodynamic Data Fusion Problems. *J. Def. Acquis. Technol.* 2019;1(1):1-8. https://doi.org/10.33530/jdaat.2019.1.1.1

9. Yuichi Kuya, Kenji Takeda and Xin Zhang. "Optimal Surrogate Modelling Approaches for Combining Experimental and Computational Fluid Dynamics Datasets," AIAA 2009-2216. *50th AIAA/ASME/ASCE/AHS/ASC Structures, Structural Dynamics, and Materials Conference.* May 2009.

10. Han, Zhong-Hua & Zimmermann, Ralf & Görtz, Stefan. (2010). A New Cokriging Method for Variable-Fidelity Surrogate Modeling of Aerodynamic Data. *48th AIAA Aerospace Sciences Meeting Including the New Horizons Forum and Aerospace Exposition.* 10.2514/6.2010-1225.

11. Han, Zhong-Hua, Zimmermann, and Stefan Görtz. "Alternative cokriging method for variable-fidelity surrogate modeling." *AIAA journal* 50.5 (2012): 1205-1210.

12. Han, Zhong-Hua & Görtz, Stefan & Zimmermann, Ralf. (2013). Improving variable-fidelity surrogate modeling via gradient-enhanced kriging and a generalized hybrid bridge function. *Aerospace Science and Technology.* 25. 177–189. 10.1016/j.ast.2012.01.006.

13. Rosenbaum, B. and Schulz, V. (2012), Comparing sampling strategies for aerodynamic Kriging surrogate models. Z. angew. *Math. Mech.,* 92: 852-868. https://doi.org/10.1002/zamm.201100112

14. Parussini, Lucia & Venturi, D. & Perdikaris, Paris & Karniadakis, George. (2017). Multi-fidelity Gaussian process regression for prediction of random fields. *Journal of Computational Physics.* 336. 36-50. 10.1016/j.jcp.2017.01.047.

15. R. Julian Rohit & Ranjan Ganguli (2022) Co-kriging based multi-fidelity uncertainty quantification of beam vibration using coarse and fine finite element meshes, *International Journal for Computational Methods in Engineering Science and Mechanics,* 23:2, 147-168, DOI: 10.1080/15502287.2021.1921883

16. Deng, Yixiang, Guang Lin, and Xiu Yang. "Multifidelity data fusion via gradient-enhanced Gaussian process regression." arXiv preprint arXiv:2008.01066 (2020).

17. Quan Lin, Dawei Hu, Jiexiang Hu, Yuansheng Cheng, Qi Zhou, A screening-based gradient-enhanced Gaussian process regression model for multi-fidelity data fusion, *Advanced Engineering Informatics,* Volume 50, 2021, 101437, ISSN 1474-0346, https://doi.org/10.1016/j.aei.2021.101437.

18. Manyu Xiao, Guohua Zhang, Piotr Breitkopf, Pierre Villon, and Weihong Zhang. 2018. Extended Co-Kriging interpolation method based on multi-fidelity data. *Appl. Math. Comput.* 323, C (April 2018), 120–131. https://doi.org/10.1016/j.amc.2017.10.055

19. Zhang, M., Jungo, A., & Bartoli, N. (2017). Disciplinary Data Fusion for Multi-Fidelity Aerodynamic Application. *6th CEAS Air & Space Conference Aerospace Europe*, 953.

20. Rumpfkeil, M.P., Beran, P.S., & Rumpfkeil, M.P. (2016). Construction of Multi-Fidelity Surrogate Models for Aerodynamic Databases.

21. Dong, H., Song, B., Wang, P. et al. Multi-fidelity information fusion based on prediction of kriging. *Struct Multidisc Optim 51,* 1267–1280 (2015). https://doi.org/10.1007/s00158-014-1213-9

22. Zhou, Qi & Wu, Yuda & Guo, Zhendong & Jiexiang, Hu & Jin, Peng. (2020). A generalized hierarchical co-Kriging model for multi-fidelity data fusion. *Structural and Multidisciplinary Optimization.* 62. 10.1007/s00158-020-02583-7.

23. Mehdi Anhichem, Sebastian Timme, Jony Castagna, Andrew Peace and Moira Maina. "Multifidelity Data Fusion Applied to Aircraft Wing Pressure Distribution," AIAA 2022-3526. *AIAA AVIATION 2022 Forum.* June 2022.

24. Feldstein, Alex & Lazzara, David & Princen, Norman & Willcox, Karen. (2019). Multifidelity Data Fusion: Application to Blended-Wing-Body Multidisciplinary Analysis Under Uncertainty. *AIAA Journal.* 58. 1-18. 10.2514/1.J058388.

25. Mukhopadhaya, Jayant, et al. "Multi-fidelity modeling of probabilistic aerodynamic databases for use in aerospace engineering." *International Journal for Uncertainty Quantification* 10.5 (2020).

26. Perdikaris, Paris et al. “Nonlinear information fusion algorithms for data-efficient multi-fidelity modelling.” *Proceedings of the Royal Society A: Mathematical, Physical and Engineering Sciences* 473 (2017): n. pag.

27. Chun Tang, Ken Gee and Scott Lawrence. "Generation of Aerodynamic Data using a Design Of Experiment and Data Fusion Approach," AIAA 2005-1137. *43rd AIAA Aerospace Sciences Meeting and Exhibit.* January 2005.

28. Mehdi Ghoreyshi, Keneth Badcock and Mark Woodgate. "Integration of Multi-Fidelity Methods for Generating an Aerodynamic Model for Flight Simulation," AIAA 2008-197. *46th AIAA Aerospace Sciences Meeting and Exhibit.* January 2008.

29. Nguyen, Nhu Van. (2009). Multidisciplinary Unmanned Combat Air Vehicle (UCAV) System Design Using Multi-Fidelity Models.

30. Nguyen, Nhu Van & Lee, Jae-Woo & Tyan, Maxim. (2015). A modified variable complexity modeling for efficient multidisciplinary aircraft conceptual design. Optimization and Engineering. 16. 485-505. 10.1007/s11081-014-9273-7.

31. Zastawny, Marian. (2016). VARIABLE FIDELITY MODELLING IN MODERN AIRCRAFT DESIGN. 6383-6397. 10.7712/100016.2264.6117.

32. Maxim Tyan, Nhu Van Nguyen & Jae-Woo Lee (2015) Improving variable-fidelity modelling by exploring global design space and radial basis function networks for aerofoil design, *Engineering Optimization*, 47:7, 885-908, DOI: 10.1080/0305215X.2014.941290

33. Belyaev, Mikhail & Burnaev, Evgeny & Kapushev, Yermek & Alestra, Stephane & Dormieux, Marc & Cavailles, Antoine & Chaillot, Davy & Ferreira, Eugenio. (2014). Building Data Fusion Surrogate Models for Spacecraft Aerodynamic Problems with Incomplete Factorial Design of Experiments. *Advanced Materials Research.* 1016. 405-412. 10.4028/www.scientific.net/AMR.1016.405.

34. Gomec, Fazil & Canıbek, Murat. (2017). Aerodynamic Database Improvement of Aircraft based on Neural Networks and Genetic Algorithms. 10.13009/EUCASS2017-226.

35. Kurt, Hüseyin & Millidere, Murat & Sezer, Emrah. (2019). Aerodynamic Database Simulation Implementation Based On Neural Network and Neural Network Parameter Selection Using Genetic Algorithms. 10.13009/EUCASS2019-679.

36. Wang, Yan & Long, Teng & Shi, Renhe & Li, Liu. (2018). Aero-Structure Coupled Optimization for High Aspect Ratio Wings Using Multi-model Fusion Method. 10.2514/6.2018-1913.

37. Tao, Jun & Sun, Gang. (2019). Application of deep learning based multi-fidelity surrogate model to robust aerodynamic design optimization. *Aerospace Science and Technology*. 92. 10.1016/j.ast.2019.07.002.

38. Renganathan, S. Ashwin & Harada, Kohei & Mavris, Dimitri. (2019). Multifidelity Data Fusion via Bayesian Inference. 10.2514/6.2019-3556.

39. Kou, Jiaqing & Zhang, Weiwei. (2019). Multi-fidelity modeling framework for nonlinear unsteady aerodynamics of airfoils. *Applied Mathematical Modelling.* 76. 10.1016/j.apm.2019.06.034.

40. Chen, Jie & Gao, Yi & Liu, Yongming. (2022). Multi-fidelity Data Aggregation using Convolutional Neural Networks. *Computer Methods in Applied Mechanics and Engineering.* 391. 114490. 10.1016/j.cma.2021.114490.

41. van den Berg, J. I., Sytsma, H. A., & Schippers, H. (1995). Computation of the flow about a F16-like configuration for several flow conditions. *13th Applied Aerodynamics Conference,* 201–211. https://doi.org/10.2514/6.1995-1786

42. Rizzi, A., & Luckring, J. M. (2014). What was learned in predicting slender airframe aerodynamics with the F16-XL aircraft. *52nd AIAA Aerospace Sciences Meeting - AIAA Science and Technology Forum and Exposition,* SciTech 2014. https://doi.org/10.2514/6.2014-0759.

43. Akgun, O., Golcuk, A. I., Kurtulus, D. F., & Kaynak, Ü. (2016). Drag analysis of a supersonic fighter aircraft. *9th International Conference on Computational Fluid Dynamics,* ICCFD 2016 - Proceedings.

44. Kodavanla, B., Kiran Burra, S., Santosh, G., Priyanka, S., Anudeep, P., & Madhavi, V. (n.d.). CFD ANALYSIS OF F-16 FALCON. *www.tjprc.org*

45. Sharma, M., Reddy, T. R., & Priyadarsini, C. I. (2013). Flow Analysis over an F-16 Aircraft Using Computational Fluid Dynamics. *International Journal of Emerging Technology and Advanced Engineering,* 3(5).

46. Matak, L., & Nikolić, K. K. (2022). CFD Analysis of F-16 Wing Airfoil Aerodynamics in Supersonic Flow. *In The Science and Development of Transport*—ZIRP 2021. https://doi.org/10.1007/978-3-030-97528-9_13.

47. Peiris, H., Nirmal, P., Bandara, H., Mahindarathne, D., Rangajeeva, S., & Bandara, R. (2015). Aerodynamics Analysis of F-16 Aircraft.

48. Kostić, Č., Bengin, A., Rašuo, B., & Damljanović, D. (2021). Calibration of the CFD code based on testing of a standard AGARD-B model for determination of aerodynamic characteristics. In Proceedings of the Institution of Mechanical Engineers, Part G: *Journal of Aerospace Engineering* (Vol. 235, Issue 10). https://doi.org/10.1177/0954410020966859

49. Huband, G. W., Shang, J. S., & Aftosmis, M. J. (1990). Numerical simulation of an f-16a at angle of attack. *Journal of Aircraft,* 27(10). https://doi.org/10.2514/3.45953

50. Ramli, M. R., Mohamed, W. M. W., Yusoff, H., Ismail, M. A., Mansor, A. A., Hussin, A., & Yamin, A. F. M. (2023). The Aerodynamic Characteristics Investigation on NACA 0012 Airfoil with Owl's Wing Serrations for Future Air Vehicle. *Journal of Advanced Research in Fluid Mechanics and Thermal Sciences,* 102(1). https://doi.org/10.37934/arfmts.102.1.171183

51. Pandya, Y., Sreevanshu, Y. G., Sharma, A., Jain, K., Jena, S., Pawar, A. A., Ranjan, K. S., & Saha, S. (2017). Aerodynamic characterization of a model aircraft using wind-tunnel testing and numerical simulations. *Proceedings of the International Conference on Recent Advances in Aerospace Engineering,* ICRAAE 2017. https://doi.org/10.1109/ICRAAE.2017.8297239

52. Kai, S., Takazawa, S., Ochi, S., Imamura, T., Yokozeki, T., & Rinoie, K. (2023). Low-Speed Wind Tunnel Testing of a Passive Camber Morphing Airfoil Using a 3D-Printed Compliant Mechanism. *Lecture Notes in Electrical Engineering, 912.* https://doi.org/10.1007/978-981-19-2689-1_78

53. Jun, G. R., Oliden, D., Potapczuk, M. G., & Tsao, J. C. (2013). Computational aerodynamic analysis of three-dimensional ice shapes on a NACA 23012 airfoil. *Transactions of Japanese Society for Medical and Biological Engineering, 51(SUPPL.).* https://doi.org/10.2514/6.2014-2202

54. Vadake, K., & Cui, J. (2015). Numerical and Experimental Study of Turbulent Flows Around Clark Y-14 Aerofoil. https://doi.org/10.1115/imece2015-50536

55. Announcements. (2023, July 24). OpenVSP. *https://openvsp.org/*

56. T. Shahid, F. Sajjad, M. Ahsan, S. Farhan, S. Salamat and M. Abbas, "Comparison of Flow-Solvers: Linear Vortex Lattice Method and Higher-Order Panel Method with Analytical and Wind Tunnel Data," *2020 3rd International Conference on Computing, Mathematics and Engineering Technologies (iCoMET),* Sukkur, Pakistan, 2020, pp. 1-7, doi: 10.1109/iCoMET48670.2020.9073909.

57. Yurov VM, Goncharenko VI, Oleshko VS, Ryapukhin AV. Calculating the Surface Layer Thickness and Surface Energy of Aircraft Materials. Inventions. 2023; 8(3):66. https://doi.org/10.3390/inventions8030066.

58. Compute mesh spacing for a given Y+ for viscous flow in CFD. (n.d.). https://www.cadence.com/en_US/home/tools/system-analysis/computational-fluid-dynamics/y-plus.html

59. Guo, B., & Ghalambor, A. (2005). Transportation. In Elsevier eBooks (pp. 219–262). https://doi.org/10.1016/b978-1-933762-41-8.50018-6

60. Alayil, Rajesh. (2014). Re: What is the best value of Maximum Aspect Ratio in Ansys Fluent? Is there any effect on converging from this value?. *Retrieved from:* https://www.researchgate.net/post/What-is-the-best-value-of-Maximum-Aspect-Ratio-in-Ansys-Fluent-Is-there-any-effect-on-converging-from-this value/543f4738d2fd64c90f8b461c/citation/download.

61. Tadepalli, S., Erdemir, A., & Cavanagh, P. R. (2011). Comparison of hexahedral and tetrahedral elements in finite element analysis of the foot and footwear. *Journal of Biomechanics,* 44(12), 2337–2343. https://doi.org/10.1016/j.jbiomech.2011.05.006

62. Rasmussen, C. E. and Williams, C. K. I. (2006). Gaussian processes for machine learning. *MIT press*.

63. Shi, R., Liu, L., Long, T., Wu, Y., and Gary Wang, G. (October 17, 2019). "Multi-Fidelity Modeling and Adaptive Co-Kriging-Based Optimization for All-Electric Geostationary Orbit Satellite Systems." *ASME. J. Mech. Des.* February 2020; 142(2): 021404. https://doi.org/10.1115/1.4044321

ÖZGEÇMİŞ

Kişisel Bilgiler

Soyadı, adı	: K******, B**** N****
Uyruğu	: T.C.
Doğum tarihi ve yeri	:
Medeni hali	:
Telefon	: 0
e-mail	:

Eğitim

Yüksek lisans	SBTÜ/ Savunma Teknolojileri	2024
Lisans	Samsun Üniversitesi / Uçak ve Uzay Mühendisliği	2020
Lise	85.Yıl Anadolu Lisesi	2015

İş Deneyimi

Yıl	Yer	Görev
2021-Halen	Sivas Bilim ve Teknoloji Üniversitesi	Araştırma Görevlisi
2023-2024	Türk Havacılık ve Uzay Sanayi	Araştırmacı

Yabancı Dil

İngilizce

Yayınlar

Kızıloğlu B N, Ostovan Y. (2023). “Examination of Co-Kriging Method to Obtain Aerodynamic Data Set For Generic Fighter Aircraft” ANKARA INTERNATIONAL CONGRESS ON SCIENTIFIC RESEARCH-IX, 213-225.

Hobiler

Bilardo, Video Oyunları, Motor Sporları

KÖKLERDEN GÖKLERE…